Marine to continental depositional systems of Outer Dinarides foreland and intra-montane basins (Eocene-Miocene, Croatia and Bosnia and Herzegovina)

By

Igor Vlahovic, Oleg Mandic, Ervin Mrinjek, Stanislav Bergant, Vlasta Cosovic, Arjan de Leeuw, Paul Enos, Hazim Hrvatovic, Dubravko Maticec, Goran Miksa, Wojciech Nemec, Davor Pavelic, Vili Pencinger, Ivo Velic & Alan Vranjkovic

With 78 figures

Field Trip Guide

29th IAS Meeting of Sedimentology Schladming/Austria

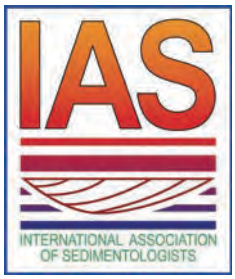

Addresses of the authors
Igor Vlahovic, Davor Pavelic, Ivo Velic, Alan Vranjkovic
University of Zagreb
Faculty of Mining, Geology and Petroleum Engineering
Pierottijeva 6
HR-10000 Zagreb
Croatia

Oleg Mandic
Department of Geology and Paleontology
Natural History Museum Vienna
Burgring 7
1010 Wien
Austria

Journal of Alpine Geology	54	S. 405-470	Wien 2012

ERVIN MRINJEK, VLASTA COSOVIC
University of Zagreb
Faculty of Science
Horvatovac 102
HR-10000 Zagreb
Croatia

WOJCIECH NEMEC
Department of Earth Science
University of Bergen
N-5007 Bergen
Norway

STANISLAV BERGANT, DUBRAVKO MATICEC, VILI PENCINGER
Croatian Geological Survey
Sachsova 2
HR-10000 Zagreb
Croatia

ARJAN DE LEEUW
CASP
West Building
181A Huntingdon Road
Cambridge
CB3 0DH
United Kingdom

PAUL ENOS
Department of Geology
University of Kansas
KS 66045 Lawrence
USA

HAZIM HRVATOVIC
Federal Institute for Geology
Sarajevo
Ustanicka 11
71210 Ilidza
Bosnia and Herzegovina

GORAN MIKSA
INA Plc.
Lovinciceva bb
HR-10000 Zagreb
Croatia

Content

1. Introduction

The Dinarides form a mountain chain extending in NW-SE direction along the northeastern Adriatic coast, connecting the Southern Calcareous Alps to the north with the Albanides and Hellenides-Taurides to the south. The mountain chain consists of a strongly tectonized, thick rock succession spanning a stratigraphic range from Carboniferous to Quaternary. The zone close to the Adriatic coast - where the field-trip area is located - is known as the Outer or Karst Dinarides, composed mainly of carbonate rocks. The more inland zone, between the Karst Dinarides and the Pannonian Basin, is known as the Inner Dinarides, composed mainly of deeper-marine sedimentary rocks and ophiolites.

Although the carbonate deposition commenced in Carboniferous and significantly increased in the Late Permian and Triassic, the major part of the carbonate deposits, which belong to the Adriatic Carbonate Platform (AdCP), formed during Jurassic and Cretaceous (Vlahovic et al. 2005 and references therein). The AdCP formed on the Adria Microplate, recording disintegration of a vast para-Tethian carbonate platform into several smaller ones during the late Early Jurassic (Toarcian). The AdCP was a relatively stable shallow-marine area until the Late Cretaceous, when it started to be gradually deformed, tectonically disintegrated and mostly emerged by SW-NE oriented compression. More or less continuous shallow-marine sedimentation across the K/T boundary is recorded only at the northwestern (Ogorelec et al. 2007) and southeastern margins of the AdCP (Gusic & Jelaska 1990, Steuber et al. 2005).

Deposition during Eocene, Oligocene and Miocene was significantly influenced by tectonic deformation of the former Adriatic Carbonate Platform. Therefore, although Outer Dinarides are famous for their thick succession of shallow-marine carbonate rocks, which were already main topic of numerous field trips, including several excursions at two IAS meetings (Split 1983, Opatija 2003), we believe that post-platform development is also very interesting.

On this field trip we will show you three different Cenozoic successions deposited above the Mesozoic platform carbonates:

(1) Massive Cenozoic carbonate breccia of the Karst Dinarides: the Velebit breccia, a brief stop on the first day of the field trip (Stop 1/1 on Fig. 1),
(2) The Eocene-Oligocene Promina Beds of the Dinaric foreland basin in northern Dalmatia, on the second day (Stops 2/1 and 2/2 on Fig. 1) and third day morning (Stops 3/1 and 3/2 on Fig. 1), and
(3) Miocene intra-montane lacustrine basins of Outer Dinarides (Croatia and Bosnia and Herzegovina), on the third day afternoon (Stop 3/3 on Fig. 1) and fourth day of the field trip (Stops 4/1 to 4/3 on Fig. 1).

Fig. 1: Location map showing driving direction across the Croatia and stops of the first day (Stop 1/1), second day (Stops 2/1 and 2/2), third day (Stops 3/1 to 3/3) and fourth day (Stops 4/1 to 4/3) of the field trip. On the last day the bus will go directly to Schladming, the venue of the 29th IAS Meeting of Sedimentology.

2. Topic One: Velebit breccia

Massive Cenozoic carbonate breccia of the Karst Dinarides: the Velebit breccia

IGOR VLAHOVIC, IVO VELIC, PAUL ENOS & ERVIN MRINJEK

2.1. Introduction

Velebit Mt. is the fourth highest Croatian mountain (1757 m, after Dinara, 1831 m, Kamesnica, 1809 m, and Biokovo, 1762 m), but is the longest, stretching for approximately 145 km. The entire mountain is protected as Nature Park (2200 km^2 area), and includes two National Parks: Northern Velebit and Paklenica. Besides numerous endemic species (the most popular of which is *Degenia velebitica*) it is famous for its deep pits, including two deepest in Croatia: 'Lukina jama' (1,392 m deep), and Slovacka jama (1,320 m), both located within the breccia zone. On our way from Gospic across the Velebit we will cross the entire succession from Carboniferous and Lower to Middle Permian clastic

rocks, Upper Permian and Lower Triassic dolomites, Middle Triassic massive diplopora limestones, Middle to Upper Triassic reddish clastic rocks, Upper Triassic Main Dolomite and Lower to Upper Jurassic limestones before reaching the zone of carbonate breccia on the SW slope of the mountain.

The massive Cenozoic carbonate breccia covers large areas along the NE Adriatic coast (VLAHOVIC et al. 2007, 2011): according to the data presented on 14 sheets of the Basic Geological Map in 1:100.000 scale the total area covered by breccia is 1011 km^2, and three largest outcrops cover 695, 115 and 22 km^2, respectively (82% of a total area; Fig. 2). The biggest outcrop is more than 100 km long, stretching along the SW slope of the Velebit Mt. The rest

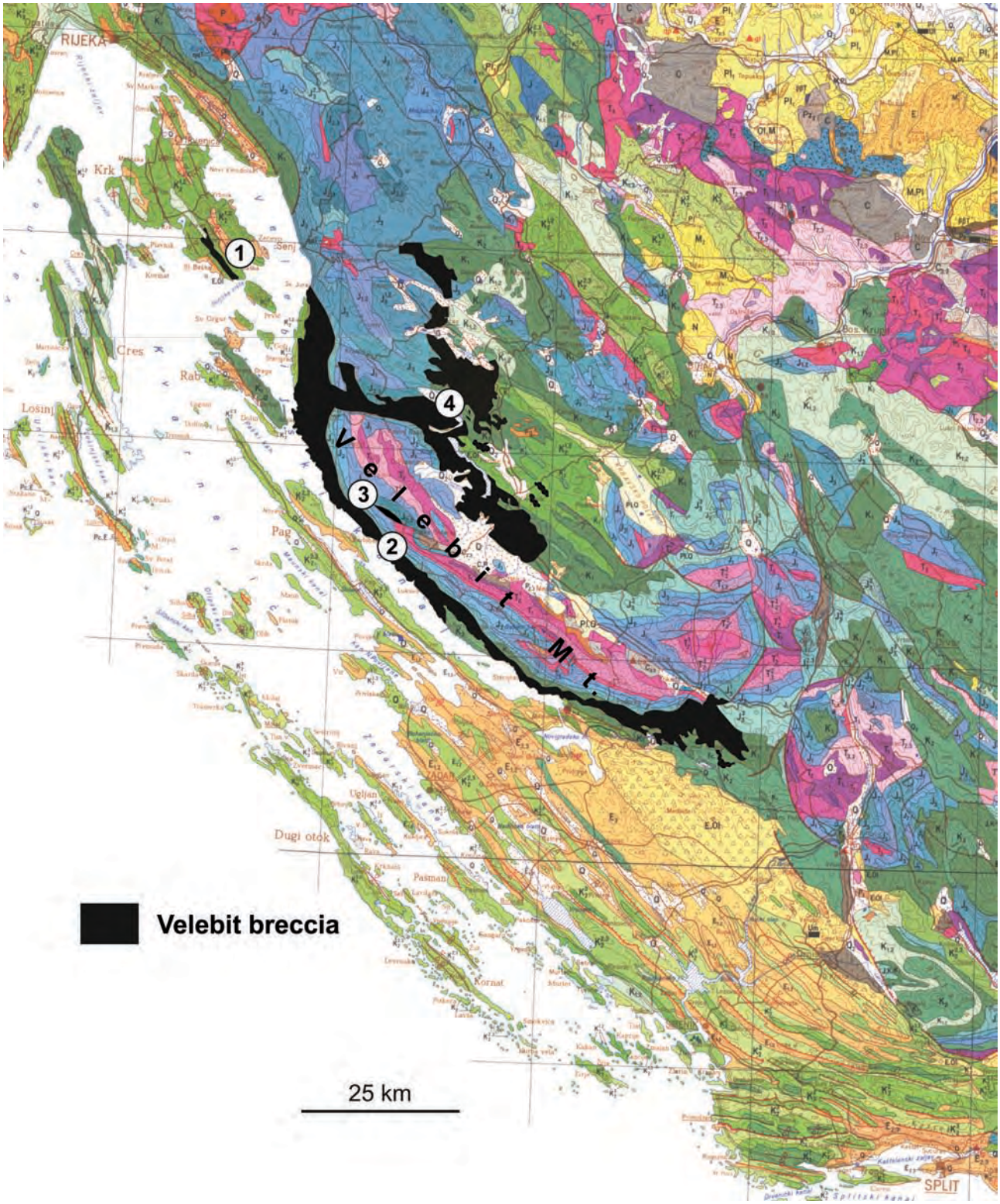

Fig. 2: Main outcrops of Velebit breccia (black): 1) island of Krk; 2) the SW slope of the Velebit Mt. (number 2 shows location of Stop 1/1); 3) Ostarije fault; 4) Lika region.

comprises more than 400 smaller outcrops. Thickness data on the breccia are few, but in places it is very thick, as indicated by more than 400 m high cliffs in the Paklenica National Park completely composed of breccia. Even greater thickness was recorded in the well made during the construction of the Sveti Rok highway tunnel through Velebit Mt.: the 350-m-deep well was located 250 m below highest peaks of Tulove Grede (which are completely built of breccia; Fig. 3), and it was fully cored and composed of breccia, so its thickness should exceed 600 m.

2.2. Previous investigations

Breccia is up to now poorly understood because of its very complex composition, usually unclear structural position and intense younger tectonic deformation. In the Austro-Hungarian geological maps it was considered as intraformational breccia due to the common predominance of Cretaceous clasts (e.g., 'Grey breccia of Lower Cretaceous' on the Medak and Sv. Rok sheet - SCHUBERT 1909, 1910), while in later maps geographical attribute representing the most important locality was added - e.g. 'Grey breccia of Velebit' on the Knin and Ervenik sheet (SCHUBERT 1920a, KERNER 1920a) and Zadar sheet (SCHUBERT 1920b, KERNER 1920b).

During the work on the Basic Geological Map of SFR Yugoslavia in 1960's and 1970's this breccia was proved to be younger then surrounding rocks on the basis of occurrences of younger clasts. However, at none of 14 sheets of the map with breccia outcrops the same combination of age and lithological description was used for its designation, confirming the very significant complexity.

During 1960's and 1970's the breccia was sometimes confused with Promina deposits, uppermost part of which is characterized by a thick succession of alluvial conglomerates, and crops out relatively close to the breccia outcrops. Therefore BAHUN (1963) proposed the term Jelar deposits for the succession composed of approximately 70% of breccia, 25% of limestones and 5% of marls or marly breccia; the name was proposed after the hill above the village of Podjelar near Gornji Kosinj in Lika (however, this hill is called Jelar only by a local people - on official topographic maps of the area it is designated as Gorica).

Since limestones represent zones of underlying rocks and not olistoliths within breccia (as indicated by typically continuous stratigraphic succession of limestones across the breccia zone), and marls are practically absent in most of the breccia areas, this lithological unit should be sensu stricto referred to as breccia, and not as deposits composed of different lithology (and in subsequent papers it was usually referred to as Jelar breccia). However, since the proposed geographical term is very local (and cannot be even found on the topographical map), and up to now used only in couple of papers in local Croatian journals, we believe that instead of the Jelar deposits another, more appropriate name should be proposed for this very specific lithological unit - the Velebit breccia. This may be better term not only because of the priority (as proposed by SCHUBERT and KERNER in 1920) but also because Velebit Mt. is a well-known topographic term and more than 80% of all breccia of this type crops out at or close to it (see Fig. 2).

2.3. Description of breccia

The breccia is massive, non-bedded, clast-supported, and lacks visible sedimentary structures (Fig. 4). Clasts are mostly angular and poorly sorted, ranging in size from less than 1 mm to several centimetres with only sporadic cobbles and boulders (Fig. 5). Almost all clasts were tectonized before final deposition, as shown by truncated, calcite-filled fractures. Rare clasts of older breccia indicate a polyphase origin (Figs. 6, 7) - in places even three generations may be found. Clasts were mostly derived from the surrounding carbonate rocks - only sporadically Eocene flysch fragments have been found. Locally clasts are from rocks that now crop out only tens of kms away (Figs. 8, 9). Rare subrounded to rounded clasts reflect some sedimentary transport. Weathered rims on clasts are absent, but pressure-solution contacts between grains are common (Fig. 10). The grey, yellowish, or reddish carbonate matrix is composed of small lithoclasts and recrystallized calcite (Fig. 11), and contains no fossils or structures indicative of subaqueous deposition.

Within the breccia, several parallel ribbons of the underlying rocks crop out in stratigraphic order, i.e. older towards the anticline axis if within folds (island of Krk) or continuously younger within monocline structure of the coastal slope of the Velebit Mt. Unlike other breccia types within the Dinarides outcrops of Velebit breccia are much larger and characterized by mostly steeply inclined to vertical gradational contacts with adjacent rocks: transitional zones up to several meters wide extend from undisturbed to gradually more tectonized limestones through completely cataclastic limestones and monomict breccia composed of clasts from adjacent limestones to ± polymictic breccias (lower part of Fig. 12). Gradual contacts are one of the main criteria differentiating Velebit

Fig. 3: Tulove grede, Velebit Mt.: peaks composed of Velebit breccia approximately 200 m higher than surrounding hills. 250 m below the highest peak a 350 m deep well was drilled, completely within breccia.

Fig. 4: Polymictic variety of Velebit breccia composed of poorly sorted angular clasts of different lithological units, including fragment of older breccia (above the hammer).

Fig. 5: Velebit breccia composed predominantly of white allochthonous Cenomanian/Turonian clasts; note the size of the clast below the hammer.

breccia from other types of breccia within the Dinarides. Significantly, breccia occurrences are mostly located along faults and overturned folds with NE vergences, which are very atypical for the Dinarides where SW vergences are much more common.

2.4. Problems regarding interpretation of the Velebit breccia

Velebit breccia was traditionally considered as talus breccia shed from the front of inferred reverse faults or overthrusts (e.g., Bahun 1974, Herak & Bahun 1979, Tari & Mrinjek 1994). However, this interpretation ignores several important facts: (i) subvertical and gradational contacts with surrounding rocks, instead of the expected inclined, irregular but sharp contacts (Fig. 12), (ii) breccias crop out at hypsometrically highest points, and (iii) stratigraphic succession does not indicate reverse faulting, especially not with supposed SW vergences.

Recent investigations indicated that there are various structural positions of Velebit breccia outcrops, and they should be studied in detail in order to determine the origin of Velebit breccia. However, all these different types have in common NE vergences of structures. The most important examples are:

(1) The SE part of the island of Krk comprises a relatively large (15 km x 1 km; 1 on Fig. 2) outcrop of a typical Velebit Breccia, within the apical part of the NW-SE oriented anticline composed of highly fractured Cenomanian limestones, transgressive, little fractured Lower-Middle Eocene limestones and Mid-Eocene flysch. The NE fold limb is overturned (inclination ~20° towards the SW).

(2) The SW slope of the Velebit Mt. is characterized by the longest and biggest outcrop of Velebit breccia (approximately 100 km long, 2-10 km wide, 2 on Fig. 2), striking parallel with the limb of the monocline in the hinterland of which there are overturned older beds located near the subsequently steepened reverse fault of NE vergence.

(3) Along the Ostarije fault, which is also of NE vergence,

Fig. 6: Block of breccia with red matrix incorporated in breccia with grey matrix. Coin is 26.5 mm in diameter.

Fig. 7: Polymictic Velebit breccia with coarser fragments including clasts of older breccia. Coin is 26.5 mm in diameter.

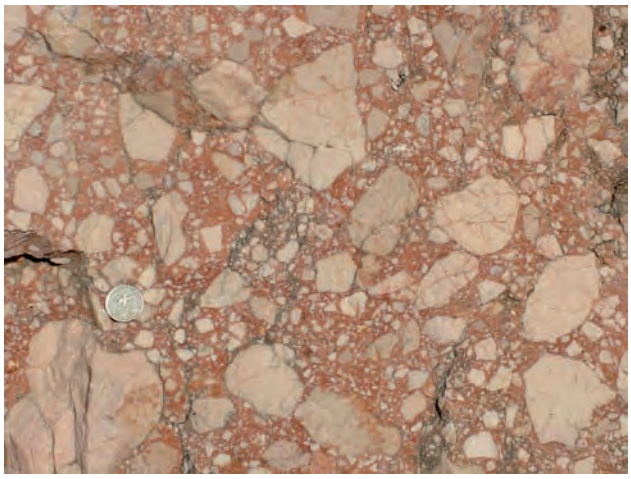

Fig. 8: Monomictic Velebit breccia composed predominantly of white allochthonous Cenomanian/ Turonian clasts in red matrix. Coin is 22.5 mm in diameter.

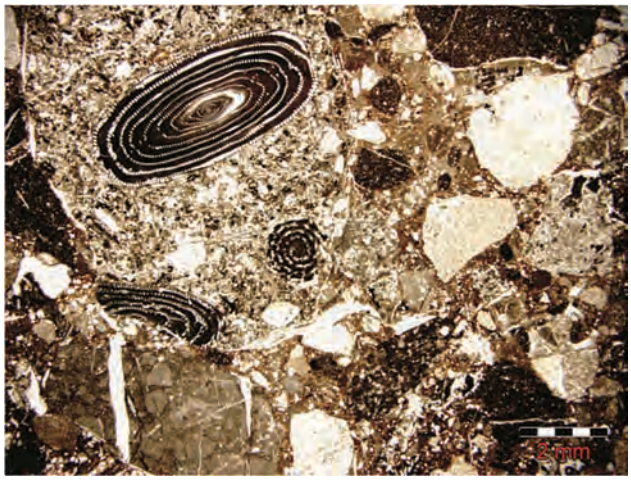

Fig. 9: Photomicrograph showing polymictic Velebit breccia including fragments of Eocene Foraminifera limestones.

in the area of Ravni and Crni Dabar there is approximately 9 km long zone of breccia (3 on Fig. 2), mostly cataclastic but also typical polymictic varieties of Velebit breccia type.

(4) In the Lika region (hinterland of the Velebit Mt.), the large area is covered by irregular breccia outcrops (4 on Fig. 2), but they seems to be relatively thin, since outcrops of underlying host-rocks are very common. Unlike previous three examples which are directly related to tectonic structures this type appear like erosional remnant of much larger breccia body of possible talus origin.

The studied outcrops of Velebit breccia represent only erosional relics of originally probably much larger outcrops. The enormous amount of carbonate material which was tectonized and mechanically disintegrated rather then chemically weathered indicate intense and rapid tectonics, and several generations of breccia clearly indicate its polyphase nature. A very interesting issue represents a lack of such breccia along the much more common structures of SW vergences, what is a topic of the recent investigations.

Possible mechanism of breccia formation may be seen at the island of Krk, where fracturing of apical parts of the overturned anticline resulted in crushing of clasts and collapse into a complex system of deep fractures largely without surficial transport. The breccia was probably initiated by intense in-situ fracturing during compression, disintegrating the carbonate rocks into cm-sized clasts within km-wide zones. Subsequent extension within overturned structures opened a complex system of deep fractures filled by breccia. Other breccias formed locally on the surface and portions were reworked by surficial processes. The resulting deposits were subsequently tectonized, further altered diagenetically, and intensely karstified and denuded during the long post-emplacement exposure (more then 15 MY), therefore resulting in a very complex appearance. This model may explain many features of the Velebit breccia found at other localities.

No fossils have been found within the matrix of the breccia

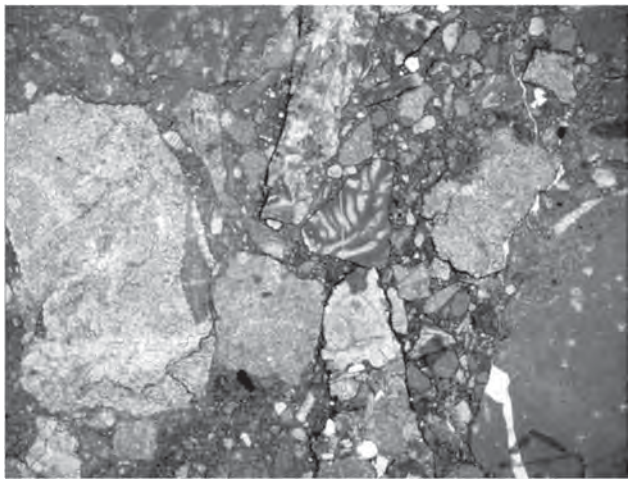

Fig. 10: Photomicrograph of Velebit breccia composed of various clasts with visible pressure solution on grain contacts.

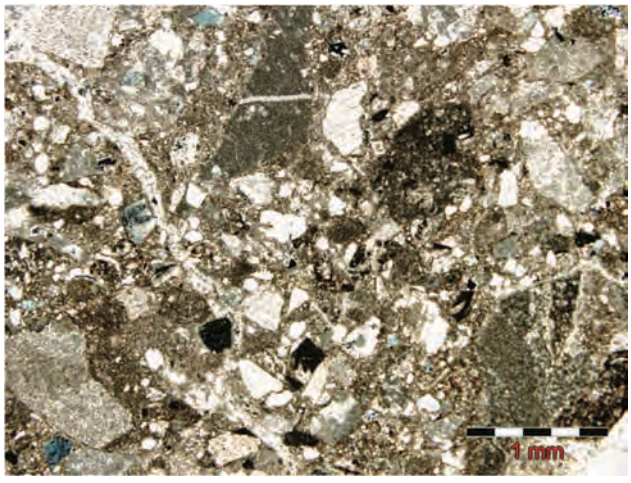

Fig. 11: Photomicrograph of Velebit breccia with carbonate matrix composed of small lithoclasts and recrystallized calcite (Fig. 11).

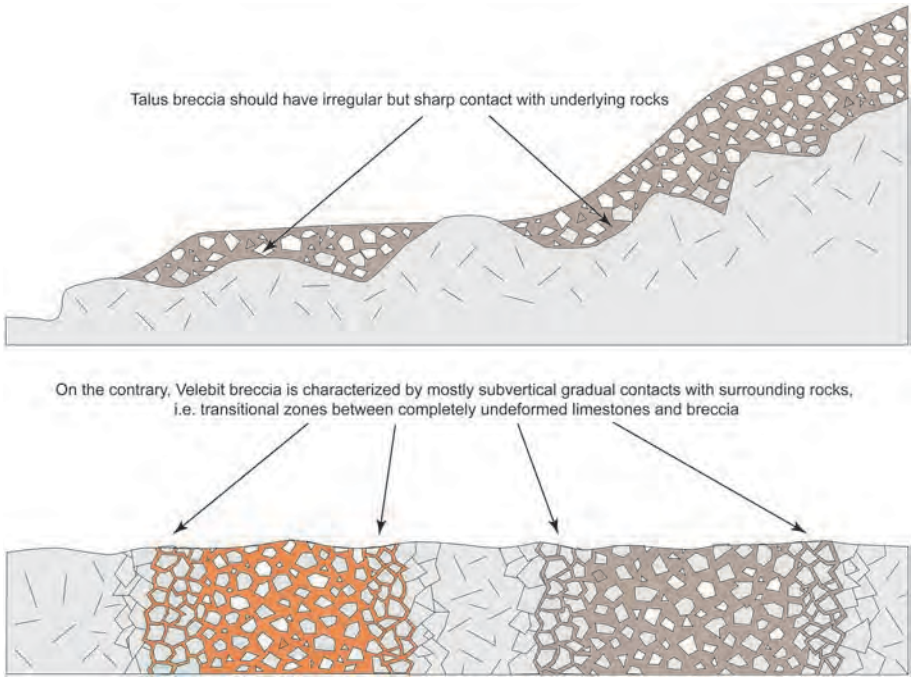

Fig. 12: Upper part: previous interpretation of Velebit breccia as talus breccia - note that most of the clasts should be allochthonous, transported from hypsometrically higher areas where supposed reversed fault should be located. Lower part: our interpretation of Velebit breccia as deposits within steep tectonized zones characterized by gradual transition from undisturbed limestones to complete breccia - note that most of the clasts originated from surrounding limestones, while only some are allochthonous.

to enable direct age determination. Velebit breccia is therefore younger than the youngest clasts within it (typically Mid-Eocene foraminiferal limestones or locally Mid-Eocene flysch). Maximum compression and uplift of the Dinarides took place from Middle to Late Eocene to Early Miocene, and these events could cause a significant tectonic deformation necessary for the formation of breccia. A post-Middle Miocene tectonic phase formed fractures within already lithified breccia. Therefore, a very rough estimate on the age of the Velebit breccia may be: not older than Middle Eocene and not younger than Early Miocene, although its age may be variable at different localities due to the variable timing of main tectonic events. However, if initial results indicating that Dinaric structures with NE vergences were formed before the structures with SW vergences will be confirmed an older age estimation will be favoured.

3. Topic Two: Promina Beds

The Eocene-Oligocene Promina Beds of the Dinaric foreland basin in northern Dalmatia

Ervin Mrinjek, Wojciech Nemec, Vili Pencinger, Goran Miksa, Igor Vlahovic, Vlasta Cosovic, Ivo Velic, Stanislav Bergan & Dubravko Maticec

3.1. Introduction

The Dinaric peripheral foreland basin of Croatia (Fig. 13) developed in front of the rising mountain chain, by tectonic deformation and marine drowning of an emerged and denudated carbonate platform. The deepening of water in the basin is reflected by the deposition of Foraminifera Limestones (with miliolid, alveolinid, nummulitid and discocyclinid limestone units), glauconite-bearing marly Transitional Beds and an extensive, thick turbiditic succession of Dalmatian Flysch. These deposits are mainly of Eocene (Ypresian-Bartonian) age. The foreland zone proximal to orogenic front accumulated a regressive molasse succession of neritic to terrestrial calciclastic deposits, mid-Eocene to Oligocene in age and ~2000 m thick, referred to as the Promina Beds. The Promina Beds recorded syn-tectonic sedimentation in an evolving thrust wedge-top (piggyback) basin (Mrinjek et al. 2010a, b, 2011). The Dalmatian Flysch filled the more distal (foredeep) zone of the foreland basin and was overlain by the Promina Beds. The upward transition from Flysch turbidites to a succession of late mid-Eocene shallow-marine ramp deposits of the Promina Beds is exposed only in the Benkovac area (Fig. 1C; Mrinjek 2008, Mrinjek & Pencinger 2008). To the SE of Lisane (Fig. 1C), the Promina Beds overlie unconformably the bedrock-covering Foraminifera Limestones and Transitional Beds.

The development of the foreland basin involved formation of a series of blind-thrust growth folds, before the soling thrust system eventually established the wedge-top basin's outer limit. The development of folds resulted in foreland compartmentalization into an array of narrow, high-relief sub-basins, where the main part of Promina Beds was deposited. The evidence of this tectonic evolution and its impact on the basin-fill succession are the main topic of this part of the field trip.

3.2. The Dalmatian Flysch and Promina Beds

3.2.1. Regional extent

The mud-rich heterolithic deposits of the Dinaric outer foreland (foredeep zone) are 200-900 m thick and have

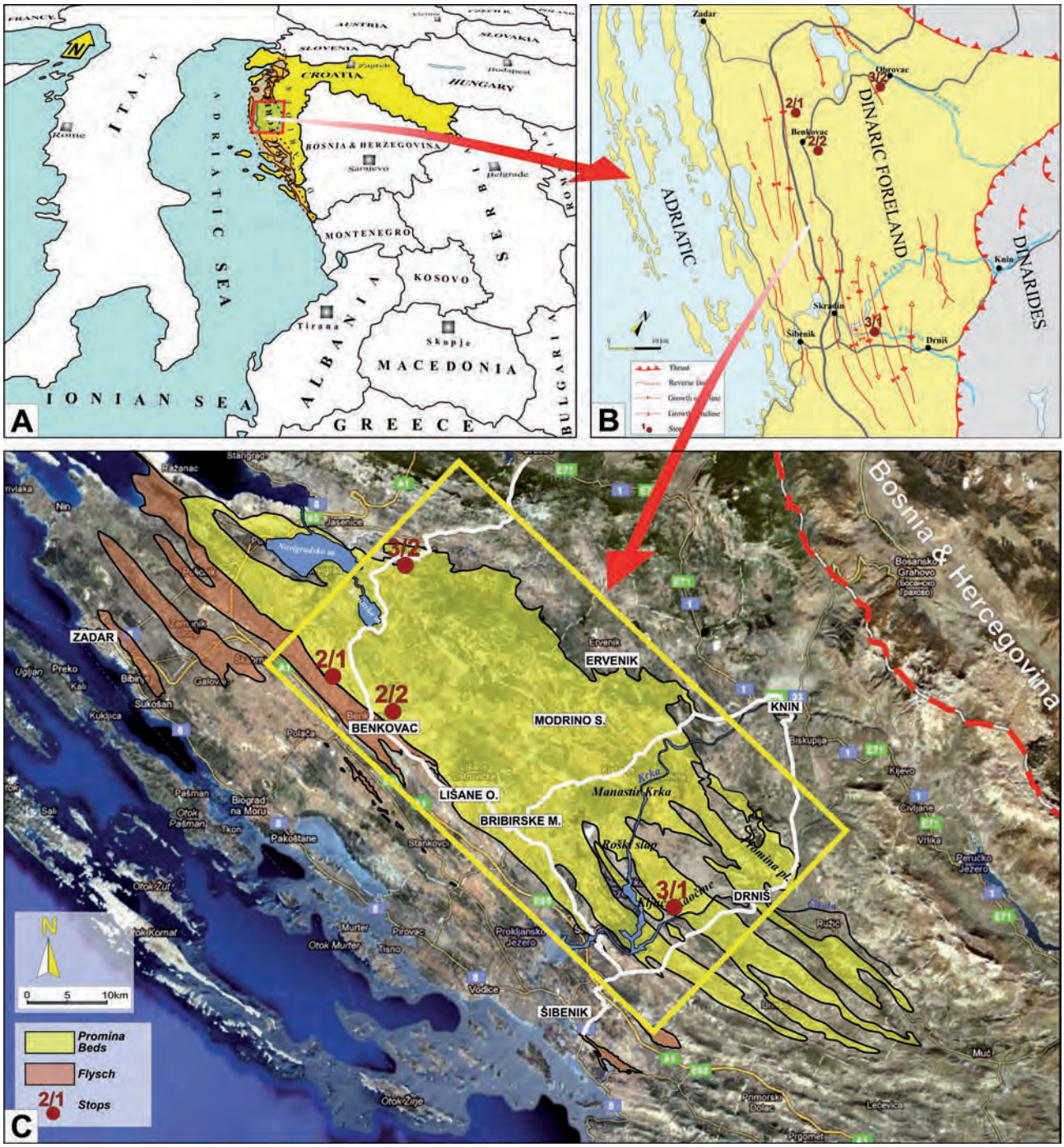

Fig. 13: Regional setting of the field-trip area (modified after PENCINGER 2012). **(A)** The location of Dinaric foreland and fold-and-thrust orogenic belt. **(B)** Simplified structural map of the Promina Beds, with the location of field-trip stops. **(C)** A generalized map showing the areal extent of the Promina Beds and Dalmatian Flysch (note the location of field-trip stops).

been generally considered to be an Eocene deep-marine turbiditic succession, referred to as the Dalmatian Flysch. The erosional relics of these deposits are preserved in several synclines along the Adriatic coast (Fig. 13B). The intervening anticlines expose bedrock composed of Late Cretaceous rudist limestones. This outcrop belt of isolated Flysch occurrences extends from the central Istria in the north to the Split and Dubrovnik areas in the south (Fig. 14). However, these deposits may not necessarily all be of turbiditic origin or even share their age, as the isolated occurrences more likely represent a diachronous range of palaeoenvironments spanning the transition from outer shelf to submarine slope and deep-water basin floor. For example, the so-called Flysch deposits in the Dubrovnik-Konavle area of southernmost Croatia (Fig. 14) have recently been reinterpreted as a succession of sublittoral shelf deposits of Oligocene to early Miocene age (PRTOLJAN et al. 2009).

The adjacent belt of similarly isolated outcrops of the Promina Beds extends from the small occurrences in

Fig. 14: The outcrop extent of the 'inner' Promina Beds and 'outer' Dalmatian Flysch in the Dinaric foreland basin of Croatia.

narrow synclines in some of the Adriatic islands in the north, such as Rab and Pag (Fig. 14), to occurrences NW of Imotski in southern Croatia and NE of Posusje in the neighbouring western Herzegovina (Fig. 14). The largest outcrop area (~1200 km^2) is in the northern Dalmatia, extending ~80 km in NW-SE direction and up to 20 m in the SW-NE direction (Figs. 13C, 14).

3.2.2. Stratigraphy and structural characteristics

The calciclastic Promina Beds in northern Dalmatia (Fig. 13C) are of the latest mid-Eocene to Oligocene age and were deposited in a range of neritic, littoral, coastal/deltaic and alluvial environments (Ivanovic et al. 1967, Babic & Zupanic 1983, 1988, 1990, Mrinjek 1993a, b, 2008, Mrinjek et al. 2005, 2007, Mrinjek & Pencinger 2008). The deposits are better preserved in the NW part of the area (Fig. 13C), where their total thickness reaches ~2000 m. Towards the SE, these deposits crop out in synclines (Figs. 13C, 15) representing isolated or semi-isolated, thrust-related compartments (narrow sub-basins) of the Promina piggyback basin (Mrinjek et al. 2011). The thickest of these occurrences, up to 900 m, is in the Cikola sub-basin north of Kljuc (Fig. 15, Stops 3/1-2, 3/1-3).

Across the Promina piggyback basin from the SW to NE (Fig. 15), the bedrock is progressively older and more deformed, overlain 'transgressively and discordantly' by the Promina Beds (Sakac 1960, 1969). The discordance is barely recognizable to the SW, but quite clear in the more proximal, NE part of the basin. The anticlines southwest of Drnis (Fig. 15) expose mainly early Palaeogene, Cretaceous and Late Jurassic rocks, but locally even Triassic. The Promina Beds occur in synclines, most of which represent the original narrow sub-basins if an evolving piggyback basin. There are two stratigraphic levels of bauxite occurrence: older bauxites at the base of Palaeogene and younger bauxites at the base of the Promina Beds. The bauxites formed on carbonate bedrock - the Upper Cretaceous limestones and the earliest Eocene Foraminiferal Limestones, respectively - and are lacking in areas where the Promina Beds overlie the marly Transitional Beds.

The youngest deposits of the Promina Beds, a coarse-grained alluvium of probably late Oligocene age, occur at the orogeny-proximal zone of the basin (Obrovac area in Fig. 15, Stops 3/2-1, 3/2-2). The alluvium overlies folded Palaeogene and Upper Cretaceous limestones, with intervening occurrences of bauxite deposits - now almost completely exploited (Babic & Zupanic 1988, Mrinjek 1993a, b, 1994). Brown coal occurrences have been recognized in the basin's proximal zone (Nikler 1982), mainly in the youngest part of the Promina Beds and towards the SE, where the basin's topographic relief was

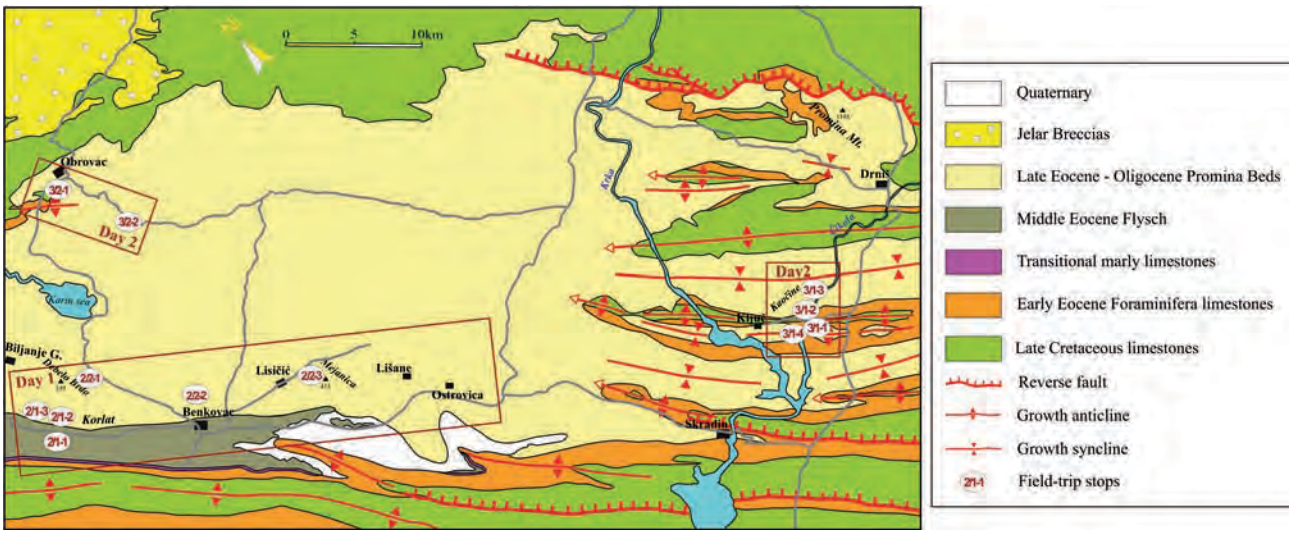

Fig. 15: Geological map of the Promina piggyback basin in northern Dalmatia, with the location of field-trip stops (modified after Pencinger 2012).

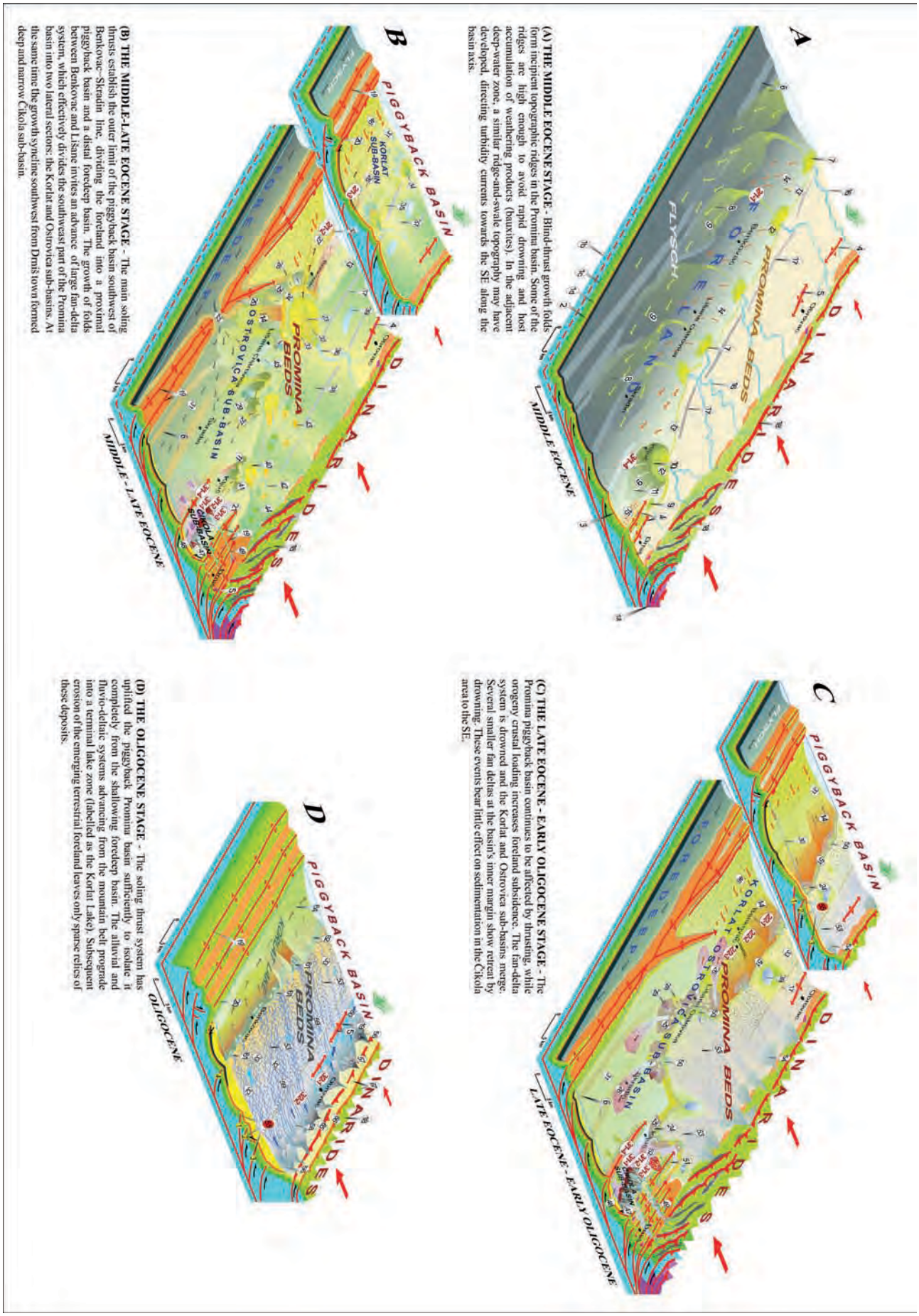

(A) THE MIDDLE EOCENE STAGE - Blind-thrust growth folds form incipient topographic ridges in the Promina basin. Some of the ridges are high enough to avoid rapid drowning and host accumulation of weathering products (bauxites). In the adjacent deep-water zone, a similar ridge-and-swale topography may have developed, directing turbidity currents towards the SE along the basin axis.

(B) THE MIDDLE-LATE EOCENE STAGE - The main soling thrusts establish the outer limit of the piggyback basin southwest of Benkovac–Skradin line, dividing the foreland into a proximal piggyback basin and a distal foredeep basin. The growth of folds between Benkovac and Lišane invites an advance of large fan-delta system, which effectively divides the southwest part of the Promina basin into two lateral sectors: the Korlat and Ostrovica sub-basins. At the same time the growth syncline southwest from Drniš town formed deep and narrow Cikola sub-basin.

(C) THE LATE EOCENE - EARLY OLIGOCENE STAGE - The Promina piggyback basin continues to be affected by thrusting, while orogeny crustal loading increases foreland subsidence. The fan-delta system is drowned and the Korlat and Ostrovica sub-basins merge. Several smaller fan deltas at the basin's inner margin show retreat by drowning. These events bear little effect on sedimentation in the Cikola area to the SE.

(D) THE OLIGOCENE STAGE - The soling thrust system has uplifted the piggyback Promina basin sufficiently to isolate it completely from the shallowing foredeep basin. The alluvial and fluvio-deltaic systems advancing from the mountain belt prograde into a terminal lake zone (labelled as the Korlat Lake). Subsequent erosion of the emerging terrestrial foreland leaves only sparse relics of these deposits.

Fig. 16: Interpreted tectono-palaeogeographic evolution of the Dinaric foreland basin in northern Dalmatia (Eocene-Oligocene time) (modified after Pencinger 2012). 1 - substrate: 1a - Triassic rocks, 1b - Jurassic limestones; 1c - Early to Late Cretaceous limestones; 1d - early to middle Eocene Foraminifera Limestones; 2 - middle Eocene Flysch deposited in the foredeep basin; 3 - middle Eocene Promina Beds deposited in piggyback basin; 4 - incipient ridges (blind-thrust anticlines) hosting accumulation of bauxites in the Promina basin; 5 - bauxites; 6 - basinfloor ridge-and-swale topography directing turbidity currents to the SE; 7 - hypothetical shelf-edge delta; 8 - prodelta/slope deposits; 9 - sediment gravity flows; 10 - hypothetical shoal-water delta; 11 - prodelta deposits; 12 - coarse-grained shelf-edge delta; 13 - coarse-grained beach zone formed by wave-reworking of mouth bars and alongshore sediment drift; 14 - storm-generated turbidity currents; 15 - shoreface resedimentation on shelf edge; 16 - bedload river; 17 - local base-level step (inferred incipient blind-thrust anticline); 18 - Dinaric fold-and-thrust belt; 19 - blind-thrust growth anticline; 20 - growth-fold branching; 21 - growth syncline; 22 - intermittent connection between foredeep and piggyback basin; 23 - prograding large gravelly Gradina delta; 24 - delta-front deposits; 25 - prodelta sediment gravity-flow deposits and synsedimentary deformations; 26 - turbidity currents; 27 - hyperpycnal flows; 28 - debris flows; 29 - slump; 30 - basinfloor topography directing sediment-gravity flows to the NW; 31 - deep-neritic lower slope and basin floor; 32 - active braided distributaries; 33 - abandoned distributaries; 34 - hypothetical delta; 35 - abandoned delta; 36 - inferred gravelly braided river; 37 - inferred abandoned braided river; 38-floodplain; 39-inferred small lakes; 40 - hypothetical sandy shoal-water delta; 41 - delta-front deposits; 42 - inferred meandering river; 43 - crevasse splays; 44 - peat-forming mires; 45 - mud mounds; 46 - deviation of olistoliths and mass-flow megabeds; 47 - slope apron of debris-flow deposits and turbidites; 48 - sandy shoreface and muddy offshore deposits; 49 - inferred antecedent braided river; 50 - 'back-stepping" fan delta; 51 - gravelly beach; 52 - submarine slope-waste deposits (colluvium); 53 - alluvial fan-toe braidplain (fluvially extended fans); 54 - alluvial fan; 55 - inferred back-stepping blind thrusts with slope back-lapping; 56 - coalescent and vertically stacked alluvial fans; 57 - subaerial debris-flow deposits; 58 - sheetflood deposits; 59 - braided-stream deposits; 60 - confined consequent braided-river system; 61 - hypothetical Gilbert-type delta; 62 - abandoned Gilbert-type delta; 63 - hypothetical braidplain shallow-water delta complex; 64 - hypothetical hydrologically open lake; 65 - active reverse fault; 66 - inactive reverse fault; 67 - highland drainage area.

more varied.

The Dalmatian Flysch and Promina beds have long been interpreted as a simple shallowing-upwards foreland succession passing from deep- to shallow-marine and to marginal-marine and alluvial facies. The most recent studies (Mrinjek 2008, Mrinjek & Pencinger 2008, Mrinjek et al. 2010a, b, 2011) indicate a more complex palaeogeographical scenario, with a deep-water distal foreland (foredeep basin) accumulating turbidites and the shallower-water proximal foreland split by blind thrusts into an array of narrow sub-basin where a range of neritic to terrestrial environments coexisted. In this way, the proximal foreland gradually evolved into a thrust wedge-top (piggyback) basin, with the farthest-reaching active thrusts as a soling system (see Ori & Friend 1984, DeCelles & Giles 1996, Mutti et al. 2009), while the foredeep was filled up and eventually overstepped by the Promina Beds. The development of the Promina basin involved formation of a series of blind-thrust growth folds, before the soling thrust system eventually extended far enough to establish the wedge-top basin's outer limit. The effects of the syn-depositional folding included: (1) formation of incipient topographic ridges that were high enough to avoid an early drowning and hosted accumulation of weathering products that gave rise to bauxites; (2) development of progressive unconformities; (3) deposition of differing facies successions on the opposite limbs of fold-growth anticlines, with both limbs recording a forced regression during the anticline growth and a transgression during the foreland bulk subsidence due to crustal loading; and (4) deposition of contrasting facies successions on the opposite limbs of fold-growth synclines, with a forced regression on one limb possibly corresponding to a transgression on the other limb in the instance of a non-synchronous movement of thrusts. The development of blind-thrust folds thus resulted in the proximal foreland's compartmentalization, with abrupt lateral changes in the thickness and facies of basin-fill succession and with a laterally-varying record of relative sea-level changes.

3.3. The outer part of the Promina Basin: the Dalmatian Flysch and selected units of the Promina Beds

3.3.1. Palaeogeographic background

The Dinaric foreland basin was formed by a compressional tectonic deformation, structural collapse and marine drowning of a pre-existing thick carbonate platform. The marine drowning was followed by the deposition of Foraminiferal Limestones and marly Transitional Beds in the early to middle Eocene, after which the proximal zone of the basin accumulated the calciclastic Promina Beds succession of deep neritic to terrestrial deposits, while the distal (foredeep) zone accumulated the coeval turbiditic succession of the Dalmatian Flysch. By the middle Eocene, blind-thrust growth folds formed incipient topographic ridges in the Promina basin, which were uplifted high enough to avoid rapid drowning and hosted accumulation of bedrock weathering products (bauxites). Similar folds with gentle ridge-and-swale topographic ridges may have formed in the foredeep zone, confining turbidity currents and directing them parallel to the basin axis (Fig. 16A). Turbidite palaeocurrent directions are mainly towards the southeast and lack of radial pattern of dispersal, which also suggests a southeastward general basinfloor inclination.

The Flysch unit in the excursion area is a middle Eocene succession of sheet-like sandstones interbedded with marls, ~850 m thick, showing slump features and occasional palaeochannels in the upper part. In a recent revisiting study, BABIC & ZUPANIC (2008) consider the unit to comprise deposits of a prodelta system prograding over a basin floor, overlain by the delta-front and delta-plain deposits of powerful, high-gradient braided rivers (Fig. 16A). The Flysch unit is underlain by the marly Transitional Beds (Figs. 17, 18) and contains a considerably higher admixture of siliciclastic component (~50 vol.%) than in the overlying Korlat unit (up to 10 vol.%) and Ostrovica unit (up to 25 vol.%).

In the middle to late Eocene, the main soling thrusts were probably established and defined the outer structural limit of the Promina piggyback basin along a line southwest of the towns of Benkovac and Skradin (Fig. 13B). The division of the foreland into a compartmentalized, shallower-water, proximal piggyback basin and a tectonically quitter, deep-water foredeep basin was then completed (MRINJEK et al. 2010, 2011). The tectonic deformation simultaneously enhanced the growth of blind-thrust anticlines within the piggyback basin, as is shown - for example - by a progressive unconformity related to a growth fold trending along the Benkovac-Lisane line (Fig. 13C). The branching of growth folds and an advance of large fan-delta system (the Gradina Unit) divided the basin into two semi-isolated lateral compartments (Fig. 16B), referred to as the Korlat sub-basin (represented by the Korlat Unit) and the Ostrovica sub-basin (represented by the lower and middle part of the Ostrovica Unit). The need to distinguish many such local "units", as successions of differing facies assemblages, reflects the Eocene compartmentalization of the basins.

The piggyback basin continued to be affected by orogenic thrusting in the late Eocene to early Oligocene, while orogen crustal loading increased the foreland bulk subsidence. The fan-delta system was drowned and the Korlat and Ostrovica sub-basins merged (Fig. 16C). A large, "back-stepping" braidplane delta was formed in the Ostrovica area (Bribir Unit) and several smaller fan deltas in the Benkovac area. In the Benkovac area, a braidplain delta-front and shoreface deposits (Otavac Unit) pass distally into deposits of a wave-dominated offshore-transition zone (Benkovac Stone Unit) and into offshore zone (Debelo Brdo Unit). In the Oligocene, the soling thrust system uplifted the piggyback basin sufficiently to isolate it completely from the shallowing foredeep basin (Fig. 16D). The alluvial and fluvio-deltaic systems advancing from the mountain belt prograded into a terminal lake zone. Subsequent erosion of the emerged terrestrial foreland left only sparse relics of these deposits.

3.3.2. Remarks on sequence stratigraphy

Except for progressive unconformities recognized in the lowest part of the Korlat Unit, the Flysch and Promina Beds lack contractional deformation by thrusting that typifies many foreland basins and complicates stratigraphic correlations. It is rather the basin's original compartmentalization and rapid lateral facies changes, together with the effects of Neogene and Quaternary erosion, which render correlations difficult and hinder sequence-stratigraphic interpretation. However, detailed facies analysis of local logs (Appendix 5, Fig. 65) indicates that the Flysch and the Promina Beds jointly show at least two transgressive system tracts (TSTs), two regressive systems tract (RSTs) and one lowstand system tract (LST), with two maximum regression surfaces (MRSs), two maximum flooding surfaces (MFSs), one major and three minor surfaces of forced regression (SFRs) and ten flooding surfaces (FS). Basin-scale correlation of these events is beyond biostratigraphic resolution, and it would be rather pointless to attempt their large-scale correlation in a compartmentalized basin with a highly differential pattern of subsidence and uplift episodes. Only tentative local-scale correlation can be made (Appendix 5, Fig. 65).

The Promina Beds succession in the Korlat-Lisicic area of the basin's outer part (Fig. 15) is divided into five lithostratigraphic units (Fig. 17; Appendix 5, logs in Fig. 65): the Korlat, Gradina, Debelo Brdo, Benkovac Stone and Otavac units. The Korlat Unit is thinning gradually eastwards (see logs PD and DC in Appendix 5, Fig. 65) and also the coeval Gradina Unit is wedge-shaped, showing a regressive to transgressive trend (see the log correlation panel in Appendix 5, Fig. 65). The Korlat Unit in log PD represents the basin's central zone, whereas the same unit in log DC and the Gradina Unit in log GR represent the basin's southeastern margin (see Fig. 16B). The two units in logs DB, BE, KI, BK, OT and ME represent the basin's northeastern margin.

The Korlat and Gradina units are lateral equivalents and their main part is considered to be a RST of Sequence 1. The TST of this sequence is the top part of the underlying Flysch Unit (BABIC & ZUPANIC 2008). The topmost part of the Korlat and Gradina units and the lowest part of the overlying Debelo Brdo Unit are thought to form the TST of Sequence 2. The boundary between Sequences 1 and 2 is a maximum regressive surface (MRS), albeit recognizable only in the Gradina Unit as a sharp boundary between the delta-front and delta-slope facies associations. The TST of Sequence 2 indicates a relatively rapid basin subsidence, which can be attributed to the crustal loading by orogeny and a back-stepping of blind-thrust activity that widened, deepened and merged the Korlat and Ostravica sub-basins (Fig. 16C). The top surfaces of the marly intervals in the lowest part of logs DB and ME are taken to be maximum flooding surfaces (Appendix 5, Fig. 65). The Benkovac Stone Unit and the coeval middle to upper part of the Debelo Brdo Unit are considered to be the RST of Sequence 2. The sharp, erosional boundary between the Benkovac Stone Unit and the overlying Otavac Unit in all outcrop sections is taken to be a surface of forced regression, because the progradation of gravelly mouth bars and foreshore zone was apparently erosive, truncating shoreface and offshore-transitional deposits (Appendix 5, Fig. 64). The Otavac Unit consists of at least three coarsening-upwards cyclothems, which are considered to be parasequences bounded by flooding surfaces and attributed to a series of minor relative sea-level rises. Two of the cyclothems seem to show an erosional unconformity

between mudstones and conglomerates, which may suggest minor forced regressions, but may as well be attributed to a rapid shoreline advance due to extreme river floods combined with powerful storms.

3.3.3. Stop 2/1-1: The Flysch Unit

Outcrop location
In the vicinity of catholic church and cemetery located about 1200 m from the road Benkovac-Smilcic (Fig. 19).

Description
The outcrops show palaeochannels, 2-14 m thick and 60-80 m wide, filled with erosional lenticular packages of fine-to very coarse-grained sandstone beds (Figs. 20, 21). The component beds are lenticular, 5-60 cm thick, showing erosional bases and low-angle truncation surfaces. The beds are internally massive or plane-parallel stratified, mainly non-graded or rarely normal-graded, and commonly amalgamated. Some beds contain stringers of imbricated nummulites, thin granule interlayers, mudclasts or plant debris. Sporadic burrows can be found. Some of the sandstone packages contain lenticular conglomerate intercalations, 0.5-2 m thick, composed of subrounded, moderately sorted granules and fine pebbles with a clast-supported texture. The conglomerates are massive, with sharp non-erosional to slightly erosional bases and common amalgamation (Fig. 22). They consist of limestone clasts (mainly mid-Eocene Foraminifera Limestones) and benthic foraminifera tests (mainly nummulites). Other components include quartz granules, chert fragments and sandstone clasts.
The lenticular packages are underlain and overlain by sheet-like to broadly lenticular sandstone beds, 10-50 cm thick, separated by mudstone beds 10-100 cm thick (Fig. 23). The sandstone beds have erosional bases and are internally massive or plane-parallel stratified, occasionally with a weak normal grading. They also locally contain mudclasts and stringers of imbricated nummulites or small pebbles. Their tops are commonly bioturbated, but burrows occur also within the beds. The sandstone is rich in mollusc shells, larger foraminifera and other skeletal particles. Plant debris is common. The mudstone is rich in planktonic foraminifera and is sporadically intercalated with thin, fine-grained sandstone layers.

Interpretation
The sedimentary facies are thought to have been deposited at the transition from subneritic lower slope to basin floor. The packages of sheet-like to broadly lenticular sandstone beds are deposits of delta-toe lobes, overlain by their feeder channels - frequently filled and rejuvenated. The depositional lobes overlain by feeder channels indicate delta progradation. Babic & Zupanic (2008) interpret the sandstone beds as deposits of catastrophic flood-related hyperpycnal flows, whereas the intervening mudstone beds with thin sandstone intercalations would be deposits of hypopycnal, buoyant deltaic plumes or dilute underflows generated by normal river discharges. The conglomerate beds may be deposits of debris flows derived by

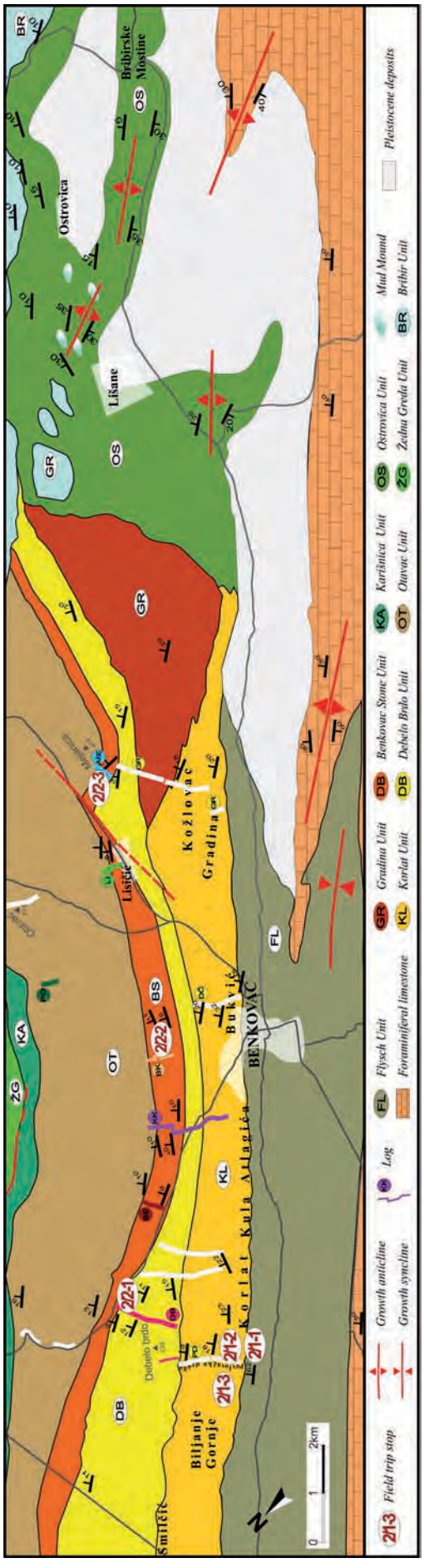

Fig. 17: Lithostratigraphic map of the Korlat-Ostrovica segment of the Dalmatian foreland basin, showing the areal distribution of basin-fill units and the location of field-trip stops 2/1-1 to 2/1-3 and 2/2-1 to 2/2-3 (modified after Pencinger 2012).

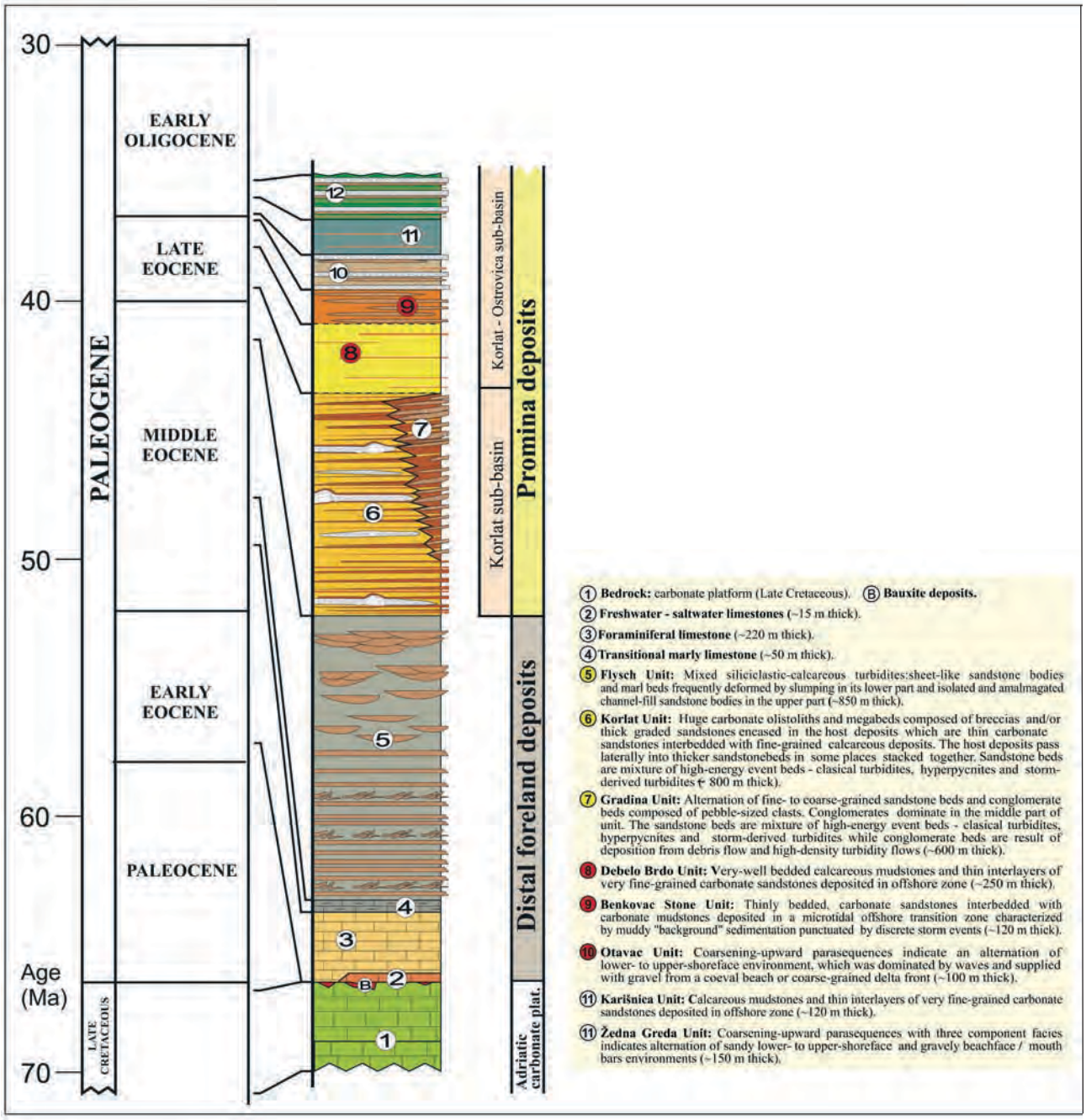

Fig. 18: Lithostratigraphic log of the distal foreland deposits and the lower part of the Promina Beds. The units in the profile pertain to the Korlat-Benkovac area (modified after PENCINGER 2012).

resedimentation of delta shoreline gravel. The lateral scatter of lobes and channels indicates multiple distributaries on the delta plain. The vertical alternation suggests possible minor relative sea-level rises followed by normal (progradational) regression.

3.3.4. Stop 2/1-2: The Korlat Unit near Galici

Outcrop location

Pavlovacka Draga gully near by the hamlet of Galici, ~1.5 km from the road Benkovac-Smilcic (Figs. 15 & 19). A twenty minutes leisurely walking is required.

Description and interpretation

Outcrop of a middle to late Eocene, calciclastic heterolithic succession composed of sheet-like sandstone beds, 3-20 cm thick, alternating with mudstones 5-200 cm thick (Appendix 1, Fig. 51). An isolated megabeds and huge limestone olistolith are visible (see Appendix 5, Fig. 65, thickness interval 180-220 m in log PD).

The sandstone beds have sharp and probably erosional bases, and are non-graded or inversely and/or normally graded. They are wholly massive, wholly planar-parallel stratified or massive to parallel stratified. Some beds show low-angle cross-stratification passing upwards into planar-parallel stratification and to low-angle cross-stratification;

Fig. 19: Satellite image showing the field-trip stops in the Korlat area.

and yet others show planar-parallel stratification with an intervening massive division (Appendix 1, Fig. 53). Most of the sandstone beds can be interpreted as hyperpycnites, products of river flood-generated turbidity currents. Some of the normal-graded beds may be deposits of storm-generated, delta-derived turbidity current surges or represent 'classical' surging flows generated by delta-slope sediment failures.

The 'background' mudstones commonly show silty streaks or more continuous laminae, thin (1-2 cm) siltstone interlayers (non-graded or inversely and/or normally graded) or thin interbeds of very fine-grained sandstone. This facies may represent such processes as: (1) deposition from hypopycnal deltaic plumes; (2) deposition by dilute very low density turbidity underflows generated at normal river discharges; (3) deposition by weak tidal currents; and/or (4) deposition by dilute turbidity currents generated by minor seasonal storms.

The monotonous heterolithic succession represents distal prodelta sediments deposited on an extensive, deep-neritic lower delta slope and basin floor. The main sediment supplier was a fluvially constructed and wave-modified, coarse-grained fan-delta system located between Benkovac and Lisani at the northeastern margin of the basin (see Fig. 16B).

The succession contains an isolated irregularly-shaped block, ~65 m long and >18 m thick, derived from the early to middle Eocene Foraminifera Limestones (Appendix 1, Fig. 55; see olistolith marked with number 3 in Appendix 1, Fig. 54. There is also a calciclastic megabed ~3 m thick (Appendix 1, Fig. 56; see also Appendix 5, Fig. 65, thickness interval 180-220 m in log PD). The megabed is bipartite, comprising a lower debritic division (0.5 m) and an upper turbiditic division (2.5 m) thick high density turbidite in the upper part. The debrite division has a matrix- to clast-supported texture and consists of unsorted, angular to subangular limestone clasts, 2-40 cm in size, derived mainly from the same Foraminifera Limestones. Matrix is composed of granules and medium- to very coarse-grained sand of similar provenance. The turbidite division is characterized by a well-developed grading from a mixture of limestone granules, coarse sand and small rip-up clasts at the base to silty mud at the top. The deposition of the megabed is attributed to a debris flow accompanied by a 'co-genetic' high-density turbidity current. Parallel to its depositional strike, the megabed can be followed laterally to olistolith 4 at the adjacent Stop

Fig. 20: A portion of channel-fill composed of three lenticular sandstone packages separated by low-angle truncation surfaces (yellow lines). The scale is 100 cm.

Fig. 21: Lenticular packages of plane-parallel stratified sandstone beds. The beds are lenticular, with erosional bases and low-angle truncation surfaces. The scale is 70 cm.

2/1-3 (Fig. 19). The emplacement of isolated olistoliths is attributed rockslide process, with the block gliding on a lubricating cushion of water-saturated seafloor mud.

3.3.5. Stop 2/1-3: The Korlat Unit near Basici

Outcrop location
In the vicinity of the hamlet of Basici, ~500 m from Stop 2/1-2 (Fig. 19).

Description and interpretation
The outcrop shows a large oblate olistolith (see number 4 in Fig. 55 in Appendix 1), 60 m long and 20 m high, in the Korlat Unit. The block was derived from the early to middle Eocene Foraminifera Limestones. The azimuth of the block's long axis is ~40° and the bedding attitude of the host deposits is 40/20°. The heterolithic deposits are strongly contorted in front of the northeastern edge of the olistolith but undisturbed at its southwestern edge (Appendix 1, Figs. 57, 58), which indicates the block's ploughing movement towards the NE.
The outcrop thus sheds more light on the provenance of the megabed and olistoliths in the Korlat Unit. The emplacement of olistolith 4 from the SW was coeval with the emplacement of other olistoliths (numbered 1-7 in Appendix 1, Fig. 54) and deposition of megabed A (Fig. 54). Their scattering along the depositional strike indicates gravitational failures of a limestone cliff and associated sedimentary slope, perhaps triggered high-magnitude seismic shock. This source area is thought to have been

Fig. 22: Lenticular beds of massive, clast-supported conglomerate stacked upon one another (amalgamated); the dashed line indicates bed boundary. Contact with underlying coarse-grained sandstones is sharp, non-erosional to slightly erosional. Note the high bed-dip angle (~60°).

Fig. 23: Sheet-like to broadly lenticular sandstone beds, 30-50 cm thick, separated by mudstone beds 20-80 cm thick. The mudstone surfaces are covered by their weathering products. The arrow in the upper right-hand part indicates a palaeochannel filled with lenticular sandstone packages.

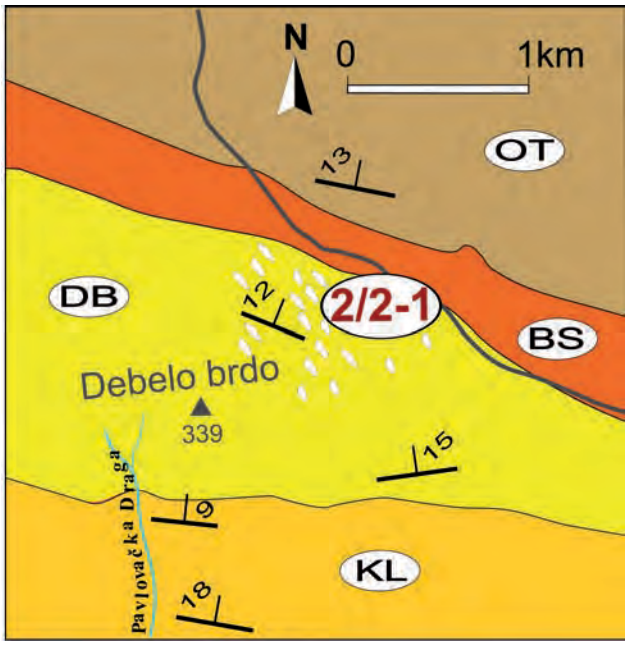

Fig. 24: Lithostratigraphic map showing the areal distribution of the basin-fill units in Debelo Brdo area and location of Stop 2/2-1.

the hinge-zone of thrust-cut growth anticline that defined the piggyback basin's outer, southwestern margin (Fig. 16B).

3.3.6. Stop 2/2-1: The Debelo Brdo Unit

Outcrop location
The outcrop is on the left-hand side of the road from Obrovac to Benkovac, in the area of Debelo Brdo hill (Figs. 15 & 24).

Description and interpretation
The numerous small quarries in the uppermost part of the Debelo Brdo Unit (see Appendix 5, log DB in Fig. 65) show an offshore facies succession which is distal palaeogeographic equivalent of the sandy Benkovac Stone Unit (subsequent Stops 2/2-2, 2/2-3). The deposits are mudstones intercalated with very thin siltstone and fine-grained sandstone beds, considered to be distal-most tempestites spread by sporadic most violent storms. The platy splitting of mudstone and sandstone beds offers a good opportunity to study the assemblage of trace fossils.

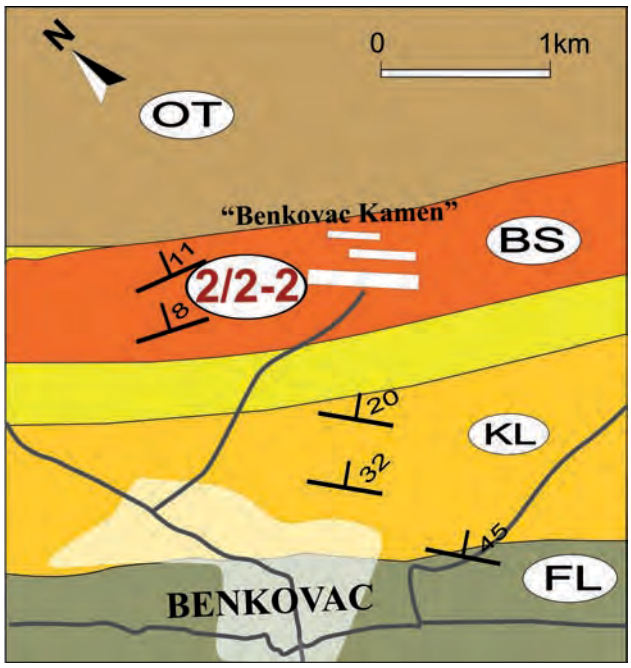

Fig. 25: Lithostratigraphic map showing the areal distribution of the basin-fill units and location of "Benkovacki Kamen" quarry.

3.3.7. Stop 2/2-2: The Benkovac Stone Unit in Benkovacki Kamen quarry

Outcrop location
The Benkovacki Kamen quarry is located ~2 km northeast of the town of Benkovac (Figs. 15, 25).

Description and interpretation
Three long outcrops parallel to the bedding strike afford a good insight into the sedimentary characteristics of the Benkovac Stone Unit (Fig. 26). The platy splitting of sandstone beds exposes large surfaces showing a wide range of trace fossils on bed soles and a range of wave ripples on bed tops (Fig. 27). Post-depositional structures include sand volcanoes and dykes of various sizes and forms.
The sedimentological and ichnological characteristics of the Benkovac Stone Unit are described in more detail in Appendix 3.

3.3.8. Stop 2/2-3: The Benkovac Stone Unit near Lisicic

Outcrop location
The Mejanica hill near the village of Lisicic (Figs. 17, 28); a 15-minute walk is required.

Description and interpretation
Due to illegal 'wild' excavation of the platy sandstone for building purpose, the Mejanica hill resembles a giant mole-hill. The randomly located excavation pits a 3D insight into the sedimentary facies of the Benkovac Stone Unit (Fig. 29; see Appendix 3, Fig. 59). In addition, many large bedding surfaces offer a trace-fossil 'El Dorado' to an ichnologist (Appendix 3, Figs. 61, 62). The succession of thinly bedded, planar parallel-stratified and wave-ripple cross-laminated sandstones intercalated with mudstones is interpreted as shoreface to offshore-transition deposits of a wave dominated shoreline. This means littoral to shallowly sublittoral environment. However, the trace-fossil assemblage includes ichnospecies that are widely considered to be characteristic of deep-water environments.
The sedimentological and ichnological characteristics of the Benkovac Stone Unit are described in more detail in Appendix 3.

Fig. 26: A modern technology in the Benkovacki Kamen quarry enables making long vertical walls and exposing large bed surfaces.

3.4. The medial to proximal part of the Promina Basin: other representative deposits of the Promina Beds

3.4.1. Palaeogeographic background

In the middle to late Eocene simultaneously with establishing of the outer limit of the piggyback basin, a synclinal swale in the medial part of the Promina basin located westsouthwest from Drnis town gradually developed into relatively deep and narrow synclinal trough referred to as the Cikola sub-basin (The Cikola sub-basin is named after a small, Cikola Canyon River) (see Figs. 15, 16B, 16C).

A coarse-grained fan-delta slope system fed by the antecedent braided rivers was formed on the steeply inclined north-eastern limb. Frequent resedimentation pulses as consequences of a high sedimentation rate and continued subsidence of the syncline followed by seismic activities formed about 800 m thick slope apron succession composed of cohesive and cohesionless debris-flow deposits and high-density to low-density turbidity flow-deposits (see log CI1, Fig. 37). Sedimentation on the opposite, less steeply inclined synclinal limb was under influence of shallow shelf processes without fluvial inputs. This considerably thinner, about 150 thick succession is composed of sandy shoreface and muddy offshore deposits. Only top of the succession contains coarse-grained beach

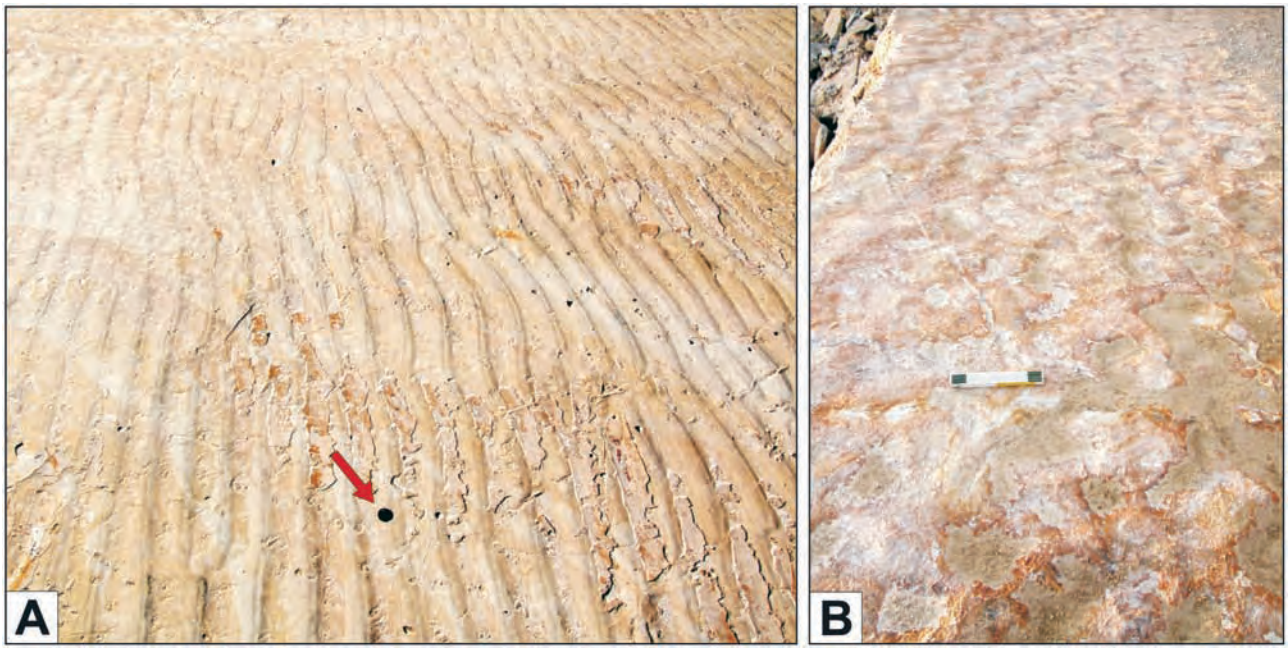

Fig. 27: Sedimentary structures nicely revealed on the upper bed surfaces. (A) Small double-crested wave ripples in subfacies 5a; ripple migration is towards the right. The coin is 2.6 cm. **(B)** 'Micro-hummocky' structures in subfacies 2a. The scale is 22 cm.

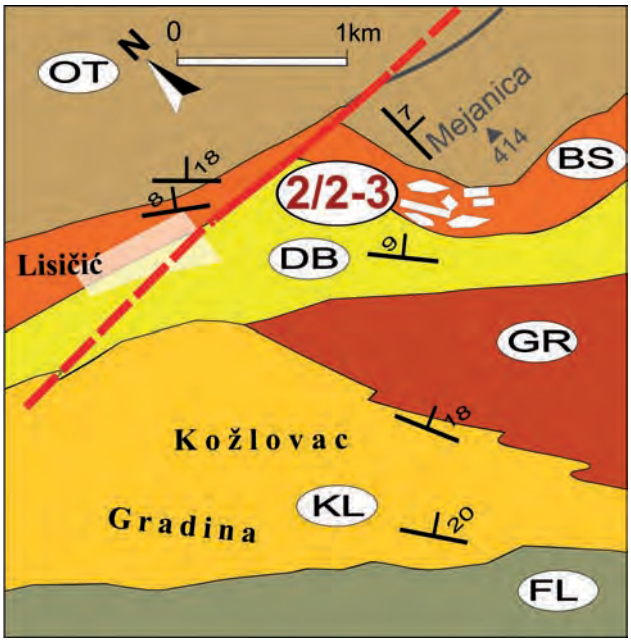

Fig. 28: Lithostratigraphic map showing the areal distribution of the basin-fill and numerous illegal excavation pits in the Lisicic area.

Fig. 29: The light-brown to grey sandstones can be readily distinguishable from the pale yellowish-grey mudstones. Note thick sandstone beds of facies S1 in the middle of succession. The thinner sandstone beds of facies S2 and S5 interbedded with mudstone beds of facies M dominate in this succession. The scale is 2 m.

deposits (see log CI2, Fig. 40). A similar sedimentary dynamic probably proceeded in the early Oligocene.

The Cikola synclinal basin-fill deposits is an instructive example of contrasting facies successions on the opposite limbs of a growing syncline, with the forced regression on one limb possibly corresponding to a transgression on the other limb, or vice versa, in the case of non-synchronous thrusting (Fig. 30).

In the Oligocene, the soling thrust system uplifted the piggyback basin sufficiently to isolate it completely from the shallowing foredeep basin (Fig. 16D). The alluvial and fluvio-deltaic systems advancing from the mountain belt prograded into a terminal lake zone. The latest Promina beds are thus entirely composed of terrestrial sediments deposited in an alluvial system (merged alluvial fans, fan-toe braidplain, fan-toe braidplain deltas and lakes) (see, Fig. 16D) with generally the south-westward palaeocurrent pattern. Only locally (Stop 3/2-1), topographic ridges (blind-thrust growth anticlines) confined and redirected stream flows subparallel to the mountain front (Figs. 16D and 48).

The proximal alluvial facies association crop out along the northeast basin margin. It includes massive, sheet-like conglomerates deposited from cohesive and cohesionless debris flow, sheetflood and braided streams implying the presence of relatively steep gradients. The distal alluvial deposits were subsequently eroded so thus distal alluvial fan environment, fan deltas and terminal lake illustrated in Fig. 16D are inferred and hypothetical.

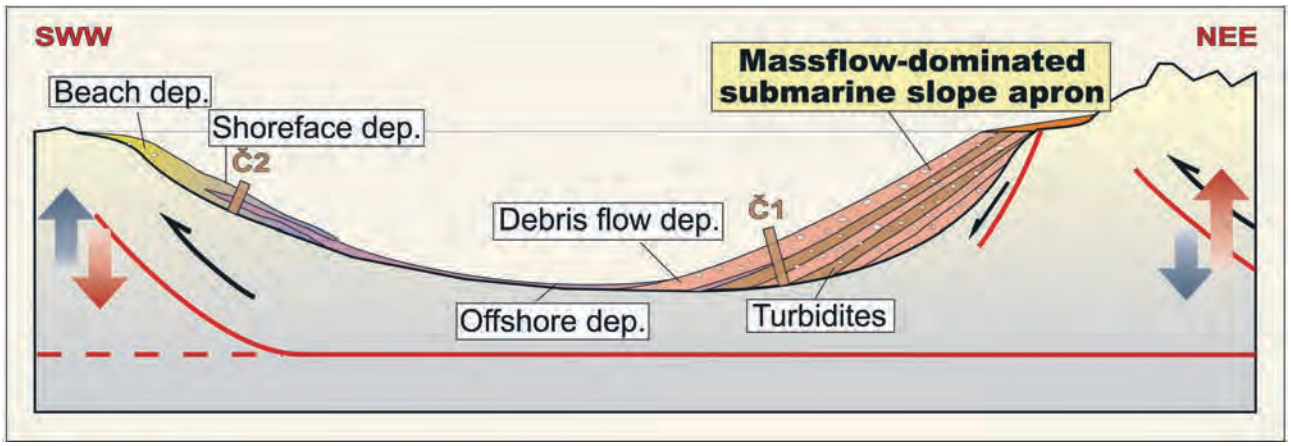

Fig. 30: Schematic cross-section from the Cikola Canyon, with contrasting facies successions deposited on the opposite limbs of a growth syncline (see logs C1 and C2). Synchronous thrusting caused coeval transgressions on both limbs. A non-synchronous, out-of-phase thrusting caused an uplift and forced regression on one limb coeval with a subsidence and transgression on the other limb.

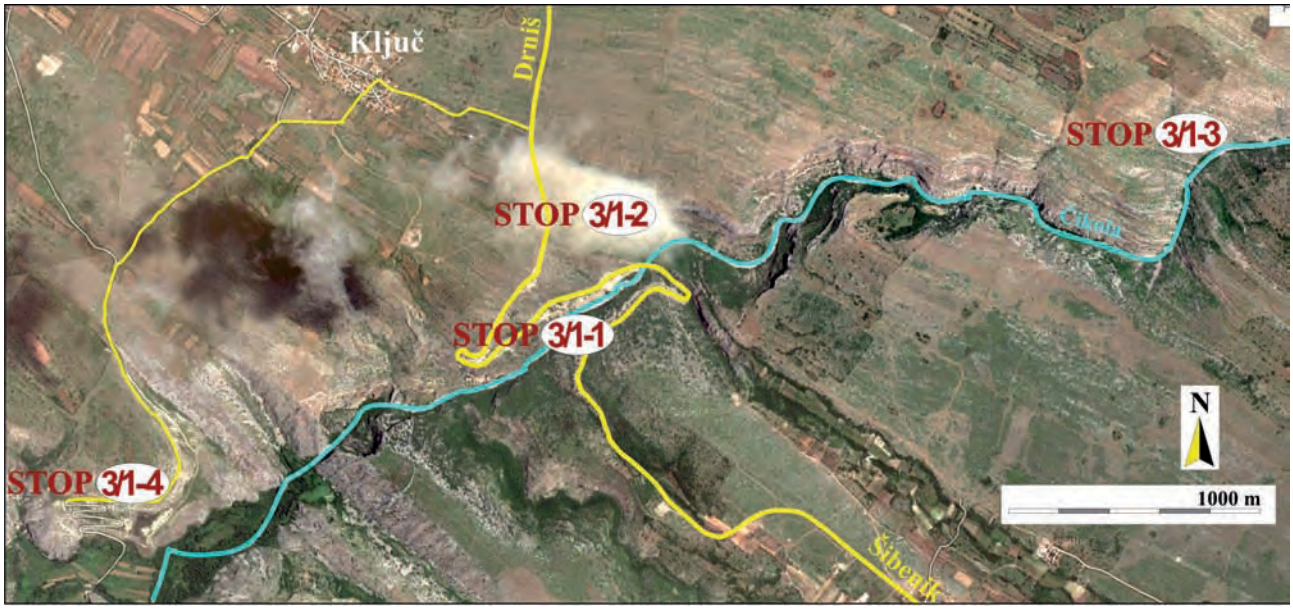

Fig. 31: Satellite image showing the field-trip stops in the Cikola Canyon area.

3.4.2. Stop 3/1-1: Panoramic view of the Cikola Canyon

Location

The lay-by alongside with the road Sibenik-Drnis offers a spectacular panoramic view of Cikola Canyon and an excellent opportunity to see an initial stage of foreland basin formation (Figs. 15, 31 and 32A).

Description and interpretation

Panoramic view of the medial part of the Cikola growth syncline (see Fig. 32B) showing the late Cretaceous limestones belonging to the Adriatic Carbonate Platform unconformably overlain by the middle Eocene Foraminifera Limestones. Initial subneritic Promina Beds conformably overlay Foraminifera Limestones. About 200 m thick the Foraminifera Limestones denotes beginning of subsidence caused by the orogenic crustal loading. The Transitional Beds are only present on the south-western synclinal limb (Stop 3/1-4, Fig. 32D) where conformably overlays the Foraminifera Limestones. The late Cretaceous limestones on the north-western limb are unconformably (angular unconformity) overlain by the slope apron Promina Beds (Fig. 32D). Progressive unconformities are noticed in the Promina Beds on the both synclinal limbs. The progressive unconformity with the rotative offlap on the north-western limb and the progressive unconformity with the rotative onlap on the limb of opposite side indicate variable rate of blind-thrusts uplifting (Figs. 32C, 32D). Note a low angular unconformity (3-4°) between the initial subneritic Promina Beds and the Transitional Marls on the southwestern limb (Stop 3/1-4, Fig. 32D).

3.4.3. Stop 3/1-2: The pre-thrusting Promina Beds deposited in axial zone of the growth syncline

Outcrop location

A steep wall of Cikola Canyon located about 400 m from the Sibenik-Drnis road (see Figs. 15, 31, 33).

Description and interpretation

About 100 m thick succession is composed of the initial (pre-thrusting) fine-grained subneritic sediments in the first 30 m. The upper part of succession are sediments of shoreface, offshore-transitional and offshore environments (Figs. 34, 35). For more detailed facies description see Fig. 36. Episodes of normal (progradational) regression in response to the limb subsidence characterise this part of succession (see Log C1 in Fig. 37, thickness interval 80-93 m). The top part of succession (thickness interval 80-93 m) contains cohesive debris- flow deposits, erosionally stacked deposits of high-density to low-density turbidity currents and "background" offshore deposits. This resedimentation pulses of shoreface to foreshore deposits

Fig. 32: A cross-section of the Cikola growth syncline with detailed figures showing progressive unconformities. **(A)** The Cikola growth syncline showing the late Cretaceous limestones unconformably overlain by the middle Eocene Foraminifera Limestones and progressive unconformities on the both limbs of the growth synclinal. **(B)** The late Cretaceous limestones are unconformably overlain by the middle Eocene Foraminifera Limestones. Initial Promina Beds conformably overlay Foraminifera Limestones. **(C)** The northwestward synclinal limb with clearly visible progressive unconformity between slope apron beds. Note an erosive angular unconformity between the Promina Beds and the late Cretaceous limestones. **(D)** The southwestward synclinal limb with a progressive unconformity between neritic Promina beds related to the synclinal growth and with low angular unconformity (3-4°) between pre-thrusting subneritic deposits and the Transitional Marls.

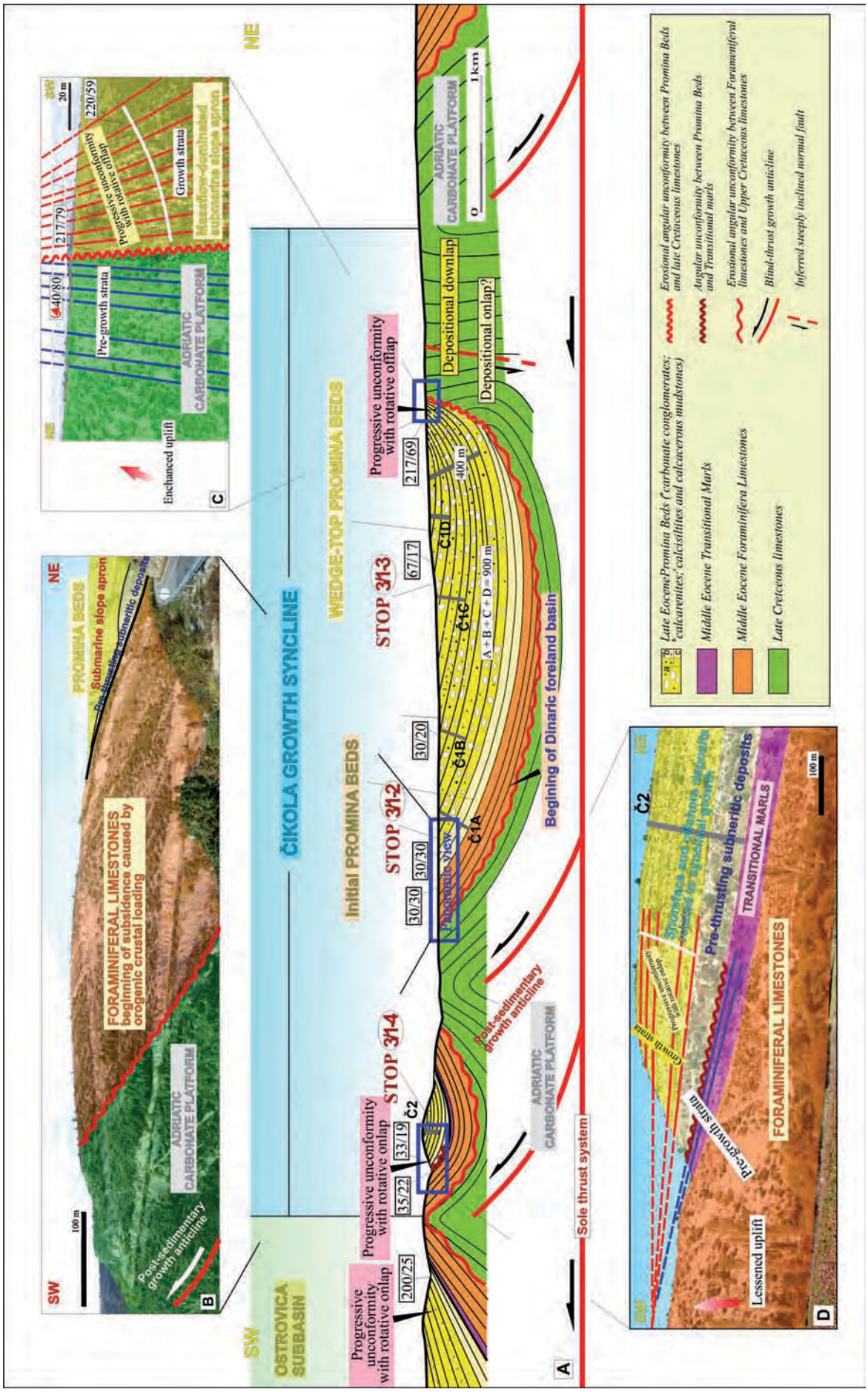
ČIKOLA GROWTH SYNCLINE
WEDGE-TOP PROMINA BEDS
Initial PROMINA BEDS
Begining of Dinaric foreland basin
Sole thrust system
OSTROVICA SUBBASIN
ADRIATIC CARBONATE PLATFORM
Progressive unconformity with rotative onlap
Progressive unconformity with rotative offlap
Depositional downlap
Depositional onlap?
Post-sedimentary growth anticline
STOP 3\1-4
STOP 3\1-2
STOP 3\1-3
Panoramic view
Č1A
Č1B
Č1C
Č1D
Č2
A+B+C+D = 900 m
400 m
1 km
Late EocenePromina Beds (*carbonate conglomerates; °calcarenites; ^calcisiltites and calcareous mudstones)
Middle Eocene Transitional Marls
Middle Eocene Foraminifera Limestones
Late Cretceous limestones
Erosional angular unconformity between Promina Beds and late Cretaceous limestones
Angular unconformity between Promina Beds and Transitional marls
Erosional angular unconformity between Foraminiferal limestones and Upper Cretaceous limestones
Blind-thrust growth anticline
Inferred steeply inclined normal fault
PROMINA BEDS
Submarine slope apron
FORAMINIFERAL LIMESTONES beginning of subsidence caused by orogenic crustal loading
Post-sedimentary growth anticline
Enchanced uplift
Pre-growth strata
Growth strata
Mass-flow-dominated submarine slope apron
Pre-growth strata
TRANSITIONAL MARLS
FORAMINIFERAL LIMESTONES
Lessened uplift
A
B
C
D

Fig. 33: A fabulous panoramic view of the Promina Beds in the Cikola Canyon.

signal limb steepening before normal faulting on the northeastward synclinal limb.

3.4.4. Stop 3/1-3. The slope apron Promina Beds deposited on the northwestern limb

Outcrop location
On the edge of the Canyon wall. A twenty minutes walking is required (Fig. 31).

Description and interpretation
Outcrops of massflow-dominated subneritic slope apron deposited on the northeastward limb of the growth syncline (see Log C1 in Fig. 37, thickness interval 320-360 m). Lenticular or sheet-like cohesive and cohesionless debris-flow conglomerates are commonly amalgamated or capped by turbidites. The high-density to low-density turbidity flow deposits are commonly stacked erosionally upon one another or capping debris-flow conglomerates (Figs. 38, 39). For more detailed facies description see Fig. 36. The sediment gravity-flow deposits are resedimentation pulses which indicate continued subsidence of syncline. The conglomerates mostly contain carbonate clasts (> 90% vol.). The most carbonate clasts are the Foraminiferal and the late Cretaceous limestones and fewer clasts of the late Jurassic age. Very rare non-carbonate clasts are various sandstones, cherts and marls.

Fig. 34: Fine- to very fine-grained sandstones bed with dome-shaped 3D ripples ("micro-hummocks") represents a tractional deposition of sand as 3D vortex ripples generated by oscillatory waves or as 3D ripples of storm-generated combined-flow currents. The scale is 22 cm.

Fig. 35: Massive calcareous mudstone beds with thin streaks, normal-graded interlaminae and lenses (pinch-and-swell laminae) of silt or very fine-grained sand. The mudstone was deposited by fallout of hemipelagic "background" suspension below the storm wave base The silt and sand interlaminae may represent a weak action of waves or tidal currents and possibly offshore excursions of highly dilute, storm-generated turbidity currents.

3.4.5. Stop 3/1-4: The subneritic and neritic Promina Beds deposited on the southwestern limb

Outcrop location
Long outcrop alongside a local macadam road in the Cikola Canyon. A thirty minutes walking is required (Figs. 31, 32D).

Description and interpretation
Sedimentary succession deposited on the southwestward limb of the growth syncline (see log C2, Fig. 40 and Fig. 36 for facies description). The most part of the succession is composed of shoreface and offshore deposits (Fig. 41). The first 39 m of succession is composed of pre-thrusting, subneritic massive marly mudstones. Several normal-regressive parasequences and forced-regressive episodes indicate slowdowns and the temporary breaks (see log C2 in Fig. 40, thickness interval 39-80 m and 109-151 m). Continued subsidence and signs of slope instability (Fig. 42) indicate the continued fold growth (thickness interval 39-109 m). Beach conglomerates on top of the succession mean an abrupt shallowing.

Fig. 36: Facies legend to log C1 and log C2 with detailed facies description.

3.4.6. Stop 3/2-1: Alluvial deposits in Karamarkusa open-pit bauxite mine

Outcrop location

The abandoned, about 300 m long open-pit bauxite mine near the road Obrovac-Benkovac (Fig. 43).

Description and interpretation

The lower part of about 50 m thick alluvial succession is composed of debris-flow and sheetflood conglomerates (see log KA in Figs. 44 and 45 for more detailed facies description). Thin overbank deposits (sandstone and marly mudstone beds) are present in the top of the lower part. The upper part, more than 15 m thick stream-flow channel-fill conglomerates erosively overlays the overbank deposits (Figs. 44B, 46). The bauxite deposits hosted by weathered late Cretaceous limestones overlain by thin fine-grained overbank deposits and thin sheetflood conglomerates are sporadically visible in the base of succession (Figs. 44, 47).

Conglomerates are composed of carbonate clasts (about 60 vol. %) and non-carbonate clasts. The most carbonate clasts are various limestones of the Palaeogene age while the clasts of Cretaceous and Jurassic age are considerably less present. Non-carbonate clasts are various sandstones, cherts, marls and coal fragments. The pebble- to cobble-sized clasts are subangular to subrounded. The sandstones are very fine- to medium-grained calcarenites, sporadically coarse to very coarse-grained, and consist mainly of various sparitic and micritic grains. Quartz grains are subordinate (less than 5 vol. %). The sand grains are subrounded to rounded and generally well to very well sorted, forming a

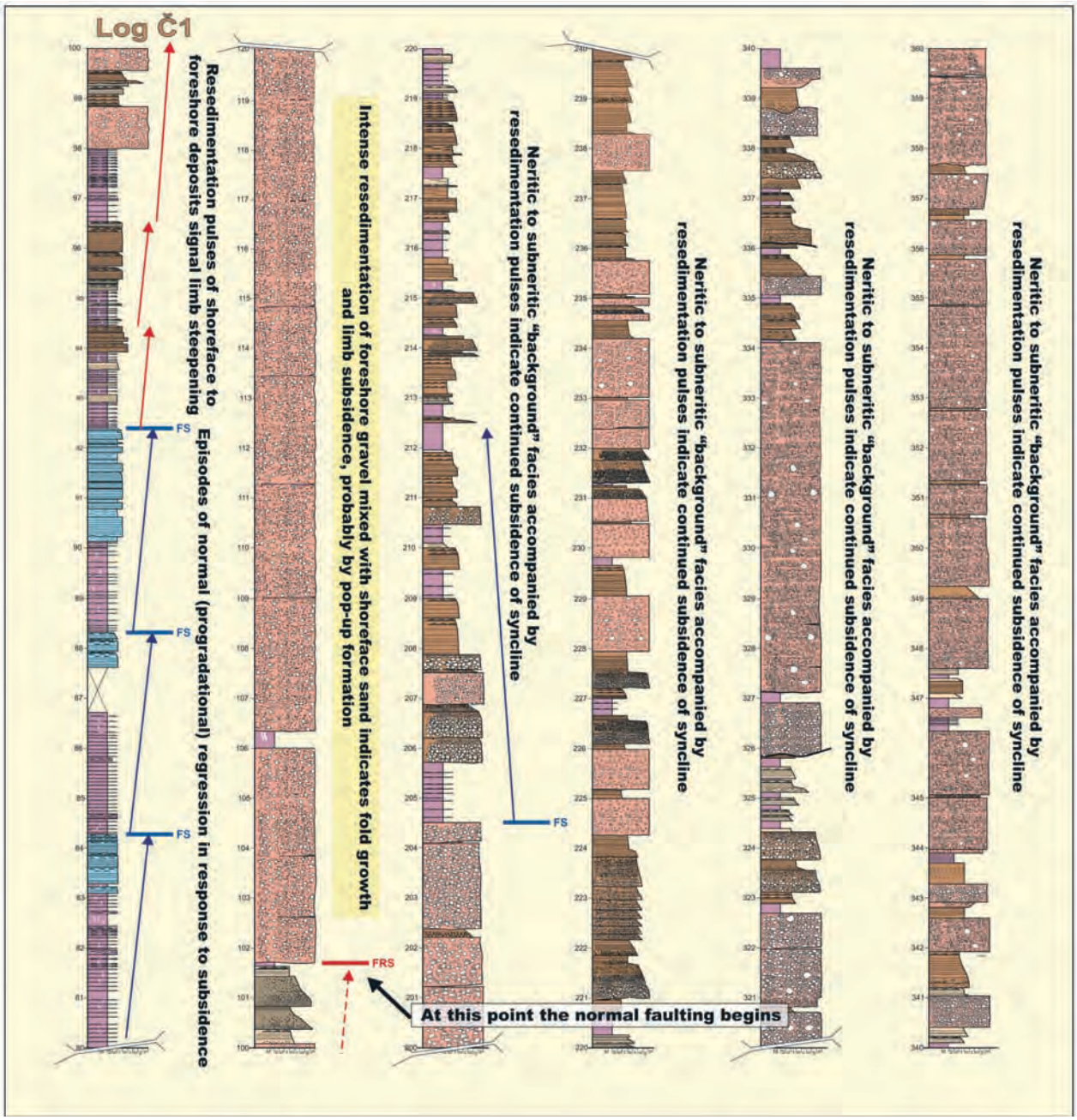

Fig. 37: Outcrop log C1, showing the component facies assemblages, normal-regressive parasequences and forced-regressive episodes.

Fig. 38: Typical appearance of the subneritic slope apron deposits in the Cikola Canyon. Sheet-like, 60-120 cm thick, matrix-supported conglomerates composed of subrounded to rounded clasts of mainly pebble to cobble size were deposited from the cohesive debris-flow. The conglomerate beds are amalgamated (the lowest part of photo) or capped by a sheet-like, 20-40 cm thick turbidites composed of fine pebble gravel to fine-grained sand (Tabc turbidites) or medium to very fine sand (Tbc turbidites) deposited from high-density to low-density turbidity currents. The scale is 2 m.

Fig. 39: Bed surface of unsorted, matrix-supported conglomerates composed of subangular to subrounded clasts of pebble to boulder size and sand- to granule size matrix. Maximum clast size is of about 80 cm. Example of cohesive debris-flow deposits. The scale is 12 cm.

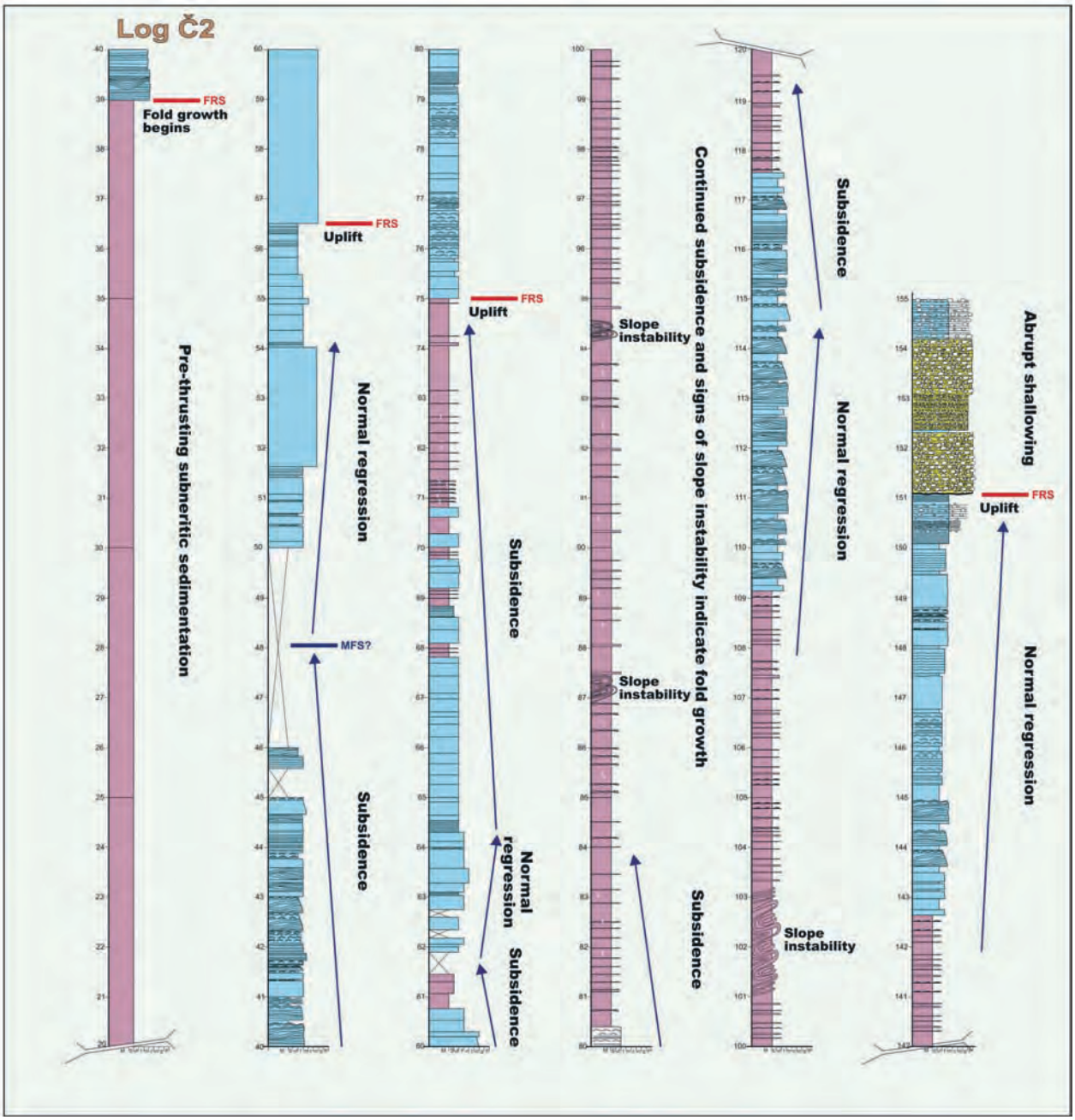

Fig. 40: Outcrop log C2, showing the component facies assemblages, normal-regressive parasequences and forced-regressive episodes.

Fig. 41: Massive calcareous mudstone beds with thin, normal-graded interlaminae and lenses of silt or very fine-grained sand deposited below the storm wave base is a dominated facies in the outcrop alongside the local macadam road in the Cikola Canyon. The scale is 12 cm.

grain-supported framework. Interstitial spaces are filled with a microcrystalline carbonate cement and/or fine-grained calcareous sediment. The mudstones are clayey micrites with scattered silt-sized carbonate and quartz grains.

Coalescent alluvial fans were formed parallel to the new mountain front on the older, probably middle to late Eocene fluvial Promina Beds (see erosive angular unconformity in Fig. 47). A local growth anticline in the vicinity of Obrovac confined and redirected stream flows to the west (consequent river system) (Fig. 48). The evidence of syndepositional tectonic deformation are progressive unconformity noticed between debris-flow and stream-flow beds and a syndepositional normal fault (Fig. 44C). The source area was uplifted and to weather exposed the middle to late Eocene Promina Beds and the late Cretaceous limestones.

Fig. 42: A small-scale slump showing contorted silt-laminated mudstone beds. The thickness of the slump unit between undisturbed silt- laminated mudstone beds is about 40 cm. Slope instability is an indication of the fold growth. The scale is 12 cm.

Fig. 43: Topographic map showing location of Stop 3/2-1.

3.4.7. Stop 3/2-2: Alluvial deposits in Bukovica area

Outcrop location

The road-cut on the right-hand side of the local road from Obrovac to Kistanje in the vicinity of the Greljevac hill (Fig. 49).

Description and interpretation

About 200 m long outcrop composed of sheetflood deposits Fig. 50). The sheetflood deposits are 30-130 cm thick "bipartite" beds with the lower part composed of pebble- and rare cobble-sized clasts while the upper part are planar parallel- stratified or massive granule sandstones or coarse to medium sandstones. The beds have a sheetlike geometry with lateral continuity of up to 20 m. The other, less present sheetflood beds consists of commonly thicker, undulatory to planar parallel-stratified sandy part. Clasts and granules are subangular to subrounded, moderately sorted and clast-supported with very poor sandy matrix. The beds have sharp, irregular to undulatory erosive bases. Conglomerates mostly contain carbonate clasts (about 90% vol). Most carbonate clasts, as well as in the Stop 3/2-1 are various limestones of the Palaeogene age. The rare non-carbonate clasts are various sandstones and cherts.

Sheetflood couplets have been deposited under a supercritical turbulent flow conditions due to the effect of the relatively high slope (about 3-5°) of the fan surface. Under these upper flow regimes cobbles and most of pebbles were carried as a bed load whereas finer pebbles and granules were in suspension along with sand and finer sediments. Standing waves intermittently forming in flow, created antidune bedforms in the gravel bedload but they were usually washed out as the standing waves broke down. The sheetflood deposits created during one flood event were hundreds of metres wide stretching from apex to the toe of the alluvial fan where they merged with sheetflood deposits of the neighbouring alluvial fans With continued lowering of alluvial slope gradient (in distal direction) thin, supercritical sheet-flows changed to thicker, subcritical stream flows (hydraulic jump). These modified fluidal flows could remould coarse-grained braidplain accumulations created by perennial, channelized streamflow in periods between sheetflood episodes (Figs. 48, 16D) (MRINJEK 1993a, 1993b, 1994).

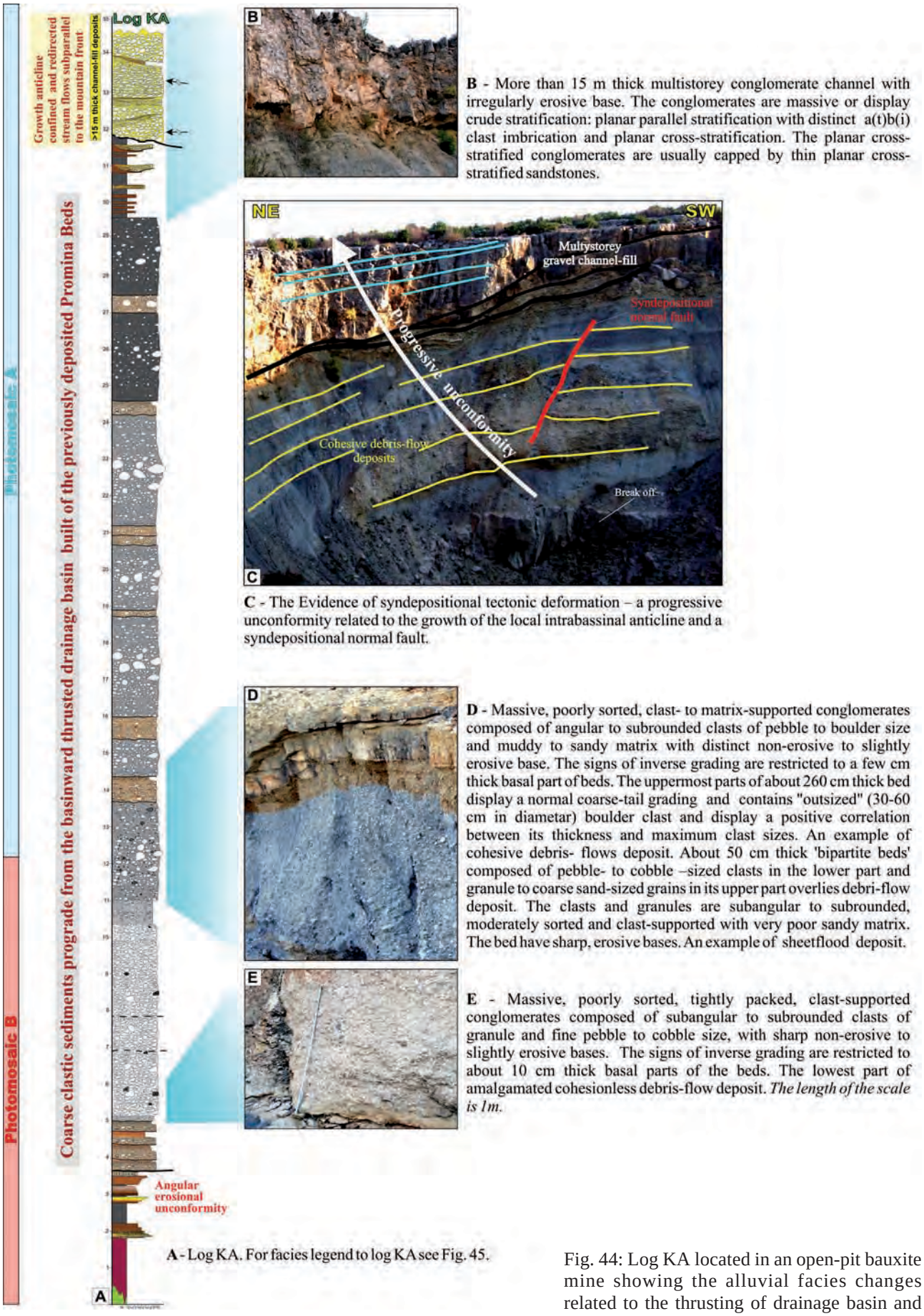

B - More than 15 m thick multistorey conglomerate channel with irregularly erosive base. The conglomerates are massive or display crude stratification: planar parallel stratification with distinct a(t)b(i) clast imbrication and planar cross-stratification. The planar cross-stratified conglomerates are usually capped by thin planar cross-stratified sandstones.

C - The Evidence of syndepositional tectonic deformation – a progressive unconformity related to the growth of the local intrabassinal anticline and a syndepositional normal fault.

D - Massive, poorly sorted, clast- to matrix-supported conglomerates composed of angular to subrounded clasts of pebble to boulder size and muddy to sandy matrix with distinct non-erosive to slightly erosive base. The signs of inverse grading are restricted to a few cm thick basal part of beds. The uppermost parts of about 260 cm thick bed display a normal coarse-tail grading and contains "outsized" (30-60 cm in diametar) boulder clast and display a positive correlation between its thickness and maximum clast sizes. An example of cohesive debris- flows deposit. About 50 cm thick 'bipartite beds' composed of pebble- to cobble –sized clasts in the lower part and granule to coarse sand-sized grains in its upper part overlies debri-flow deposit. The clasts and granules are subangular to subrounded, moderately sorted and clast-supported with very poor sandy matrix. The bed have sharp, erosive bases. An example of sheetflood deposit.

E - Massive, poorly sorted, tightly packed, clast-supported conglomerates composed of subangular to subrounded clasts of granule and fine pebble to cobble size, with sharp non-erosive to slightly erosive bases. The signs of inverse grading are restricted to about 10 cm thick basal parts of the beds. The lowest part of amalgamated cohesionless debris-flow deposit. *The length of the scale is 1m.*

A - Log KA. For facies legend to log KA see Fig. 45.

Fig. 44: Log KA located in an open-pit bauxite mine showing the alluvial facies changes related to the thrusting of drainage basin and the growth of a local intrabasinal anticline.

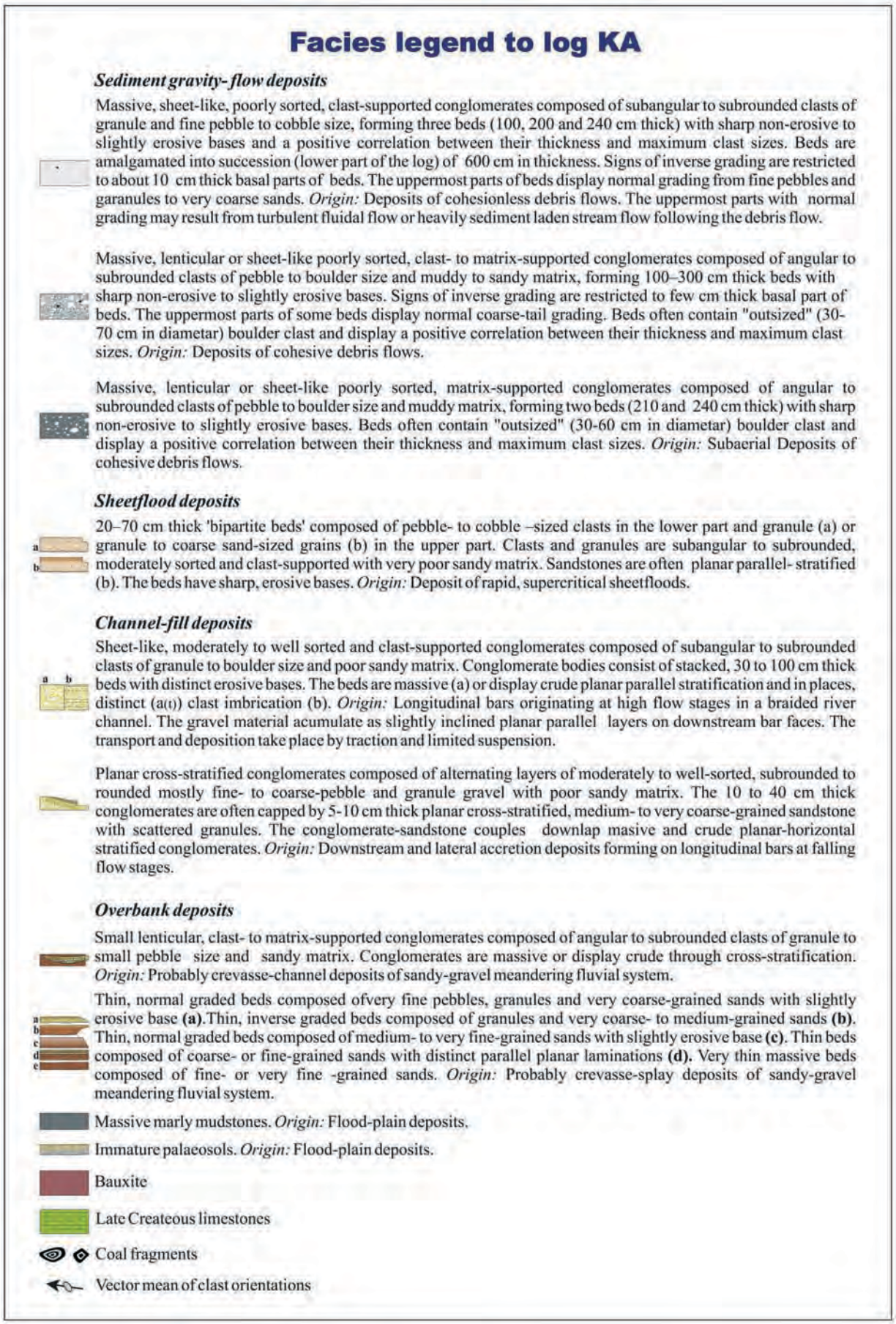

Fig. 45: Facies legend to log KA with detailed alluvial facies description.

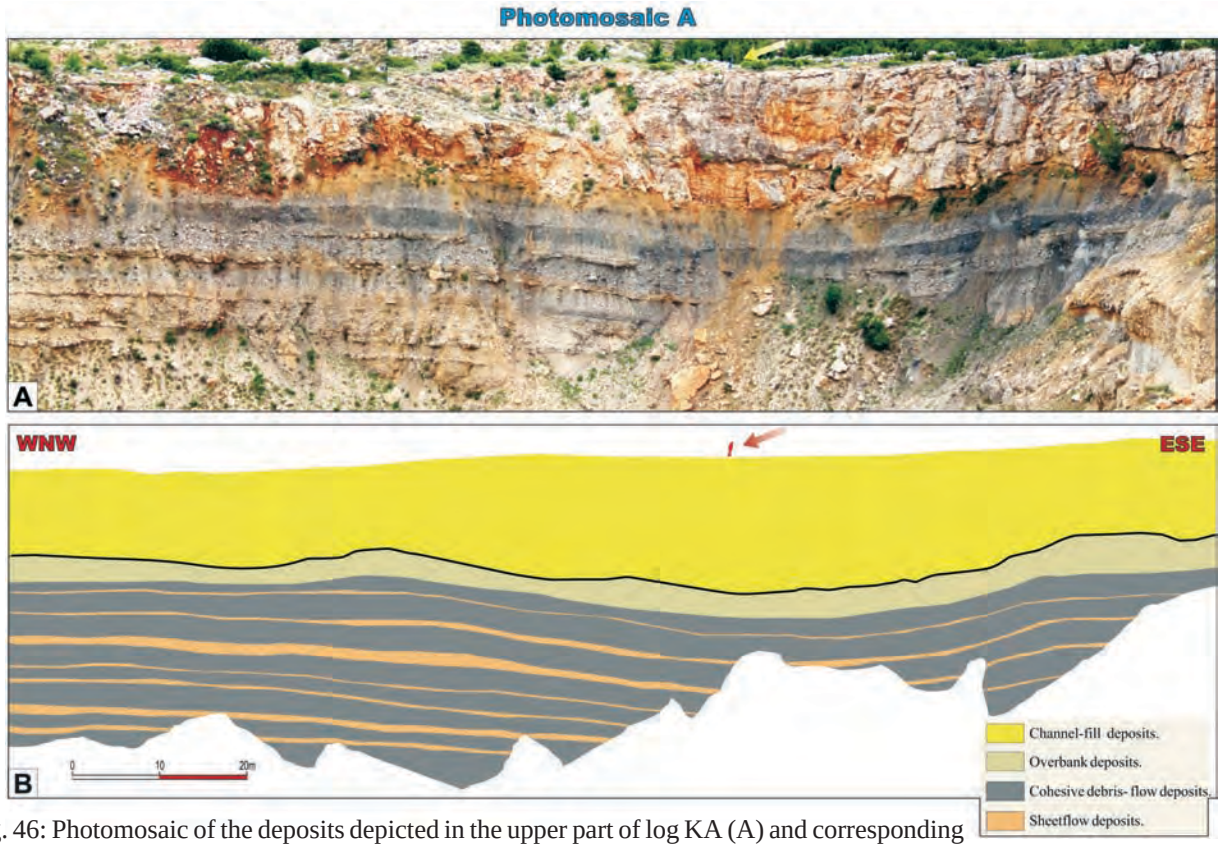

Fig. 46: Photomosaic of the deposits depicted in the upper part of log KA (A) and corresponding sketch (B), show the sheet-like beds of debris-flow and the sheetflood deposits capped by multistorey gravel channel-fill.

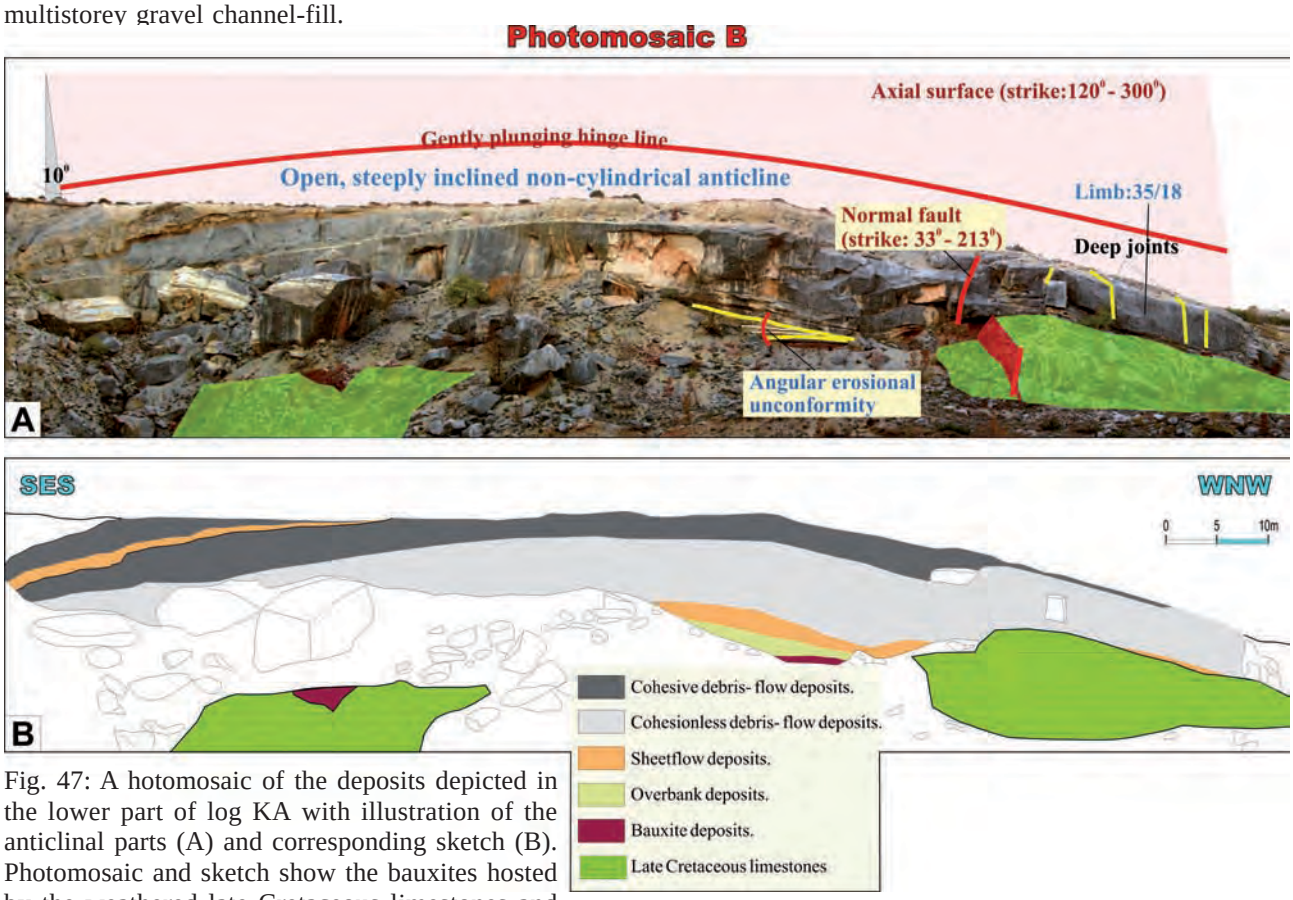

Fig. 47: A hotomosaic of the deposits depicted in the lower part of log KA with illustration of the anticlinal parts (A) and corresponding sketch (B). Photomosaic and sketch show the bauxites hosted by the weathered late Cretaceous limestones and overlying debris-flow and sheetflood deposits. The Karamarkusa open-pit bauxite mine is located in the hinge zone of the local growth anticline.

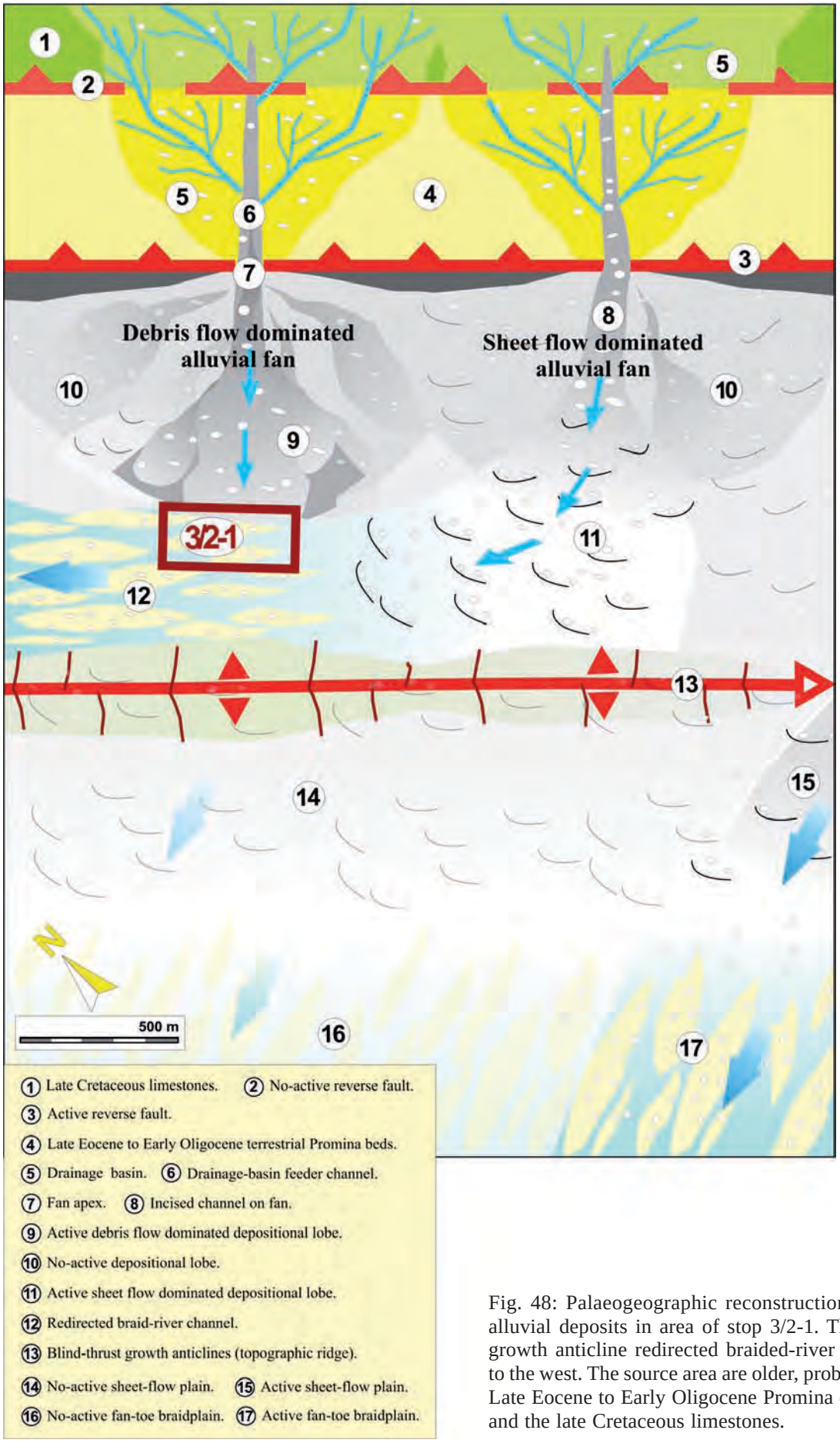

Fig. 48: Palaeogeographic reconstruction of the alluvial deposits in area of stop 3/2-1. The local growth anticline redirected braided-river channel to the west. The source area are older, probably the Late Eocene to Early Oligocene Promina deposits and the late Cretaceous limestones.

Fig. 49: Topographic map showing location of Stop 3/2-2.

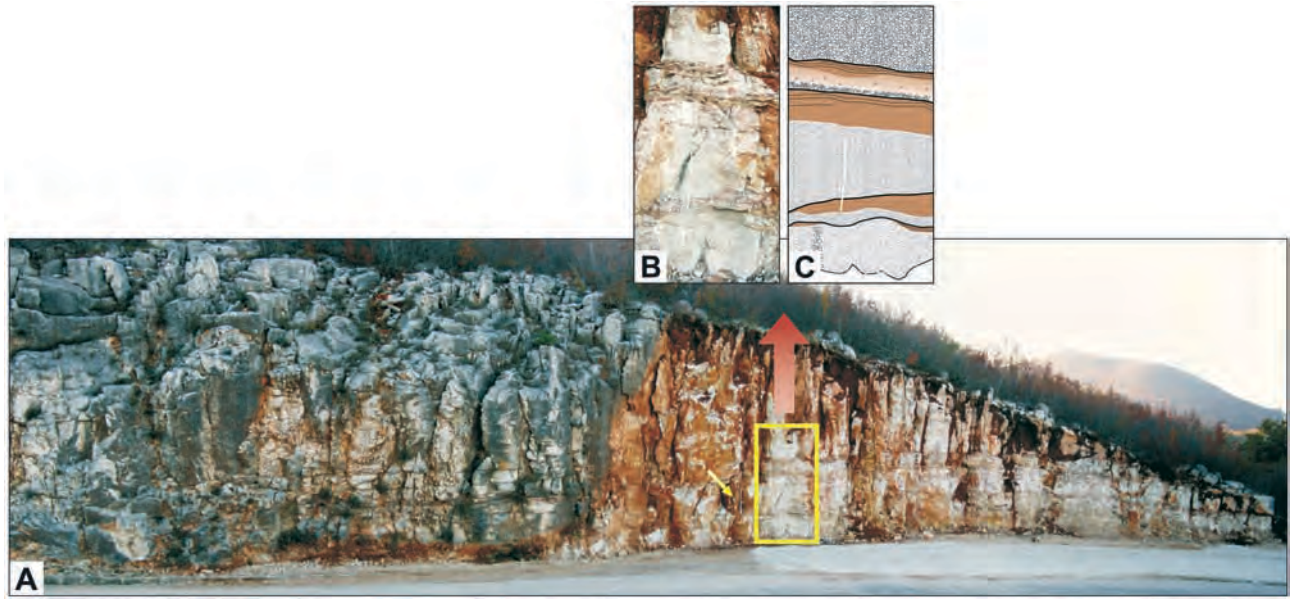

Fig. 50: Road-cut outcrop of sheetflood deposits. **(A)** Photomosaic showing sheetflood deposits composed of 30-130 cm thick "depositional couplets" consisting of pebble- and rare cobble-sized clasts in the lower part and of stratified or massive granule sandstones or coarse to medium sandstones in the upper part. Depositional couplets have a discontinuous sheetlike geometry with lateral continuity for up to 20 m and sharp, irregular to undulatory erosive bases. **(B)** Detail photo and corresponding sketch **(C)** showing sheetflood "couplets" with different thicknesses. Note well sorted, subrounded and clast-supported pebbles and granules with very poor sandy matrix and sharp, irregular to undulatory erosive bases. Sandy parts of the sheetflood couplets are partly eroded. The scale is 1 m.

Appendix 1
The Korlat Unit

Description and interpretation

The Korlat Unit is a middle to late Eocene succession of well-bedded heterolithic calciclastic deposits about 750 m thick (Fig. 51). It is composed of 3-40 cm thick carbonate sandstones interbedded with 5-300 cm thick „background“ calcareous mudstones deposited on a deep-neritic distal fan-delta slope and basin floor (MRINJEK et al. 2010a, b) (Figs 17, 18). The deposits of the basal part of the Korlat Unit represent an initial transition from the piggyback to the foredeep zone, increasingly affected by the growth of blind-thrust anticlines. The effect of syndepositional folding was the development of classic progressive unconformities (Fig. 52) and a decrease in siliciclastic component observed in the lower part of the Korlat Unit. Sandstone beds in the NW part of the unit are predominantly thinner and tabular, with laterally continuous thickness for hundreds of meters (Stops 2/1-2, 2/1-3). In the SE part sandstone beds are thicker, and some of them are stacked together and laterally pinch-out suggesting deposition within poorly defined wide channels. Outstanding characteristic throughout Korlat Unit are sporadic occurrence of huge, 60-280 m long and 7-20 m thick carbonate olistoliths and 2-7 m thick carbonate megabeds (Stops 2/1-2. 2/1-3) spawned by seismic activity along a long blind-thrust growth folds that established the wedge-top basin's outer limit (Fig. 16B). Sandstone beds are a mixture of hyperpycnites (river flood-generated turbidites), tempestites (storm-generated turbidites) and "classical" (Bouma-type) turbidites.

Fig. 51: Very well-bedded heterolithic calciclastic succession of 3-40 cm thick carbonate sandstones interbedded with 5-300 cm thick "background" calcareous mudstones. Note a low bed deep-angle (about 20°).

Hyperpycnites are 3-30 cm thick, fine- to very fine-grained, ungraded, inversely and/or normally graded sandstone beds. Their bedding surfaces may be gradational, sharp or erosional. Beds can be fully massive (Bouma-like Ta), fully planar-parallel laminated (like Tb) or contain intervals of massive and planar-parallel lamination (like Tab); massive to planar-parallel lamination to low-angle cross lamination (like Tabc); low-angle cross lamination to planar-parallel lamination to low-angle cross lamination (like Tcbc); planar-parallel lamination to massive to planar-parallel lamination (like Tbab) (Fig. 53). Recognizable structures suggest deposition from sustained, but fluctuating flows (waning flows or waxing to waning flows). Flood-generated hyperpycnal flows have been generated on fan-delta front where they could incised channels feeding sand lobes located on a deep-neritic distal fan-delta slope and basin floor.

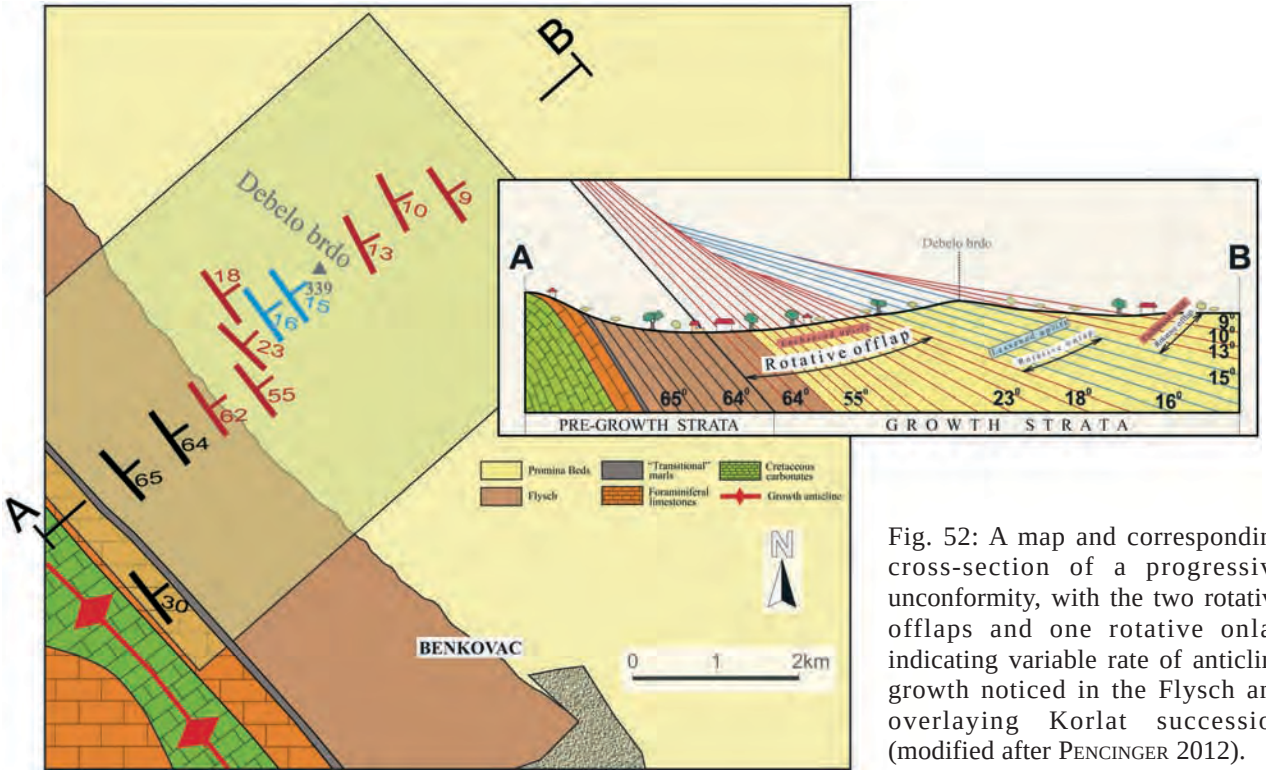

Fig. 52: A map and corresponding cross-section of a progressive unconformity, with the two rotative offlaps and one rotative onlap indicating variable rate of anticline growth noticed in the Flysch and overlaying Korlat succession (modified after PENCINGER 2012).

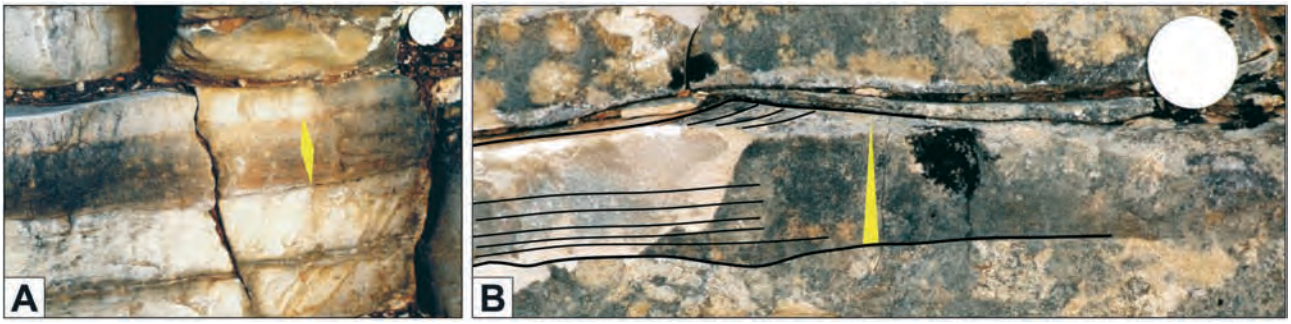

Fig. 53: Hyperpycnal flow deposits of the Korlat Unit. **(A)** Close-up view of an inversely to normally graded hyperpycnite consisting of fine- and medium-grained sandstones (like Tbab). The bed is 5-6 cm thin. Note that the hyperpycnite has a sharp, slightly erosive base while its top passes gradually into overlying mudstone bed. Such structures suggest deposition from sustained, but fluctuating flows (waxing to waning flow condition). Note underlying „background" mudstone beds with very thin (3-4 mm) silty laminae that can be ambiguously interpreted. **(B)** Close-up view of a normally graded hyperpycnite consisting of fine- to very fine-grained sandstone. The lower part of bed is planar-parallel laminated while the upper part is low-angle cross laminated (isolated ripple) (like Tbc). Note a sharp, slightly erosive base and a slightly undulating but relatively sharp top surface. The coin (scale) is 2.2 cm.

Tempestites, which may resemble incomplete Bouma-type turbidites Ta Tab or Tb, have been deposited from storm-generated currents. These heavily sediment-laden currents were initiated by episodic erosional storm events on delta fronts or shoreface and after this boosted seawards reaching to deep neritic slope and basin floor. 'Classical' turbidites comprise complete Bouma sequences (Ta-e) 30-40 cm thick, or are incomplete, representing base cut-off sequences (Tbcde Tde, Tcde) 10-20 cm thick. They are characterized by well developed grading from very coarse-sized sand grains and small rip clasts in the base (complete sequences) or medium- to fine-sized grains (incomplete sequences) to mud at the top of both sequences types. Classical turbidites could be generated by slides and slumps on the gravitationally unstable fan-delta fronts.

The northwestward current directions can be attributed to the NW basin inclination whereas the lack of radial sand dispersal can be indication of the incipient synclinal swales on the basin-floor which could promote mainly linear sand dispersal although some currents coming from the northeastern margin could spread obliquely across the slope towards basin axis. Impressive thickness and monotonous character of the Korlat Unit in distal, northwestern part of the basin suggest ponding of turbidity currents and topographically closed part of sub-basin (see Fig. 16B)

The olistoliths are isolated and coherent bodies of elongated or irregular shape. Elongated olistoliths are 60-280 m long and 7-20 m thick (Fig. 55), whereas irregular olistoliths are considerably smaller, being 12-15 m in length and 3-6 m thick. Elongated olistoliths are oriented and 'slightly plunged' in the NE direction. The host (heterolithic) deposits in the base and in the front of the NE edges of individual olistoliths are intensively distorted and bended (Fig. 57). In the base of SW edges of olistoliths host beds are undisturbed and their orientation corresponds to the local bed orientation (Fig. 58). Megabeds are composed of 0.3-1 m thick breccias beds and/or 1-6 m thick normally graded beds fine ranging in grain size from fine pebble and granule to silt and mud-sized grains. The contact between parts is rather distinct. Olistoliths and breccias are composed exclusively of various Early-Middle Eocene Foraminiferal Limestones.

The individual megabeds can be followed laterally parallel to strike direction. Significant variation in their thickness can be noticed if breccias part is lack or is thinning and this is usually case where they overly isolated olistoliths. The beds do not cut into underlying host deposits. The breccias consist of unsorted to poorly sorted, angular to subangular clasts, 2-60 cm in diameter. Clasts are matrix- to clast-supported. The matrix is composed of

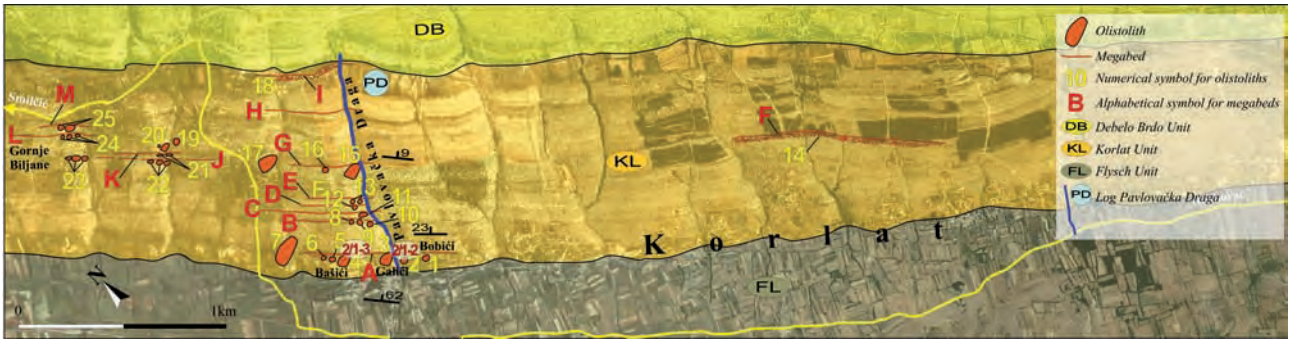

Fig. 54: Lithostratigraphic map of the Korlat area showing position of the olistoliths (numerically marked) and megabeds (alphabetically marked). At the most of olistoliths and megabeds are located at Gornje Biljane village and Pavlovacka Draga gully. Modified from Mrinjek et al. (2010).

Fig. 55: Olistolith 3 with irregular shape, about 65 m long and > 18 m thick, composed of massive, early-middle Eocene Foraminifera Limestones. Azimuth of its length axis is about 40°. The orientation of host beds is 41/23. Olistolith 3 is coeval with olistolith 4. Megabed A crops out between oliostoliths parallelly to its strike direction. The upper surface of the both olistoliths crop out since the megabed and subsequent host deposits are eroded.

granules and medium- to very coarse-sized grains with the same composition to the clasts. Most of breccia beds are chaotic but some beds and certain parts of chaotic beds display an indistinct normal or inverse grading. The normally graded beds can show indistinct parallel planar stratification and undulating stratification (Fig. 56). Very rare bottom marks are NE-SW orientated.

Individual sliding of the olistoliths towards the NE may have been facilitated by a cushion of water-saturated muds directly under the moving blocks which have effectively reduced the resistance to the basal shearing. Structural characteristics of megabeds indicate origin from two kinds of the sediment gravity flow: lower parts have probably originated from a cohesive debris flows or non-cohesive debris flows which could have generated high-density turbidity currents responsible for deposition of the upper parts.

Fig. 56: The megabed A is compound of 0.5 m thick debrite in the lower part and about 2.5 m thick high density turbidite in the upper part. The clast to matrix debrites consist of unsorted, angular to subangular clasts, 2-40 cm in diameter. Turbidite is characterized by well developed grading from small rip clasts and granule-sized grains in the base to mud-sized grains on the top. Note indistinct parallel planar stratification in the middle part of turbidite. The scale (see arrow) is 22 cm.

A total of 27 counted olistoliths and 11 megabeds are located in 11 horizons oriented parallel to the strike direction of the host deposits, i.e. parallel to the basin axis (Fig. 56). Their apron-like distribution and slide direction of olistoliths indicate slope failures along the southwestward basin margin (the limb of the growth anticline which established the wedge-top basin's outer limit). The slope failures probably were consequence of normal faulting along the anticline limb (Fig. 16B).

Fig. 57: The host heterolithic deposits at the northeastern edge of olistolith 4 are strongly contorted, with a nearly vertical dip angle.

Fig. 58: The host heterolithic deposits at the base of the southwestern edge of olistolith 4 are undisturbed.

Appendix 2
The Gradina Unit

Description and interpretation

The Gradina Unit is an about 420-m thick, well-bedded succession extending between Benkovac town and Lisane village (Fig. 17). The unit is coeval with the upper parts of Korlat and Ostrovica Units (Fig. 18). Underlying deposits are fully covered and we suppose that they belong to the lower parts of Korlat and Ostrovica units (Ostrovica Unit and Bribir Unit are not topic of the field excursion and hence are characterized here in only broad terms).

Proximal fan-delta slope deposits

The lower part of succession (the lower 200 m, see log GR in Fig. 65) consists of 5-70 cm thick, sheet-like or broadly lenticular sandstone beds that are separated by 2-100 cm thick 'background' deposits and sporadic intercalations of 50 to 200 cm thick, lenticular conglomerate beds. Sandstones are very fine- to medium-grained, massive, normally graded, inversely graded, inversely to normally graded with planar or slightly undulatory erosional bases. Sandstone beds are a mixture of hyperpycnites (river flood-generated turbidites), tempestites (storm-generated turbidites) and "classical" (Bouma-type) turbidites deposited on a proximal fan-delta slope (Mrinjek et al. 2010a, 2010b) below the mean fairweather wave base.

The sand beds that can be attributed hyperpycnal flows are fully massive (Bouma-like Ta), massive to planar-parallel laminated (like Tab) or planar-parallel laminated to massive to planar-parallel laminated (like Tbab). Some beds are normal graded with planar parallel lamination and hummocky-cross lamination with asymmetrical combined-flow ripples on their top or only hummocky-cross laminated and asymmetrical combined-flow ripples. Their structural characteristics suggest deposition between the mean fairweather wave base and storm wave base during erosional storm events. The sand beds that could be attributed to "classical" turbidites are 30-50 cm thick with clearly developed normal grading from small rip clasts and granules to mud grains. They look very like to complete Bouma sequences (Ta-e), or incomplete Bouma sequences (Tbcde, Tde, Tcde). Rare, 60-70 cm thick turbidites with massive division are probably deposit of high-density turbidity currents. The both types of turbidites have been probably initiated by sliding and slumping on gravitationally unstable fan-delta fronts. It is important to note that bellow storm wave base distinction between 'classical' turbidites and storm-generated turbidites is very unreliable.

Most mudstone contain silty laminae in the form of flat streaks and thin (1-2 thick cm) normally graded siltstone and very fine-grained sandstone beds commonly with many slightly erosional bases. Some very fine-grained sandstone beds are distinct lenses with signs of pinch-and-swell lamination. The vertical spacing of these interlayers varies from a few centimetres to 30 cm or more, and they are commonly disrupted and deformed by animal burrows. Mudstone beds represent quiet-water sedimentation (fallout of hemipelagic muddy suspension) accompanied by widespread biogenic activity (seafloor burrowing), while sparse incursions of silt and very fine-grained sands can be attributed to very low density turbidity flows generated during normal river discharge and/or to deposits of minor seasonal storms. The fine-grained sandstone beds with pinch-and-swell lamination probably represent sediment-starved small ripples of wave or tidal origin.

The middle part of the succession (about 110 m thick; see log GR in Fig. 65, thickness interval 200-310 m) can be described as a vertical alternation of two facies associations.

Distal fan delta-front facies association

This association consists of 10 to 100 cm thick sandstone beds interbedded with 2 to 50 cm mudstone beds. The sandstone beds are commonly amalgamated. The sandstone beds are characterized by structures and textures which can be attributed to sandy debrites, hyperpycnites, storm-derived turbidites and "classical turbidites. Their distal equivalents have the same characteristics as sandstone beds in the lower part of succession and thus represent distal mouth bar association deposited below upper shoreface zone. Mudstone beds are "background" deposits and they are identical to the mudstone beds in the lower part of succession. Five sandy component facies can be distinguished:

- *Massive pebbly sandstones* are 10-30 cm thick beds composed of medium to very coarse-grained sands and randomly scattered fine pebbles and granules. The beds are broadly lenticular with slightly erosive bases. Poor sorting, absence of mud and ungraded texture suggest deposition from cohesionless, sandy debris flows on distal fan-delta front.
- *Inversely graded pebbly sandstones* are 10-30 cm thick beds composed of poorly sorted medium-grained sandstone that pass upwards into granule and/or fine pebbly sandstones. The conglomeratic intervals are 5-10 cm thin, poorly sorted with sandy matrix. The beds are sheet-like with flat, nonerosional bases. The absence of mud indicates deposition of cohesionless debris-flow in the distal part of fan-delta front.
- *Non-graded sandstones* are 10-100 cm thick beds composed of grain sizes that range from coarse to fine sands. The beds are massive, sheet-like, with sharp, clearly erosive or slightly erosive bases. Their characteristics suggests deposition from heavily sediment-laden flows such as high-density turbidity currents or hyperpycnal flows.
- *Normally graded sandstones* are 10-80 cm thick beds that grade upwards either from fine pebbles or granules into medium- and fine-grained sandstones or from medium-grained sandstones into very fine-grained sandstones. The upper part of beds may show indistinct planar-parallel laminations. The beds have irregular, clearly erosive bases and flat upper bed surfaces. Conglomeratic intervals are 5-30 cm thick, moderately sorted and matrix- to clast-supported. The sandstone beds with conglomeratic intervals in their lowest part are 30-80 thick and probably deposited from high-density turbidity flows. Thinner sandstone beds (10-40 cm thick) that grade from medium to very fine sands are probably deposited from low-density turbidity

currents.

- *Planar-parallel laminated sandstones* are 5-50 cm thick beds composed of grain sizes that range from fine- to medium-sized sands. Planar parallel laminations suggest deposition from unidirectional upper flow regime currents or from bidirectional oscillatory currents The process of laminae formation needs variations of current velocities and grain sizes and thus most likely sediment transport mechanisms could be high-density turbidity currents, dense hyperpycnal currents or storm-derived turbidites.

Proximal fan delta-front deposits

This facies association is 1.5-8 m thick, comprising composite packages of various conglomeratic beds generated by traction currents and mass-flow processes. Conglomeratic beds represent mouth-bar and beachface facies deposited on proximal fan-delta front. Five mouth-bar facies and one beachface facies can be distinguished:

- *Massive, clast-supported conglomerates* composed of subangular to subrounded, moderately sorted clasts of fine pebble to cobble size, with sharp non-erosive to slightly erosive bases and a positive correlation between their thickness and maximum clast sizes. The beds are 80-150 cm thick and can be amalgamated into successions of 200 to 300 cm in thickness. They commonly found in the middle and upper part of packages. Their characteristics suggest deposition from cohesionless debris flow.
- *Plane-parallel stratified conglomerates* composed of subangular to subrounded and moderately to well sorted clasts of granule to fine pebble size, with sharp, slightly erosive bases. 10-50 cm thick sheet-like beds are clast-supported, ungraded or very rarely normally graded showing crude plane-parallel stratification. The beds are also amalgamated forming successions of 100-250 m in thickness. They are mostly found in the upper part of packages. Facies represent deposition from tractive currents during periods of high river discharge. The normally graded beds indicate deposition during waning flood.
- *Massive, matrix-supported conglomerates* composed subangular to subrounded and poorly to moderately sorted clasts of granule to fine pebble size with muddy to sandy matrix. The beds are broadly lenticular with sharp, non-erosive bases. The bed thickness is 20-50 cm and show a positive correlation between their thickness and maximum clast sizes. They are found in the lower and middle part of packages. Their characteristics suggest deposition from cohesive debris flow.
- *Inversely graded, matrix-supported conglomerates* composed of subangular to subrounded, poorly sorted clasts of fine pebble to cobble size. They show „coarse-tail“ inverse grading. The bed thickness varies between 20 and 50 cm. The beds have sheet-like geometry, non-erosive or slightly erosive bases. Non-erosive or slightly erosive bases, disorganized fabric and the inverse grading suggest deposition from cohesive debris flows. They are found in the lower and middle part of packages.
- *Normally graded, clast-supported conglomerates* are 30-70 cm thick beds that grade upwards from coarse pebbles into fine pebbles and granules. The beds consist of subangular to subrounded, moderately sorted and matrix- to clast-supported clasts. The beds have irregular, clearly erosive bases. The beds commonly occur in the middle part of packages. Clearly visible normal grading and erosive surfaces suggest deposition from high-density turbidity flows.
- *Planar parallel-stratified conglomerates* with alternating layers of well-sorted, mostly fine- to coarse-pebble and granule gravel. Clasts are rounded to well rounded, with spheres and rods often segregated from discs and blades, but occasionally mixed. The conglomerate beds are 15 to 350 cm thick, with a clast-supported and sand-filled framework. Bed boundaries are planar to slightly undulating, commonly erosional. Northeast- to north-dipping a(t)b(*i*) imbrication is recorded within some beds. Structural and textural characteristics indicate deposition from swash and backwash traction in a beachface setting. These conglomeratic beds are product of wave reworking and lateral distribution along coast line of mouth bar deposits. In the Gradina Unit, the beachface deposits are commonly found on the top of mouth bar units where they are usually overlain by transgressive (flooding) surfaces.

The mouth bars were created in front of channel mouth. Their upward growth continued until their exposure to wave reworking and consequent full filling of mouth channels. The beachface deposits that occur on the top of progradational mouth bar indicate the period of low or non-sediment supply as result of lateral shifting of feeder channels as consequence of the mouth channels dumping, or as result of sediment trapping in coastal zone as consequence of relative sea-level rising. Mass flows, originating either by gravitationally failure of unstable mouth bars gravels or from highly concentrated river floods and/or storm erosion, were able to transport sediments far from fan-delta front reaching delta slope and basin floor environments (the Korlat Unit).

The upper part of succession (about 110 m thick, see Log GR in Fig. 65, thickness interval 310-420 m) consists of 5-50 cm thick, sheet-like or broadly lenticular sandstone beds which are separated by 10-100 cm thick ‘background’ mudstone deposits. They are identical to the sandstone and mudstone beds in the lower part of succession and can be interpreted as proximal delta slope deposits.

The Gradina Unit represents a sandy gravel fan-delta complex whose braided distributary plain has been probably formed by progradation of a solitary braided river. A steady, long-standing progradation of fan-delta complex accompanied by “the growth fold branching“ reduced the wedge-top basin’s interior between Benkovac and Lisane gradually splitting basin into two, partly isolated, Korlat and Ostrovica sub-basins (Fig. 16B). Through relatively long-period fan-delta complex was an important sediment supplier for the both sub-basins.

Appendix 3
The Benkovac Stone Unit

Lithostratigraphy

The Benkovac Stone Unit is about 140 m thick heterolithic succession in the lower part Promina Beds. The unit crops out as a narrow, NW-SE trending belt located between Smilcic village and the Mejanica hill (see Figs. 16, 17). The belt area has a low topographic relief covered with short vegetation and the general rock bedding here is gently inclined towards the northeast. The Benkovac Stone belt probably extends for more than 5 km toward SE. This area is covered with very dense vegetation and thus lateral relation with a coeval upper part of Bribir Unit is indistinct. The Benkovac Stone Unit is underlain by Debelo Brdo and overlain by Otavac Unit (Fig. 18). These contiguous lithostratigraphic units also occur in areas covered with dense vegetation, where their exposure is generally poor. Field observations suggest conformable, transitional boundary with the underlying Debelo Brdo Unit, while the boundary with overlying Otavac Unit is sharp and erosive.

With its tabular bedding and platy splitting pattern, the Benkovac Stone, has long been an important local source of building stone (hence the unit's name), and the numerous small quarries allow detailed study of this calciclastic succession. This sandstone-rich heterolithic succession is readily distinguishable from the underlying and overlying units. The Benkovac Stone Unit consists of carbonate sandstones (up to 35 cm thick, but mainly thinner) interbedded with finer-grained calcareous deposits. Its late Eocene age was established on the basis of large benthic foraminifera (nummulitids, discocyclinids) and small globigerinids.

The sandstones are very fine- to fine-grained calcarenites, sporadically medium-grained, and consist mainly of various sparitic and micritic grains. Quartz grains are subordinate (less than 10 vol.%). The sand grains are subrounded to rounded and generally well to very well sorted, forming a grain-supported framework with mostly point or planar grain contacts. Interstitial spaces are filled with a microcrystalline carbonate cement and/or fine-grained calcareous sediment. The finer-grained interbeds are carbonate siltstones and mudstones, moderately to strongly burrowed. The siltstones are calcisiltites composed mainly of medium to coarse silt-sized carbonate grains and up to 10 vol. % quartz grains. The calcareous mudstones are slightly clayey micrites with scattered silt-sized carbonate and quartz grains.

Calcareous sandstone facies

The carbonate sandstone beds are predominantly tabular and separated by mudstone layers, with relatively few beds amalgamated, stacked directly upon one another. They can vary considerably in thickness. The light-brown to grey sandstones are readily distinguishable from the pale yellowish-grey mudstones, even though their weathering patterns are not necessarily dissimilar. The thicker beds have been characterised by planar parallel stratification, hummocky cross-lamination and flat parallel lamination or slightly undulatory convolute stratification. The thinner beds have slightly erosional and uneven bases, whereas the tops are slightly undulatory ('wavy') and occasionally transitional to the overlying mudstone. The thinnest sandy to silty beds (0.5-3 cm) are characterized by gently undulatory erosional bases and an undulatory, pinch-and-swell internal lamination. The sand volcanoes and dykes occur locally on isolated bedding surfaces and in vertical beds section. The sandstone beds have been classified into six facies and five subfacies (Fig. 59), which are described and interpreted below.

Facies S1: tripartite sandstone beds with plane-parallel stratification, hummocky cross-stratification and undulatory parallel lamination

These are the thickest sandstone beds, with average thicknesses in the range of 5 to 25 cm. Their basal surfaces are sharp and erosional, with an irregular relief of 1 to 7 cm, whereas their tops are slightly uneven or undulatory, with a relief of 2 to 6 cm (Fig. 59A). The beds are normally graded, with the particle size ranging from medium to fine or very fine sand. Even the thicker beds most often consist of fine to very fine sand and commonly coarse silt at the top. The basal surfaces locally show load casts, which are bulbous or irregularly-shaped features lacking preferred orientation. Basal mudstone injections in the form of load-flame structures occur in places. Gutter casts are sporadically found at the bases of the thickest beds. These isolated grooves are 1-2 cm deep and 4-5 cm wide, filled with sand and occasionally bearing mudstone intraclasts. The groove orientation shows a NE-SW to N-S trend.

Internally, these sandstone beds characteristically consist of three divisions. The lower division (*P*) is 3 to 20 cm thick and shows planar parallel lamination although it is locally poorly recognizable in some beds. The laminae are 0.2-0.4 cm thick, almost perfectly flat in the lower part and slightly undulatory in the upper part. Grain size varies from fine or medium to very fine sand. In the thickest beds of this facies (30-40 cm), the parallel-stratified division is often underlain by a medium-grained sand horizon, 1 to 3 cm thick, which is rich in mudstone intraclasts. The mudclasts are angular, 0.5 to 6 cm long and flat-lying, parallel to the basal surface and sandstone strata.

The overlying, middle division (*H*) is 4 to 15 cm thick and shows medium- to small-scale hummocky cross-lamination (Harms et al. 1975). Grain size varies between fine and very fine sand on a bed to bed basis, but the division itself shows little internal grading. The strata are gently undulating, typi-cally <10°, varying between convex- (hummocky) and concave-upward (swaley) in shape. The lateral spacing (wavelength) of the hummocks is mainly from 15 to 20 cm, and their relief (amplitude) is 1 to 2 cm. The strata are only 0.1 to 0.3 cm in thickness, which also varies laterally with their inclination. These small-scale structures are similar to the „micro-hummocky" cross-lamination of Kreisa (1981), attributed to 3D vortex ripples (Harms et al. 1982, their figs. 2-14 and 3-16). Some beds show larger-scale hummocky structures at the transition of division *P* to *H* which have a wavelength in excess of

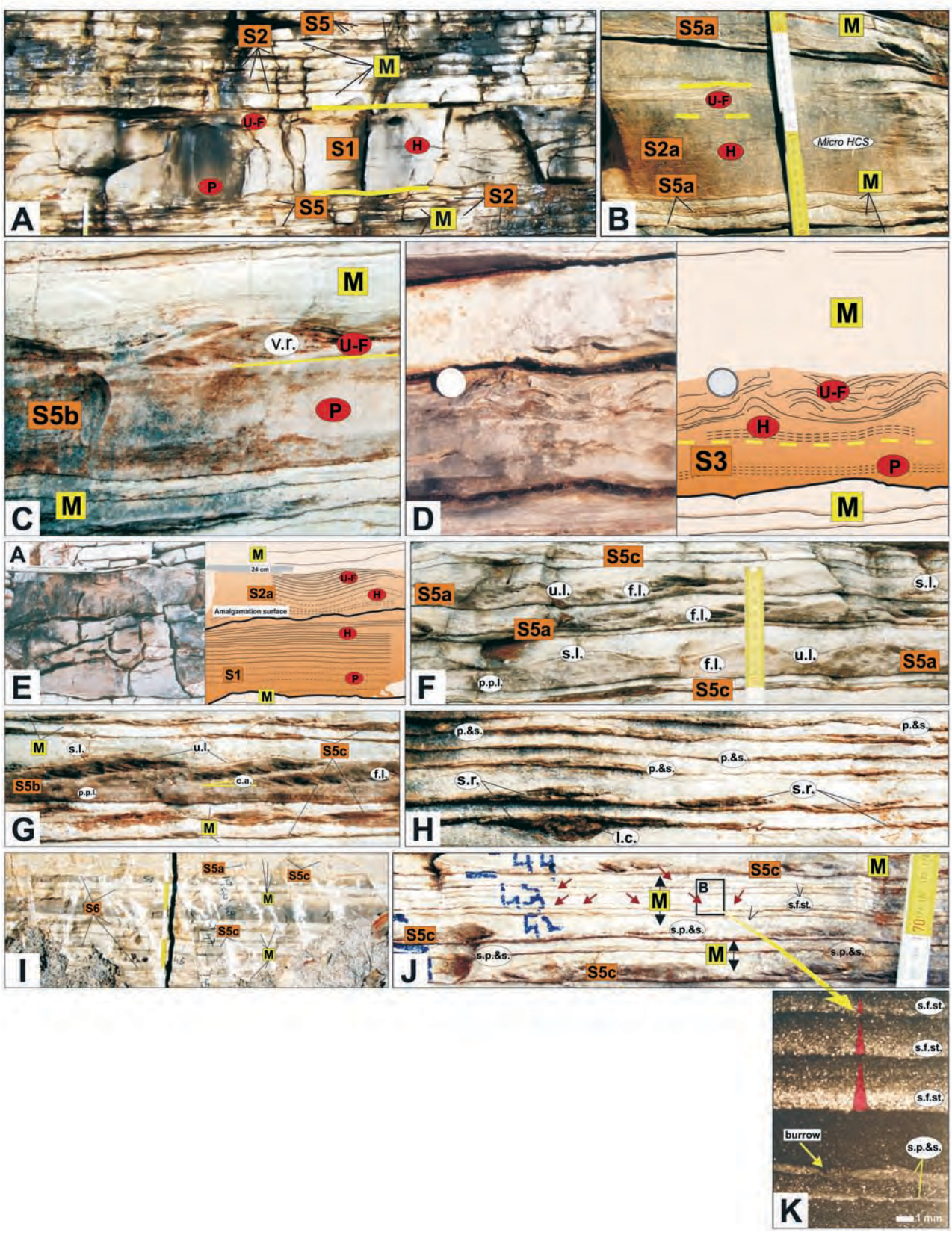
A
S2
S5
M
U-F
S1
H
P
S5
S2
M
B
S5a
M
U-F
S2a
H
Micro HCS
S5a
M
C
M
V.r.
U-F
S5b
P
M
D
M
U-F
H
S3
P
M
E
A
M
24 cm
U-F
S2a
H
Amalgamation surface
H
S1
P
M
F
S5c
S5a
u.l.
f.l.
s.l.
f.l.
S5a
s.l.
f.l.
u.l.
S5a
p.p.l.
S5c
G
M
s.l.
u.l.
S5c
S5b
p.p.l.
c.a.
f.l.
M
H
p.&s.
p.&s.
p.&s.
p.&s.
S.r.
S.r.
l.c.
I
S5a
S5c
S6
M
S5c
M
J
S5c
M
B
M
s.f.st.
S5c
s.p.&s.
M
s.p.&s.
s.p.&s.
S5c
K
s.f.st.
s.f.st.
s.f.st.
burrow
s.p.&s.
1 mm

Fig. 59: Sedimentary facies of the Benkovac Stone Unit (modified after PENCINGER 2012).
(A) Close-up view of a carbonate sandstone bed of facies S1 from the site of log Mejanica. The bed thickness is 34-40 cm. Note that the sandstone bed has a sharp, erosive base and consists of a planar parallel-laminated division P (15 cm thick) overlain by hummocky cross-laminated division H (13-15 cm) and capped with an undulatory to flat laminated division U-F (2-3cm). The wavelength of hummock forms is about 20 cm, but is considerably greater at the transition of divisions P to H, where medium-scale hummocky cross-stratification (HCS) is recognizable. Note also the mudstone intraclasts in the basal part of division P. The underlying and overlying deposits are mudstones of facies M with thin sandstone interbeds of facies S2 and S5. The scale is 14 cm.
(B) A portion of the deposits depicted in log Lisicic (see Fig. 65) showing a carbonate sandstone bed of subfacies S2a. The bed thickness is 9-10 cm. The bed has a sharp, erosive base and consists of a hummocky cross-laminated division H (micro-HCS) (7-8 cm thick) that gradually pass into U-F division (3-4 cm thick). The sandstone bed is underlain and overlain by mudstone beds (Facies M) interbedded with very thin (1-2 cm) sandstone beds of subfacies S5a.
(C) A portion of the deposits depicted in log Mejanica (see Fig. 65) showing a carbonate sandstone bed of subfacies S5b. The bed thickness is 5-7 cm. The bed has a sharp, erosive base and consists of a planar parallel-laminated division P (about 4 cm thick) that abruptly pass into U-F division (3-4 cm thick). Thin isolated intrasets of asymmetrical wave-ripple cross-lamination (w.r.) occur in this division. Asymmetrical ripples have an amplitude of 1.5 cm and wavelength of about 10 cm. The sandstone bed is underlain and overlain by mudstone beds (facies M) with silty interlayers in the form of flat streaks and distinct lenses with signs of pinch-and-swell lamination.
(D) Convoluted sandstone bed of facies S3 and a corresponding sketch from the site of log Benkovac (see Fig. 65). Before hydroplastic deformation the sandstone bed probably pertained to Facies S1. Deformation is limited to the bed's upper part and typically occur as steep antiforms composed of deformed and locally disrupted laminae. The underlying and overlying deposits are silt-streaked mudstones of facies M. The coin (scale) is 2.2 cm.
(E) Compound, amalgamated sandstone bed of facies S4 and a corresponding sketch; detail from log Mejanica (see Fig. 65). Note the sequence of component bed divisions, including planar parallel stratification (P), hummocky cross-stratification (H) and undulatory to flat parallel lamination (U-F). The lower division H shows broader, medium-scale hummocky cross-stratification (HCS), whereas the upper division H shows "micro" hummocky cross-lamination (ripple-scale hummocks). The underlying and overlying deposits are silt-streaked mudstones of facies M.
(F) A portion of the deposits depicted in log Mejanica (see Fig. 65) showing three carbonate sandstone bed of subfacies S5a. The beds with slightly erosive bases have well-preserved asymmetrical ripple forms, 1-1.5 cm in amplitude and 11-14 cm in wavelength. Some cross-sets are underlain by a set of 2 or 3 planar laminae (p.p.l.) covering the erosional basal surface. Note the well-developed foreset laminae (f.l.), with discordant silty laminae on the stoss side and a "sweeping" drape of undulatory laminae (u.l.) on their tops. The dip direction of foreset laminae (ripple migration azimuth) is to the southeast. The underlying and overlying deposits are mudstones of facies M interbedded with thin sandstone beds of subfacies S5c.
(G) A portion of the deposits depicted in log Mejanica (see Fig. 65) showing a 2.5-3.5 cm thick carbonate sandstone bed of subfacies S2b. The bed has slightly erosional base covered by 2 or 3 planar laminae (p.p.l.) and consists of three superimposed sets of asymmetrical, climbing-ripple cross-lamination. The wavelengths of asymmetrical ripple forms are 11-14 cm, whereas their amplitudes vary between 1 and 1.5 cm. Note the well-developed foreset laminae (f.l.), with discordant silty laminae on the stoss side (s.l.) and a "sweeping" drape of undulatory laminae (u.l.) on the bed top. The angle of climb (c.a.) is 10°. The dip direction of foreset laminae (ripple migration azimuth) is to the southeast. The underlying and overlying deposits are mudstones of facies M interbedded with thin sandstone beds of subfacies S5c.
(H) A portion of the deposits depicted in log Mejanica (see Fig. 65) showing 0.3-1.5 cm thin, very fine-grained carbonate sandstone beds (the lower part of photo) and 0.2-1 cm thin sandy to silty laminae of subfacies S5c. The beds and laminae have slightly erosive bases. The laminae show undulatory, pinch and swell internal lamination (p.&s.). Two thin beds in the lower part of photo contain small solitary lenticular cross-sets (small, sediment-starved translatory ripples) (s.r.). The solitary ripple of the lowest bed is deformed by loading (l.c.).
(I) Massive and normal graded, very fine sandstone to siltstone beds of facies S6 interbedded with mudstone beds of facies M and thin sandstone beds of subfacies S5a and S5c.The bed thickness varies between 1 and 8 cm. The beds have sharp and slightly erosive bases whereas their tops are flat or slightly undulatory (thicker beds). Log Benkovac Kamen.
(J) A portion of the deposits depicted in log Mejanica (see Fig. 65) showing 1-3.5 cm thick calcareous mudstone beds of Facies M interbedded with thin sandstone beds and laminae of subfacies S5c. The mudstone beds contain thin (1-3 mm) silty laminae in the form of normal graded flat streaks (s.f.st.) and distinct lenses with signs of pinch-and-swell lamination (s.p.&s.). The vertical spacing of these interlayers varies from 0.2 to 1 cm, and they are disrupted and deformed by animal burrows.
(K) Microscopic detail of a silt-streaked calcareous mudstone of facies M. Note three 1-3 mm thin, normal graded silty streaks (s.f.st.) with sharp erosive bases (the upper part of photo) and silty lenses with pinch-and-swell lamination (s.p.&s.) disrupted by burrows (the lower part of photo).

50-60 cm and can be regarded as „true“ hummocky cross-stratification, representing combined-flow conditions (HARMS et al. 1975, DOTT & BOURGEOIS 1982, MYROW & SOUTHARD 1996).
In most cases, at least two or three superimposed sets of hummocky lamination are recognizable in division *H*. The strata within the sets (first-order bounding surface *sensu* DOTT & BOURGEOIS 1982) are concordant with the set's lower bounding surface (second-order bounding surface), which itself is slightly erosional. The transi-tion from division *P* to *H* is either gradual or sharp and slightly erosional.
The upper division (U-*F*) is 1 to 5 cm thick, consists of very fine sand or coarse silt and shows undulatory to flat parallel lamination. In contrast to the lower division, the laminae here are only 0.1-0.2 cm in thickness and commonly show an upward change from slightly undulatory to flat, which renders their lower boundary transitional. In some cases, thin isolated intrasets of asymmetrical wave-ripple cross-lamination occur in this division .The transition from division *H* to *U-F* is gradual.

Facies S2: bipartite sandstone beds with planar-parallel stratification or hummocky cross-stratification and planar parallel lamination
The beds of this bipartite sandstone facies are similar to those of the previous one, but are generally thinner (average thicknesses of 4-10 cm). Their basal surfaces are sharp and erosional, with an irregular relief of 1 to 3 cm and sporadic load casts. Their upper surfaces are slightly uneven or undulatory. The beds are normally graded, with the particle size ranging from fine to very fine sand and coarse silt. The structure of the lower division form the basis for the distinction of two subfacies.

Subfacies S2a: bipartite sandstone beds with hummocky cross-stratification and undulatory parallel lamination
The lower, 2-8 cm thick division **(**H) shows hummocky-cross lamination composed of slightly thinner laminae. The wavelength of hummocks is also somewhat smaller (10-15 cm). The overlying upper division (U-*F*) is a thin (1-2 cm) set of slightly undulatory to flat parallel laminae composed of very fine sand to coarse silt. Division U-*F* is occasionally indistinct, either poorly developed or virtually absent. The transition from lower to upper division is rather gradual (Fig. 59B).

Subfacies S2b: bipartite sandstone beds with planar-parallel stratification and undulatory parallel lamination
The lower division (*P*) is 2 to 6 cm thick and shows planar parallel lamination. The laminae are 0.2-0.3 cm thick and perfectly flat. the Grain size varies from fine to very fine sand (Fig. 55). The overlying upper division (U-*F*) also is a thin 1-2 cm thin set of undulatory to flat parallel laminae composed of very fine sand to coarse. Thin isolated intrasets of asymmetrical wave-ripple cross-lamination frequently occur in this division (Fig. 59C). The transition from division *H* to *U-F* is very abrupt.

Facies S3: sandstone beds with convolute stratification
These are sandstone beds that show internal hydroplastic deformation in the form of convolute stratification, although could originally be similar to any of the previous sandstone facies. Average bed thicknesses are mainly in the range of 5 to 25 cm, and the deformation is often stronger in the bed's upper part or is locally limited to only this part. The convolutions typically occur as steep antiforms composed of deformed and locally disrupted or homogenized strata (Fig. 59D). The antiforms are commonly asymmetrical, but generally lack preferential orientation or a recognizable spatial pattern**.**

Facies S4: amalgamated sandstone beds
This facies is relatively rare and consists of amalgamated sandstone beds, which themselves represent one or more of the previous facies. The component beds are stacked erosionally upon one another with no intervening mudstone layers. These composite, amalgamated beds are recognizable by their greater thicknesses (up to 40 cm), multiple normal grading and a more complex vertical sequence of structural divisions (Fig. 59E).

Facies S5: cross-laminated sandstone beds
These are thin sandstone beds (2-5 cm), composed of very fine sand or coarse to medium silt and generally lacking any obvious grain-size grading. Their bases are slightly erosional and uneven or undulatory, whereas the tops are slightly undulatory („wavy“) and occasionally transitional to the overlying silty mudstone. Many of these sandstone beds, much like the overlying and underlying mudstone layers, are moderately to strongly burrowed. Internally, the sandstone beds show a wide range of wave-ripple cross-lamination types, which form the basis for the distinction of three subfacies (see below). The wave-ripple cross-lamination is recognizable by the presence of uneven or undulatory basal surfaces and lower laminae sets, draped or offshooting geometry of foreset laminae, and chevron-like or form-discordant internal laminae sets (see DE RAAF et al. 1977, COLLINSON & THOMPSON 1982).

Subfacies S5a: sandstone beds with translatory ripples
These beds have undulatory boundaries with well-preserved asymmetrical ripple forms, 1-1.5 cm in amplitude and 6-20 cm in wavelength (Fig. 59F). Some cross-sets are underlain by a set of 2 or 3 planar laminae covering the erosional basal surface. The well-developed foreset laminae, with discordant silty laminae on the stoss side and a „sweeping“ drape of undulatory laminae are typical of migrating, translatory wave ripples (ALLEN 1982). The dip directions of foreset laminae (ripple migration azimuths) are very variable but two trends of migration are predominant, one in range between western and northwestern directions and other in range between southern and southeastern directions.

Subfacies S5b: sandstone beds with climbing ripples
These beds are slightly thicker, have undulatory and slightly erosional bases, and consist of two or three superimposed sets of asymmetrical, climbing-ripple cross-lamination with preserved stoss-side laminae. The angle

of climb varies from 8 to 12° (Fig. 59G). Ripple dimensions are similar to those of the previous subfacies, and the dip directions of foreset laminae also similarly range between western and northwestern directions and southern and southeastern directions. As in the previous subfacies, a basal set of 2-3 flat or slightly undulatory laminae can often be seen covering the underlying erosional surface. A similar set of 'sweeping' undulatory laminae occurs often at the bed top.

Subfacies S5c: sandstone beds with pinch-and-swell lamination

These sandy to silty thin beds and laminae are the thinnest (0.2-1.5 cm), character-ized by gently undulatory erosional bases and an undulatory, pinch-and-swell internal lamination (similar to the "rolling-grain" ripples of Harms et al. 1982 - fig. 3-16), occasionally associated with thin, solitary len-ticular cross-sets (small, sediment-starved translatory ripples - Allen 1982) (Fig. 59H).

Facies S6: massive sandstone beds with normal grading

These are very common, but very thin (1-8 cm), fine-grained sandstone beds that lack recognizable internal lamination. Their basal surfaces are sharp and slightly erosional, with a local-scale relief of 0.5 to 1 cm, whereas the tops are flat or only slightly undulatory. The beds are normally graded, ranging in grain size from very fine sand to coarse silt (Fig. 59I). The thicker beds locally show traces of primary lamination, which suggests a secondary process of sediment homogenization. The 'structureless' (massive) appearance of these deposits is thus probably a result of their bioturbation and/or subsequent pervasive weathering at outcrop.

Calcareous mudstone facies M

The layers of facies M are a few mm to 30 cm thick, very common and laterally continuous mudstone interbeds. Most beds contain thin (1-5 mm) silty interlayers in the form of flat streaks and distinct lenses with signs of pinch-and-swell lamination (Fig. 59J), apparently representing sediment-starved small ripples of wave or tidal origin (see Reineck & Singh 1975; and the 'rolling-grain' ripples of Harms et al. 1982). The interlayers usually show normal grading from coarse to fine silt, and many have slightly erosional bases (Fig. 59K). The vertical spacing of these interlayers varies from a few millimetres to 20 cm or more, and they are commonly disrupted and deformed by animal burrows.

Other features

Sand volcanoe

Small circular or elliptical sand volcanoes composed of fine and very fine sandstones with mudstone intraclasts occur locally on isolated bedding surfaces in the mudstone Facies M (Fig. 60A). These conical features are typically 15-36 cm in dia-eter and 2-6 cm in relief, apparently represent seafloor sand extrusions buried by younger mud. A numerous such features have been found on open mudstone surfaces.

Sand dikes

Tabular and discordant, vertical to subvertical sandstone bodies caused by the injection of liquified sands from below. They can be seen as an irregular strips on the mudstone bed surfaces ranging in the length from a few decimetres to more than 10 m. The strips are few cm to 20 cm wide

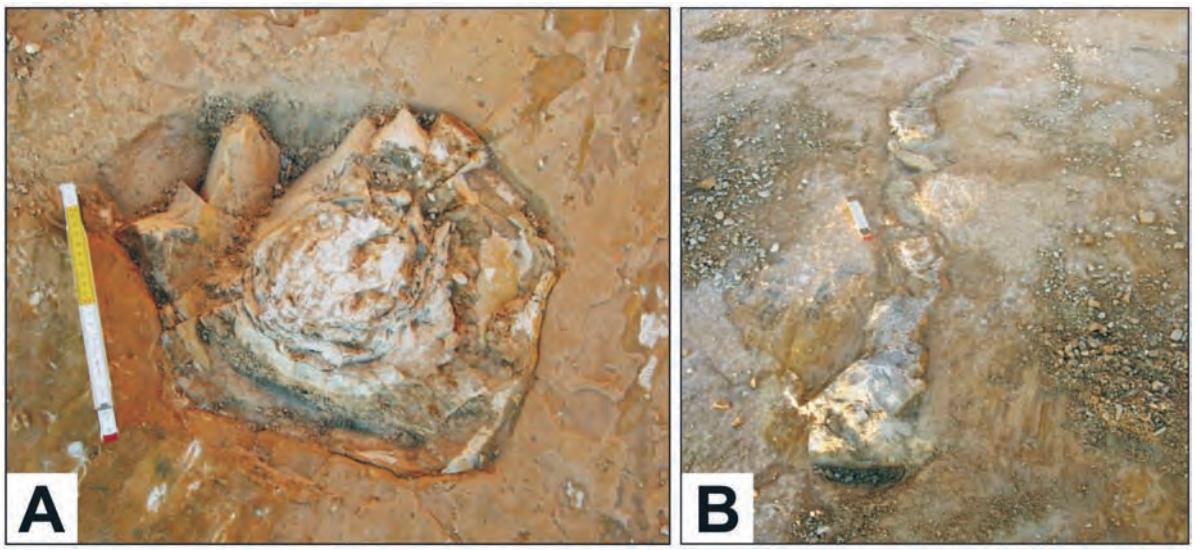

Fig. 60: Post-depositional structures due to fluidization. **(A)** Small sand volcanoes composed of fine and very fine sandstones with mudstone intraclasts in calcareous mudstone Facies M; bedding surface details from the site of log BK (Fig. 65). This volcano has a slightly elliptical plan-view shape with the longer axis of 32 cm and cone relief of 6 cm, and apparently represent sea-floor sand extrusions buried by younger mud. The scale is 22 cm. **(B)** Sand dikes in calcareous mudstone Facies M; bedding surface details from the site of log BK (Fig. 65). The dikes appears as an irregular, about 4 m long strip on the mudstone bed surface. The scale is 22 cm.

and up to 10 cm thick (Fig. 60B). In some cases mudstone intraclasts derived from overlying mudstone by shearing stress can be noticed inside injected sands. They can be commonly seen on some bed surfaces in the "Benkovacki kamen" quarry.

Facies interpretation

The internal characteristics of the sandstone facies S1-S6, together with their sheet-like bedding geometry indicate sand deposition by waves in combination with unidirectional currents (MRINJEK et al. 2005, see DE RAAF et al. 1977, HAMBLLN & WALKER 1979, DOTT & BOURGEOIS 1982, LECKIE & WALKER 1982, WALKER et al. 1983). The intervening, silt-streaked mudstone layers of Facies M indicate quiet-water conditions dominated by hemipelagic suspension fallout and biogenic activity, with the sand-starved seafloor episodically affected by very weak wave action and/or tidal currents. The intimate association of the discrete, erosional sandstone sheets rhythmically alternating with mudstone layers indicates episodic deposition from storm events in an offshore transition zone, which means a shelf bathymetric area extending between the average fair-weather wave base and the average storm wave base. The offshore transition zone thus occurs outside the shoreface zone (perennially affected by waves) and is subject to episodic incursions of sand during storm events ('event' sedimentation *sensu* EINSELE & SEILACHER 1982). The actual width, or seaward distance, of these zones depends on the local seafloor inclination and may vary from a few hundred metres to several kilometres (READING & COLLINSON 1996). Accordingly, the sandstone facies are considered to be tempestites (storm deposits), embedded in a 'background' mudstone facies (fair-weather deposits).
The sandstone beds of **facies S1** show planar parallel lamination (division *P*) overlain by medium- to small-scale hummocky cross-stratification (division *H*) and capped with undulatory to flat parallel lamination (division U-*F*). If the sporadic medium-scale hummocky cross-stratification is ignored, the sequence of stratification types can be attributed to the action of oscillatory waves (see the bedform stability diagrams in HARMS et al. 1982 - figs. 2-14), with the temporal trajectory of seafloor hydraulic regime beginning in the plane-bed field and re-entering this field again after crossing the field of 3D vortex ripples (see also WALKER et al. 1983, MYROW & SOUTHARD 1996). The action of a geostrophic current in such a case would be limited to supplying sand to the offshore transition zone, and to aiding briefly the devel-opment of medium-scale hummocks. Alternatively, the basal division *P* could partly or entirely be deposited by a geostrophic current, if the latter was sufficiently powerful, laden with sediment and characterized by high suspension fallout rate, such that tractional plane-bed transport occurred (see LOWE 1988, fig. 3). The action of waves would then directly follow that of the density-modified current. This possibility is particularly likely for beds that show medium-scale hummocky cross-stratification in the lower part of their division *H*, because this stratification type is widely attributed to a combined-flow regime.
The sandstone beds of **subfacies S2a** show a hummocky cross-laminated division *H* overlain by an undulatory to flat parallel-laminated division *U-F*, which can be attributed to oscillatory waves - with the temporal trajectory of the hydraulic regime commencing in the stability field of 3D vortex ripples and passing into the plane-bed field as the sediment supplied becomes finer-grained (see HARMS et al. 1982, figs. 2-14). In this case, the sand delivered to the offshore transition zone by a waning geostrophic current would be thoroughly worked by waves.
The sandstone beds of **subfacies S2b** show a planar parallel lamination (division *P*) overlain by an undulatory to flat parallel-laminated division *U-F*. Commencing in the stability field of plane-bed (division P) the hydraulic regime temporarily passed into stability field of 3D vortex ripples or even into stability field of 2D ripples as the sediment supplied becomes finer-grained. With waning of orbital speed accompanied by supply of very fine grains, the hydraulic regime re-entered into plane-bed stability field (division *U-F*) (see HARMS et al. 1982, figs. 2-14).
It is worth pointing out that the action of waves on the seafloor in the offshore transition zone will cease abruptly as soon as the wave base detaches itself from the seafloor. This means that the storm event of sand deposition can abruptly be terminated at a non-zero level of general wave energy; and that is why most tempestites have not only sharp bases, but also sharp tops, which are often also undulatory, showing well-preserved ripple forms.
The sandstone beds of facies S1 and S2 also stand out by their greater thicknesses, implying the strongest storm events that affected the offshore transition zone in the present case. Geostrophic currents would play a greater role in the deposition of facies S1, attributed to the strongest storm. In this context, the significance of sandstone facies S4 would be to represent strong storms that closely followed one another, such that little or no fair-weather sedimentation took place between these events.
The erosional bases and normal grading of these tempestite beds are consistent with the notion of an initial, strong ebb-surge followed by a waning geostrophic current that supplied increasingly fine-grained sediment to the offshore transition zone. The sporadic occurrence of gutter casts at the bases of facies S1 beds may theoretically be due to either oscillatory waves or combined-flow currents (MYROW & SOUTHARD 1996). However, some authors suggested that a unimodal orientation of gutter casts may indicate unidirectional currents, possibly density-modified (HAMBLIN & WALKER 1979, LECKIE & WALKER 1982, WALKER et al. 1983). The NE-SW to N-S trend of the gutter casts in the present case is roughly perpendicular or oblique with respect to the inferred palaeoshoreline, which may support the notion of strong ebb-surges or powerful geostrophic currents. This interpretation is further supported by the occurrence of mudclast-rich horizons, considered to be lag deposits of powerful, erosive currents (SEPKOSKI 1982, WALKER et al. 1983). The fact that the mudclast lags are uncommon may reflect either their limited preservation potential or deposition from somewhat exceptional currents.
The convoluted sandstone beds of **facies S3** were apparently deposited in a similar way to those of facies S1 and S2, but

underwent a late syndepositional or early post-depositional hydroplastic deformation. These deformed beds indicate partial sediment liquefaction, but are relatively rare, and hence the cause of the deformation itself can be regarded as a rare factor. The seafloor was clearly affected by sporadic shallow liquefaction, as is also indicated by the horizons of sand dykes and mud volcanoes. Their origin is attributed to the upwelling of pore-water springs through liquified quickmud (Reineck & Singh 1975), which may occur in response to a rapid sediment deposition, cyclic seafloor loading by storm waves or shaking by seismic „ground-roll" wave (i.e., the combined S and L shock waves propagating at ground level). The same factors, or the shearing by an overpassing current (Sanders 1965), could occasionally liquefy the seafloor when it was covered with sand (facies S1 or S2), rather than mud, and hence result in facies S3 (see Middleton & Hampton 1973). A more intense liquefaction and/or pervasive bioturbation are thought to have similarly produced **facies 6**, which seems to have resulted from a sporadic internal homogenization of freshly-deposited sand beds of facies S5.

The sandstone **subfacies S5a** and **S5b** indicate storm events with a prevalent role of geostrophic currents, which were sand-laden and characterized by a moderate (subfacies S5a) to high suspension fallout rate (facies S5b) (see Harms et al. 1982). These beds are thin and fine grained, which implies relatively weak, highly subcritical (Harms et al. 1975) and low-density currents (*sensu* Lowe 1982). The orientation of ripple cross-lamination indicates currents flowing towards the west (obliquely offshore) or northwest (alongshore).

At the other end of the whole spectrum of tempestites are the very thin and fine-grained beds of **facies S5c**, whose geometry and internal features indicate sand-starved vortex

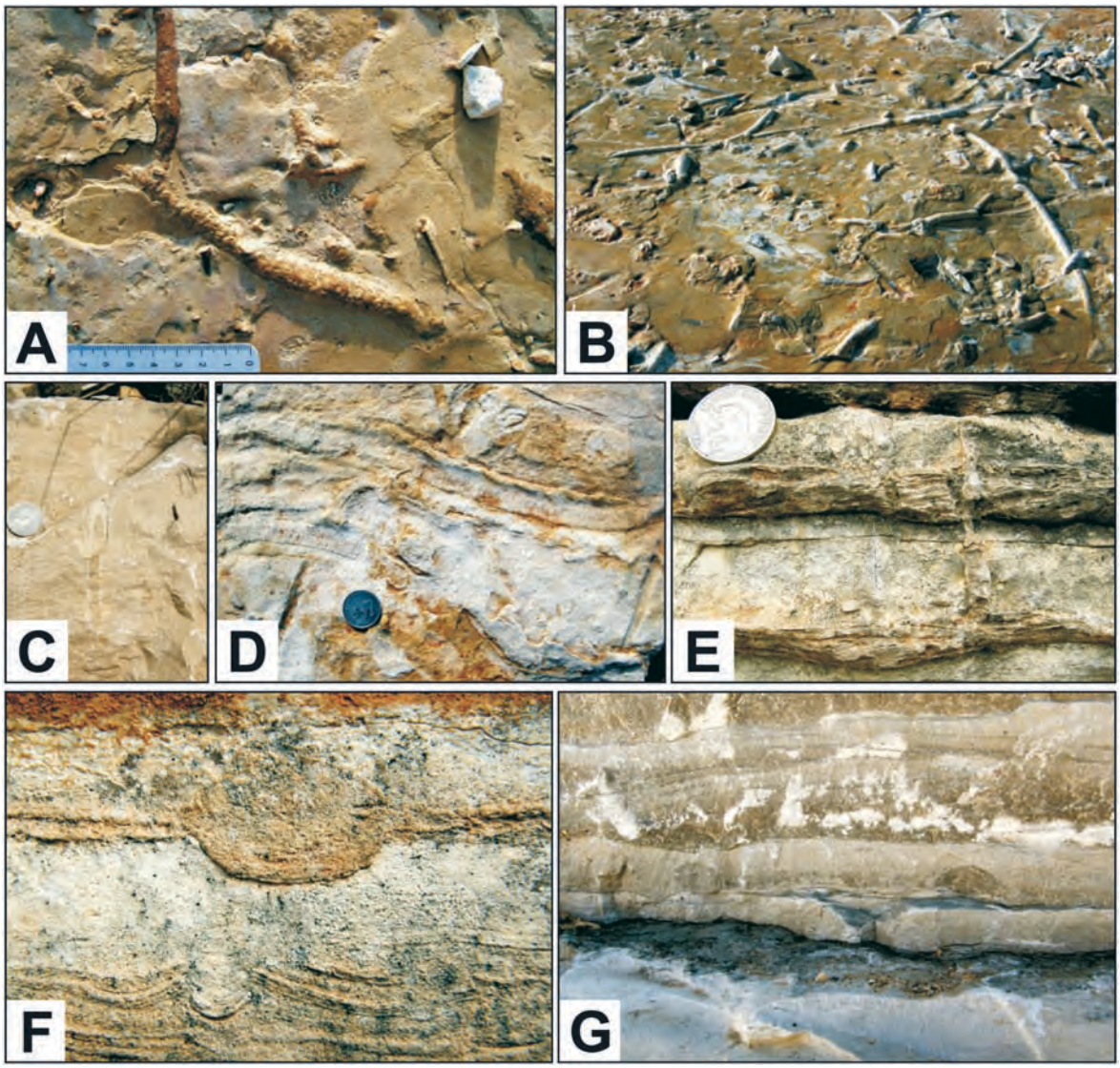

Fig. 61: Trace fossils in the calcareous sandstone facies of Benkovac Stone Unit (modified after Pencinger 2012). **(A)** *Ophiomorpha nodosa*, endichnial full relief in sandstone, Benkovacki Kamen quarry. **(B)** *Thalassinoides* isp., endichnial full relief in sandstone, Kimont quarry. **(C)** *Palaeophycus* isp., full relief in sandstone, Kimont quarry. The coin (scale) is 2.2 cm. **(D)** *Scolicia prisca*, epichnial full relief in sandstone, Kimont quarry. The coin (scale) is 2.6 cm. **(E)** *Arenicolites* isp., full relief in sandstone, Lisicic quarry. The coin (scale) is 2.6 cm. **(F)** *Teichichnus* isp., full relief in sandstone, Lisicic quarry. **(G)** *Rhizocorallium* isp., full relief in sandstone, Kimont quarry.

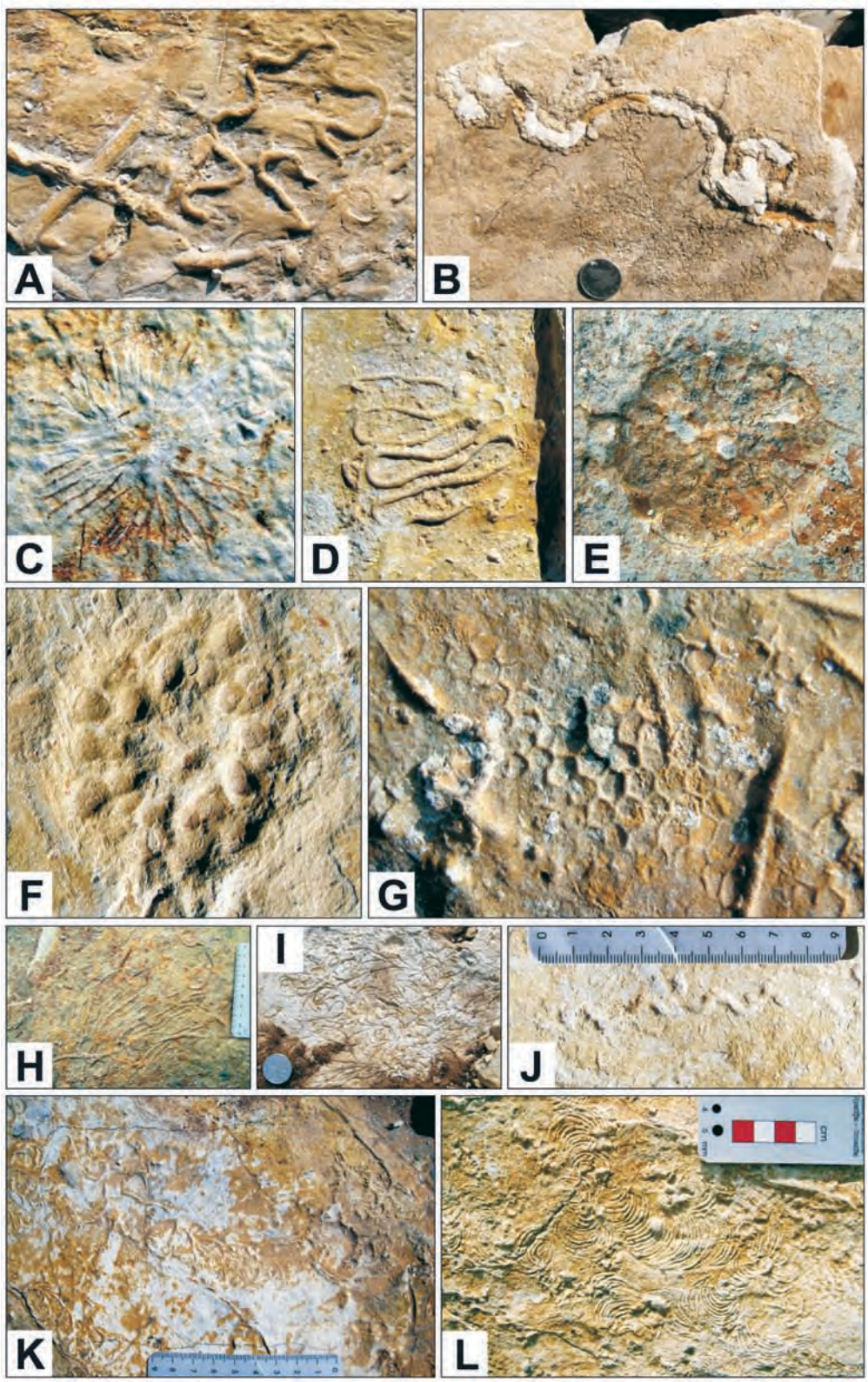

Fig. 62: Trace fossils from mudstone facies of The Debelo Brdo and Benkovac Stone units (modified after PENCINGER 2012). **(A)** *Cosmorhaphe lobata*, hypichnial semi-relief, Debelo Brdo quarry. **(B)** *Nereites missouriensis*, epichnial form in sandstone, Debelo Brdo. Quarry. The coin (scale) is 2.2 cm. **(C)** *Glockerichnus glockeri*, hypichnial semi-relief, Lisicic quarry. **(D)** *Helminthorhaphe japonica*, hypichnial semi-relief, Debelo Brdo quarry. **(E)** *Gyrophyllites* isp., epichnial form in sandstone, Benkovacki Kamen quarry. **(F)** *Atollites* isp., epichnial form in sandstone, Lisicic quarry. **(G)** *Paleodictyon strozzii*, hypichnial semi-relief, Debelo Brdo quarry. **(H)** *Urohelminthoidea appendiculata*, hypichnial semi-relief, Benkovacki Kamen quarry. (I) *Chondrites recurvus*, endichnial full relief, Debelo Brdo quarry. The coin (scale) is 2.6 cm. **(J)** *Belorhaphe zickzack*, hypichnial semi-relief, Benkovacki Kamen quarry. **(K)** *Polykampton* isp., epichnial form in sandstone, Mejanica quarry. **(L)** *Hydrancylus* isp., epichnial form in sandstone, Benkovacki Kamen quarry.

ripple and rolling-grain ripples, implying weak action of "pure" oscillatory waves (ALLEN 1982, HARMS et al. 1982). The silt-streaked calcareous mudstones of **facies M** represent quiet-water sedimentation during the inter-storm periods of fair-weather conditions, accompanied by widespread biogenic activity (seafloor burrowing). The fallout of hemipelagic muddy suspension was frequently interrupted by sparse incursions of silt, which can be attributed to weak tidal currents and/or minor seasonal storms.

Spatial distribution of facies

The sedimentary succession is characterized by tabular bedding, with the sheet-like sandstone and mudstone beds showing lateral continuity on an outcrop scale of up to several hundred metres. Two of the thickest sandstone beds of facies S1 can be correlated as markers, on an outcrop to outcrop basis, parallel to the inferred palaeoshoreline.
The succession of alternating sandstone and mudstone beds shows considerable variation in their thick-nesses, but little obvious vertical organization. The only recognizable trend is that the thicker beds of facies S1 are more common, and the mudstone beds of facies M are thinner and less bioturbated, in the middle part of the succession. This stratigraphic pattern may reflect a temporal change in relative sea level, sediment supply or sea-wave climate. An episode of an accelerated shoreline advance seems likely to have been the case, because it would inevitably increase the frequency and magnitude of storm events affecting the offshore transition zone, and thus increase the supply of sand to the latter. The subsequent, temporal recession of the shoreline could be due to any of the three factors mentioned above, but was most likely caused by a relative sea-level rise.

The Benkovac Stone ichnofauna: deep-water trace fossils in a shallow-water environment

Trace fossils in the sandstone beds are represented by numerous polychaete and arthropod burrows and burrows of irregular echinoids - *Palaeophycus*, *Teichichnus*, *Scolicia* ispp., *Rhizocorallium* and *Thalassinoides* (Fig. 61). Tracemakers exploited the sediments for the short time, searching for the organic particles (plant debris, etc.) mixed into the sediment during the tempestite formation. Trace fossils in mudstone beds show a quite different and broader ichnodiversity; the most important are graphoglyptid traces (*Helminthorhaphe*, *Cosmorhaphe*, *Urohelminthoida*, *Belorhaphe*, etc.) with *Paleodictyon*, nereitids, medusiform burrows (gyrophyllitids), asterosomids, chondritids, lophoctenids, *Zoophycos* group and asterozoan traces (Fig. 62).
Graphoglyptids are generally rare, except for ichnospecies *Paleodictyon strozzii*, one of the most common trace fossils in the Benkovac Stone Unit. Lophoctenids, represented by few excellently preserved records of *Polykampton* (Fig. 62K) are also rare and found only occasionally (a cast of one such bedding planes with *Polykampton* was included in Adolf Seilacher's world-famous exhibition 'Fossil Art'). *Zoophycos* appears as large, more than 1 m wide forms which mark narrow transitional zone between underlying Debelo Brdo Unit and Benkovac Stone Unit and probably suggest specific palaeoecological conditions around the offshore transition zone. Chondritids, asterosomids and graphoglyptid *Cosmorhaphe* are characteristic traces for the lower part, being most frequent immediately after disappearance of *Zoophycos* in succession, although these traces also occasionally occur in the younger part of the succession. *Glockerichnus* occurs in the topmost part of the unit. *Nereites*, represented with its different preservational varieties, together with *Paleodictyon strozzii* and gyrophyllitids, is the most common and ubiquitous trace fossil in the Benkovac Stone Unit. *Paleodictyon* and *Helminthorhaphe* are the only graphoglyptids present in beds below Benkovac Stone Unit - in the Korlat and Debelo Brdo units.
Ichnoassemblages from the Benkovac Stone Unit are similar in composition to those found in many European flysch basins (UCHMAN 1995, 1999, 2001). These ichnoassemblages interpreted as ichnoassemblages of offshore-transition environment are an exception to the standard ichnofacies distribution which consider *Zoophycos* and *Nereites* ichnofacies as discrete deep-marine ichnofacies (FREY & SEILACHER 1980). Especially interesting is the preservation of trace fossil *Paleodictyon* as clear epirelief, since ubiquitous occurrence of ichnospecies *P. strozzii* almost always coincides with possible appearance of microbial mats.
Traces like *Treptichnus* and few forms of *Paleodictyon* occur only in combination with microbial mat sedimentary structures and seems to indicate a possible presence of this specific sedimentary environment.
The Benkovac Stone Unit shows great variety of different ichnospecies, which is rather the result of different modes of preservation than the result of tracemaker biodiversity. A few forms of burrows cannot be assigned to any group of trace fossils (forms similar to gyrophyllitid, some phycosiphonid forms of burrows and others). Erosive exhumation of mudstone-related traces by deposition of calcarenites (casting of the traces) has also been responsible for preservation of many trace fossils in the Benkovac Stone Unit. This preservation mode prevailed in younger parts of the studied unit, while the evidence of microbial mats occurs even later.
Variable content of food, plenty of dissolved oxygen, salinity levels, sediment supply and sediment deposition rate, permanent circulation of water and water turbidity seems to be the more important factors than bathymetry for development of various ichnoassemblages (PEMBERTON et al. 1992, PERVESLER & UCHMAN 2004, UCHMAN et al. 2004). In this case, considering that the offshore-transition environment affected by storm-generated currents can be very similar to deep marine environments affected by turbidity currents, the *Nereites* and *Zoophycos* tracemakers could survive relatively abrupt shallowing from subneritic (foredeep basin) to neritic (piggyback basin) in the foreland environment.

Appendix 4
The Debelo Brdo Unit

Lithostratigraphy

The Debelo Brdo Unit (The Debelo Brdo Unit is named after Debelo Brdo hill ravaged by illegal excavation pits**)** underlies the Benkovac Stone Unit and is 230 to 280 m thick succession of well-bedded heterolithic calciclastic deposits composed of 10-40 cm thick, calcareous mudstone beds with thin interlayers of very fine carbonate sandstones and siltstones interbedded with 1-5 cm thick, very fine-grained carbonate sandstone beds. The calcareous mudstones are slightly clayey micrites with scattered silt-sized carbonate and very rare quartz grains. The unit crops out between Smilcic village and Mejanica hill (Figs. 16C, 17). As in the case of Benkovac Stone Unit, the Debelo Brdo Unit probably extends farther to the east. This zone and lateral relation with the lower part of the Bribir Unit above Lisane village is covered by dense vegetation. Field observations suggest conformable, transitional boundary with the underlying Korlat and Ostrovica units (Figs. 18, 65).
An interval of marly mudstone beds has been revealed in the lower part of succession. These beds are massive, with very rare silty laminae. The marly mudstone contain large benthic foraminifera (nummulitids, discocyclinids) and small pelagic globigerinids of Late Eocene age. The marly interval is about 10 m thick in the area of Debelo Brdo hill and is gradually thinning in southeastern direction so that its thickness on Mejanica hill is less than 2 m (Fig. 65).

Facies description and interpretation

Two sedimentary facies have been distinguished in the Debelo Brdo Unit:

Mudstone facies

This mudstone facies forms beds 10-40 cm thick and laterally extensive, interspersed with 1-5 mm thick silty laminae in the form of flat streaks and distinct lenses with signs of pinch-and-swell lamination similar to 'rolling-grain' ripples. The interlayers usually show normal grading from coarse to fine silt, and many have slightly erosional bases. The vertical spacing of these interlayers varies from a few centimetres to 50 cm, and they are commonly disrupted and deformed by animal burrows (Fig. 63A). This facies is very similar to facies M of the Benkovac Stone Unit.

Sandstone facies

These are 0.2-3 cm thin, very fine sandstone beds in the form of distinct and laterally connected, 10-12 cm long lenses. The lenses have uneven or undulatory erosive basis. Their tops are occasion-ally transitional to the overlying mudstone. The lenses commonly show ripple cross-lamination or pinch-and-swell internal lamination and represent sediment-starved translatory ripples (Fig. 63B). Many of these sandstone beds are moderately burrowed. This facies is very similar to subfacies S5c described in the Benkovac Stone Unit.

This facies assemblage indicates deposition below the average storm wave base (offshore zone). The calcareous mudstones represent quiet-water sedimentation during the inter-storm periods accompanied by widespread biogenic activity. The fallout of hemipelagic muddy suspension was frequently interrupted by sparse incursions of silt, which can be attributed to weak tidal currents and/or minor seasonal storms. The sediment-starved ripples and the general lack of deposits analogous to subfacies S5a and S5b found in the Benkovac Stone Unit indicates that only few, density-modified (turbidity-driven) geostrophic currents have reached this distal shelf zone.

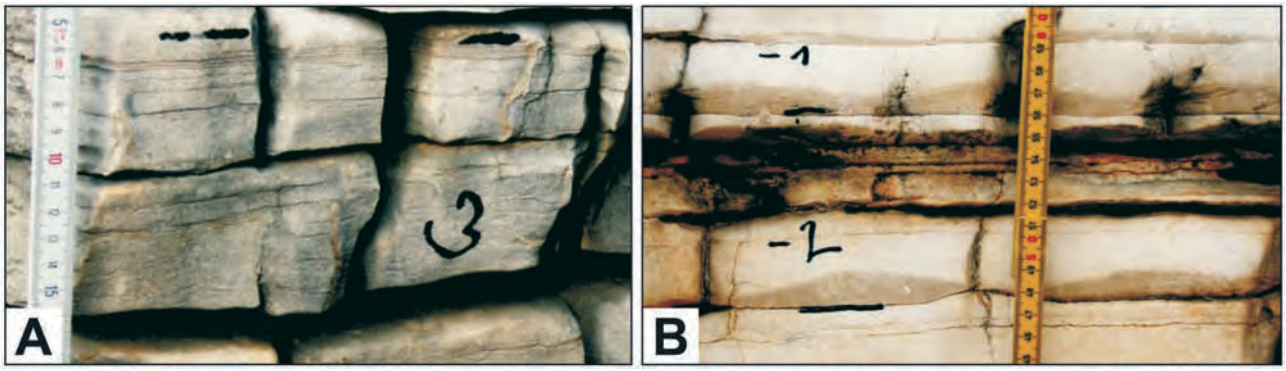

Fig. 63: A portion of the deposits depicted in log Debelo Brdo (see Fig. 65). **(A)** Mudstone facies with 1-5 mm thick silty laminae in the form of flat streaks and distinct lenses with signs of pinch-and-swell lamination. The laminae show normal grading from coarse to fine silt, and many have slightly erosional bases. The vertical spacing of interlayers varies from a few millimetres to 3 cm. **(B)** Very fine sandstone beds in the form of distinct and laterally connected, 10-12 cm long and 0.2-1.5 cm thick lenses. The lenses have undulatory erosive basis and show ripple cross-lamination. The underlying and overlying deposits are mudstone beds with silty laminae.

Appendix 5
The Otavac Unit

Description

The Otavac Unit (Otavac Unit is named after Otavac hill located 3 km northwards from Lisicic village**)** overlies the Benkovac Stone Unit. It is a ~100 m thick succession of carbonate conglomerates, sandstones and subordinate mudstones that crops out as a broad, NW-SE trending belt located in area of low topographic relief covered with dense vegetation (see Figs. 17, 18). An erosional unconformity between the basal conglomeratic beds of the Otavac Unit and the heterolithic deposits of the Benkovac Stone Unit defines a clear boundary between these units (Fig. 64). The Otavac Unit is probably coeval with the upper part of the Bribir Unit (Fig. 17).

The conglomerates are clast-supported and typically have a bimodal grain-size distribution, with a pebble framework and sand- to granule-size matrix. Gravel clasts are subrounded to rounded, derived from Cretaceous limestones and sub-ordinately also from rocks of Palaeogene, Jurassic and Triassic age (rare fragments of sandstone, marl, chert, dolomite and rudist molluscs). The conglomerates form sheet-like and lenticular beds 0.3-2.5 m thick, with uneven erosional bases, crude planar or gently inclined stratification and commonly also a tractional, 'rolling' clast fabric of *a*(t)*b*(i) type. Their lateral extent is estimated to be at least several hundred metres. The conglomerate sheets are most often isolated, both underlain and overlain by sandstones or occasionally mudstone facies.

The calcareous sandstones are mainly coarse-grained, but include also very fine, fine- and medium-grained varieties, and are similar in their mineral composition to the sandstone facies of the Benkovac Stone Unit. Granules are commonly scattered in coarse-grained sandstones. Sandstone beds are 0.1-1.5 m thick and show planar cross-, trough cross-, planar parallel, low-angle inclined and locally hummocky or swaley cross-stratification. Some beds are nearly massive ('structureless') and amalgamated into units 3-4 m thick.

The calcareous mudstones are silt-streaked with moderate to abundant bioturbation and similar to those in the Benkovac Stone and Debelo Brdo units. They form 5-40 cm thick isolated layers or up to 2.5 m thick units of stacked mudstone beds.

Interpretation

The lenticular conglomerates represent mouth bar gravels deposited on a braidplain delta front. The sheet-like conglomerates can be interpreted as beach gravels generated by reworking and lateral redistribution of mouth bar gravels.

The coarse- to medium-grained and 0.5 to 1.5 m thick sandstone beds amalgamated into 3-4 m thick units with planar or trough cross-stratification and locally with swaley cross-stratification or nearly massive can be attributed to storm-affected shoreface deposits. The fine- to very fine-grained and less than 0.5 m thick sandstone beds with planar parallel, low-angle inclined and hummocky cross-stratification, interbedded with 5-10 cm thick mudstone beds can be attributed to storm-affected deposits of offshore-transitional zone.

The isolated mudstone beds and the mudstone units composed of stacked mudstone beds indicate deposition in offshore zone (below the average storm wave base).

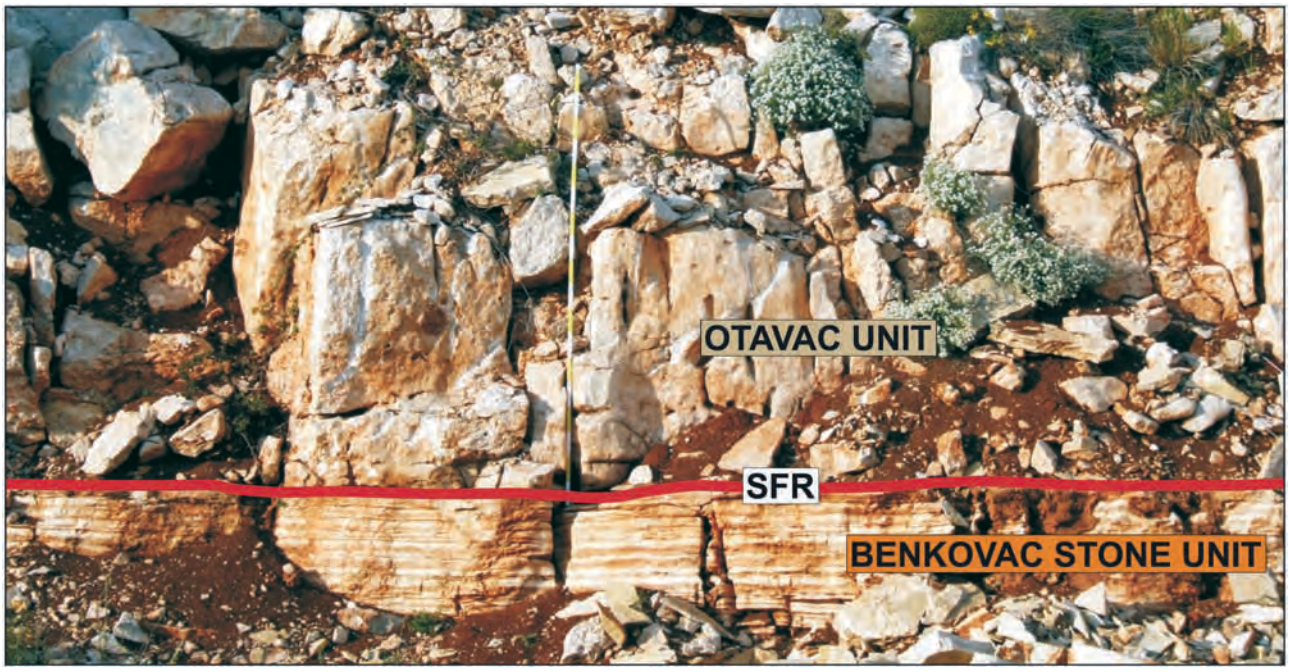

Fig. 64: Sharp and erosional boundary between mouth-bar conglomerates (Otavac Unit) and heterolithic deposits of offshore-transitional zone (Benkovac Stone Unit) (modified after Pencinger 2012). The erosional disconformity is here interpreted as a surface of forced regression. Log LI. The scale is 180 cm.

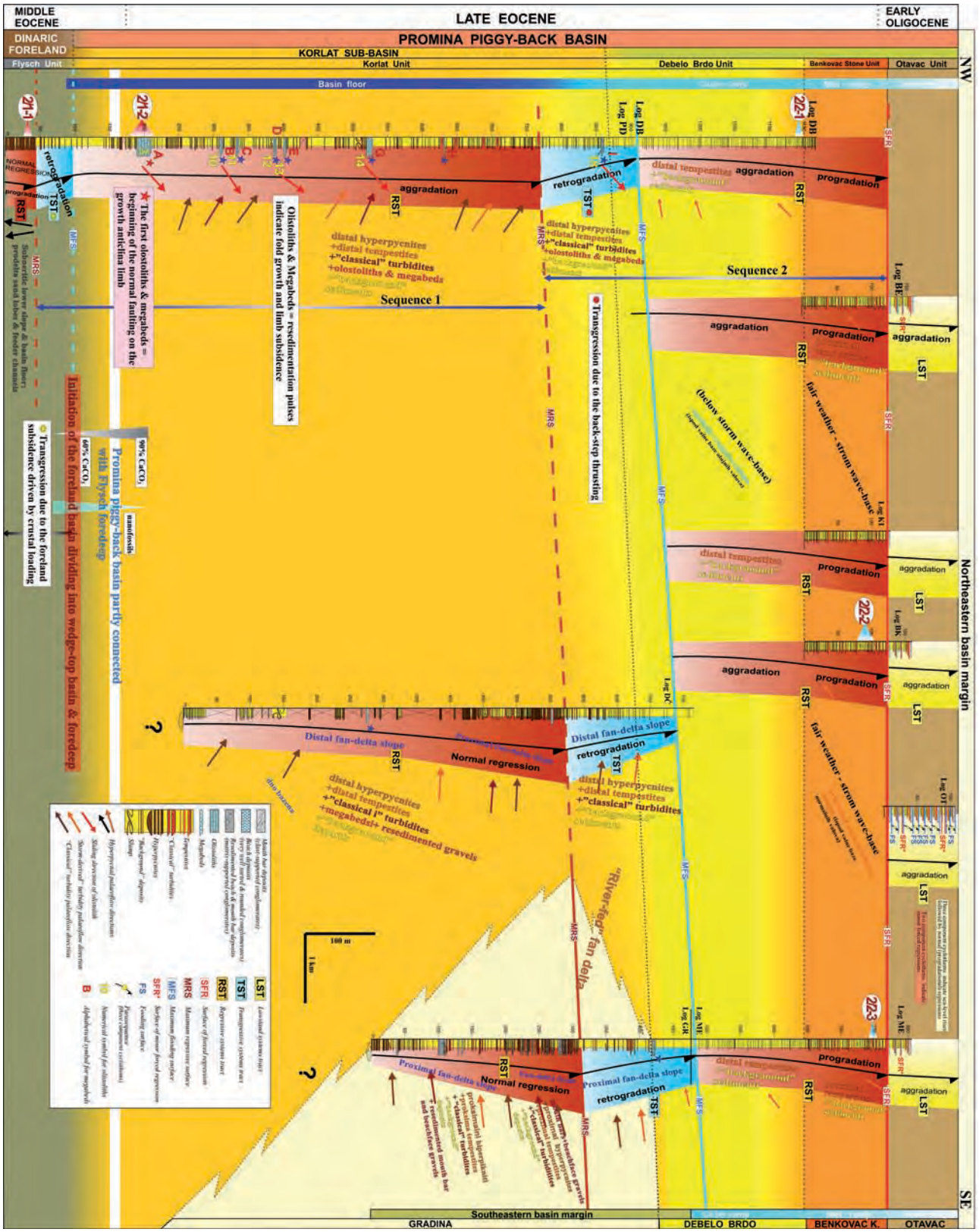

Fig. 65: Interpretative log-correlation panel showing stratigraphic distribution of the middle Eocene Flysch Unit and the middle to late Eocene Promina Beds Unit and their sequence-stratigraphic interpretation (modified after PENCINGER 2012). The log correlation pertains to the area between Korlat and Lisicic village.

The three component facies of the Otavac Unit tend to form two types of coarsening-upward cyclothems comprising either mudstone-sandstone-conglomerate or more rarely mudstone-conglomerate. At least 12 such cyclothems, each several metres thick, have been recognized as stacked upon one another in the stratigraphic succession. The cyclothemic organization of the Otavac Unit can be attributed to a series of minor relative sea-level rises. The three component cyclothems (mudstone-sandstone-conglomerate) indicate sea-level rises followed by normal (progradational) regressions. They are bounded by flooding surfaces and therefore can be also interpreted as parasequences (Fig. 65). The sporadic two component cyclothems (mudstone-conglomerate) may indicate minor forced regressions and in this case erosive disconformity between mudstones and conglomerates represent a surface of forced regressions (see Fig. 65). It should be noted that sporadic two component cyclothems may also represent episodes of a rapid shoreline advance due to extreme river floods combined with powerful storms.

Appendix 6
The Ostrovica and Bribir Units

The Ostrovica and Bribir unit are not subject of the field trip, but are relevant to its topic and hence are characterized briefly here for completeness.

The Ostrovica Unit

This unit is an about 600-m thick succession of the middle to late Eocene age (coeval with the Korlat and Gradina units), that crops out on very wide area between Lisane village and Skradin town (see Figs. 15, 16B, 17). The unit is underlain by Flysch deposits. This boundary is poorly visibly due to dense vegetation. The boundary with underlying Bribir Unit is erosive and clearly visible on the field. The Ostrovica succession is characterised by monotonic alternation of 5-40 cm thick and laterally continuous beds of biocalcarenites and marly biocalcarenites (Mrinjek 2008). The marly limestones vary from wackestone to packstone type. The beds commonly underwent the highest degree of bioturbation and therefore appear "structureless" (massive). The hummocky- and planar parallel-stratification can be seen only sporadically. Quartz and clay grains are present up to 25 vol. % except in the top part of succession where their presence is negligible. The macrofossils fragments (bivalves, gastropods, corals, bryozoans, echinoids, plant fragments) and microfossils (fragments or whole tests) are very common. The foraminiferal fauna contain larger benthic foraminifera (nummulitids) and small rotaliids, miliolids, textulariids (*Haddonia* sp.), *Operculina* sp. and orthophragminids (*Discocyclina* sp., *Asterocyclina* sp.). The rate of planktonic foraminifera slowly decreases going from the lower to the upper part of unit. The laterally persistent 5 to 30 cm thick intervals within beds with stream oriented nummulits, bryozoans, gastropods and corals can be frequently seen within marly limestones and marls.

The rarely seen structural characteristics and fossils content suggest deposition in the offshore-transitional and offshore zones affected by discrete storm events, relatively high sediment supply and continuous basin subsidence, with probably frequent minor changes in relative sea-level during the highstand normal regression. The general shallowing upwards trend of the succession (the highstand normal regression) is indicated by decreasing rate of planktonic foraminifera.

Bioclastic mud mounds interbedded with marly limestones and marls outcrop within Ostrovica succession in the area of Lisane village (Fig. 17). The mounds are 0.5-3 m thick and up to 110 m wide slightly convex-up lenses, spherical to elliptical in plan view. They are composed of nodular and/or well bedded wackestone and floatstone with various bioclasts including solitary corals, bivalves, rare gastropods, echinoid plates and spines, bryozoans, coralline algae and foraminifers (among which rotaliids, miliolids, textulariids, *Asterigerina*/*Amphistegina* sp., *Operculina*, *Nummulites*, *Orbitoclypeus*). Coralline algae largely encrust the sediments and form small rhodoliths. Scattered coral colonies are not preserved as a framework. The mounds are local carbonate factories "installed" in the photic zone on topographic ridges (incipient blind-thrust anticlines).

The Bribir Unit

This unit is an about 100-m thick succession of late Eocene age that consists of six carbonate conglomerate bodies interbedded with packages of carbonate sandstone and mudstone beds (Mrinjek et al. 2007, Mrinjek 2008).

Lenticular and sheet-like conglomerates are 4-10 m thick and laterally very extensive (500-1000 m in strike direction). The lenticular conglomerates represent mouth bar deposits (proximal delta front) of a large fan-toe braidplain delta whereas the sheet-like conglomerates can be interpreted as beach gravels generated by reworking and lateral redistribution of mouth bar gravels (see Figs. 16C, 17).

The thicker and commonly amalgamated sandstone beds of the upper part of the 5-8 m thick, sheet-like sandstone-mudstone packages can be interpreted as distal delta front facies deposited in the shoreface zone sporadically affected by storms. The thinner sandstone beds interbedded by mudstone beds of the lower part of the packages represent the prodelta facies deposited bellow the average fair-weather wave base.

The sandstone-mudstone packages with overlying conglomerates bodies stacked one upon another form 6 recognizable coarsening-upwards parasequences that represent series of minor relative sea-level rises during lowstand normal regression.

4. Topic Three: Miocene lacustrine basins

Miocene intra-montane lacustrine basins of Outer Dinarides (Croatia and Bosnia and Herzegovina)

OLEG MANDIC, ALAN VRANJKOVIC, DAVOR PAVELIC, HAZIM HRVATOVIC & ARJAN DE LEEUW

4.1. Introduction

During the period of substantial Miocene climatic changes (Fig. 66), a series of long-living lakes occupied the intra-montane basins (Fig. 67) of the Dinaric Alps in Southeastern Europe (HARZHAUSER & MANDIC 2008, 2010, JIMÉNEZ-MORENO et al. 2008, DE LEEUW et al. 2010, 2011, 2012, MANDIC et al. 2011, 2012). Settled on the western margin of the Dinaride-Anatolian Island landmass (Fig. 66), they occupied a highly interesting palaeogeographic position sandwiched between the Paratethys and the proto-Mediterranean seas (Fig. 68) in an area known to be highly sensitive to climatic changes (RÖGL 1999, HARZHAUSER & PILLER 2007). The origin and disintegration of lacustrine settings were bound to the post-collisional tectonic evolution of the Dinaride fold and thrust belt (SCHMID et al. 2008). After the southwestwards back-stepping of wedge-top molasse basins in the Early Oligocene (KORBAR 2009), dextral strike-slip movement on the Periadriatic and mid-Hungarian sutures during the Late Oligocene were compensated in the Dinarides by tectonic wrenching (HRVATOVIC 2006). Accommodating the extension from the back-arc rifting in the Pannonian basin, the longitudinal strike-slip faults become reactivated in the Early Miocene allowing the subsidence and accumulation of large sediment piles (Fig. 66) in the intra-montane basins (ILIC & NEUBAUER 2005, DE LEEUW et al. 2012).

The Dinarid Lake System (DLS) formed in the early Miocene in today NW-SE trending intra-mountain basins between the slowly rising Dinarid mountain chains (DE LEEUW et al. 2012). The comparatively low terrigenous input supported the diversification of lacustrine environments, including both deep- and shallow-water habitats. This habitat diversification sparked the spectacular Miocene radiation of the benthic fauna (HARZHAUSER & MANDIC 2008, 2010). Subsequent rifting in the Pannonian Basin System triggered the marine flooding of the northern DLS area and reduced its extension to the External Dinarides. Geographically, the deposits of the

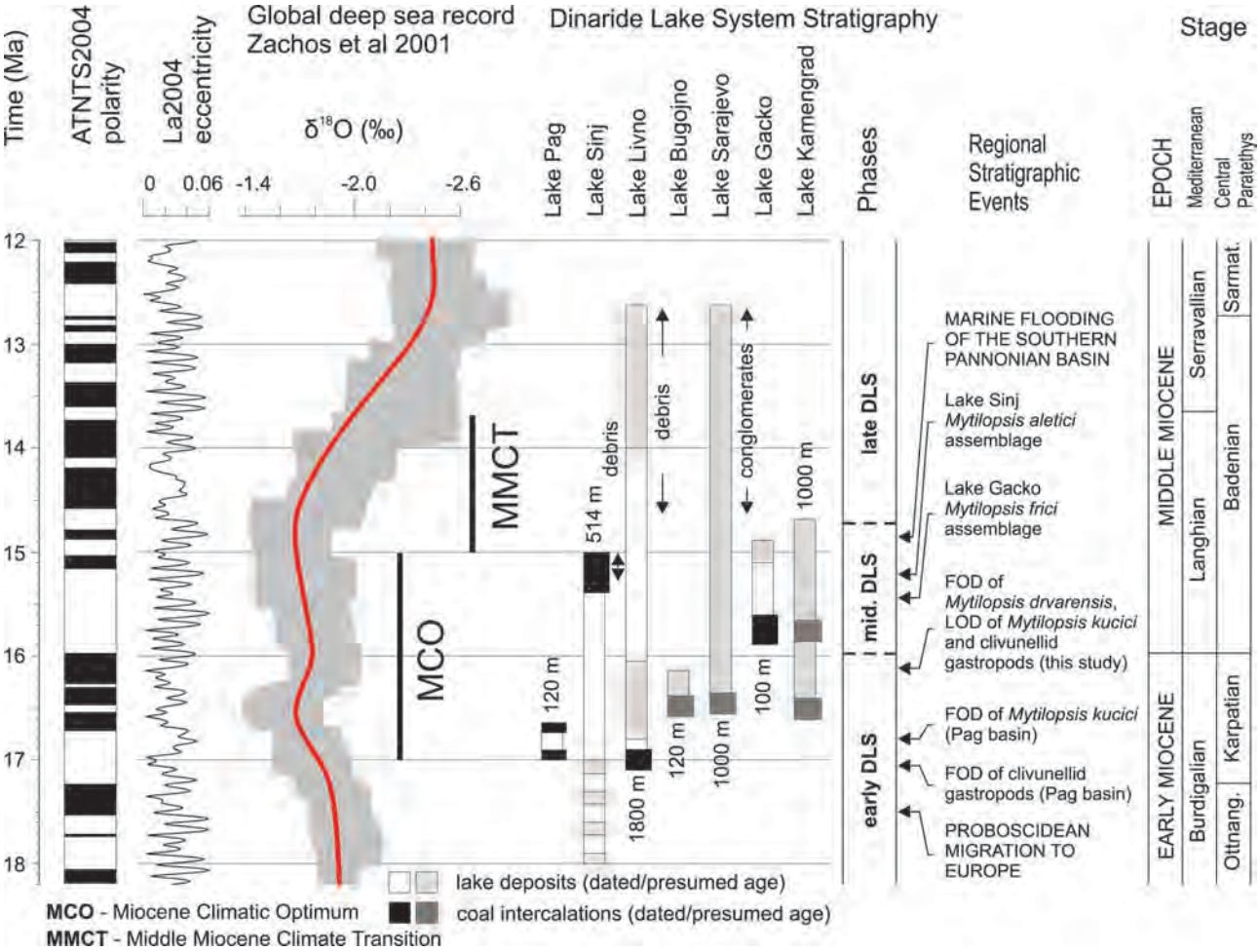

Fig. 66: MCO, MMCT and their stratigraphic correlation with DLS successions. Coal seams and detritic beds in the sections from the Dinaride intra-mountainous basins are indicated. The DLS stratigraphy is based on results from integrated Ar/Ar geochronology and magnetostratigraphy (modified after DE LEEUW et al. 2011).

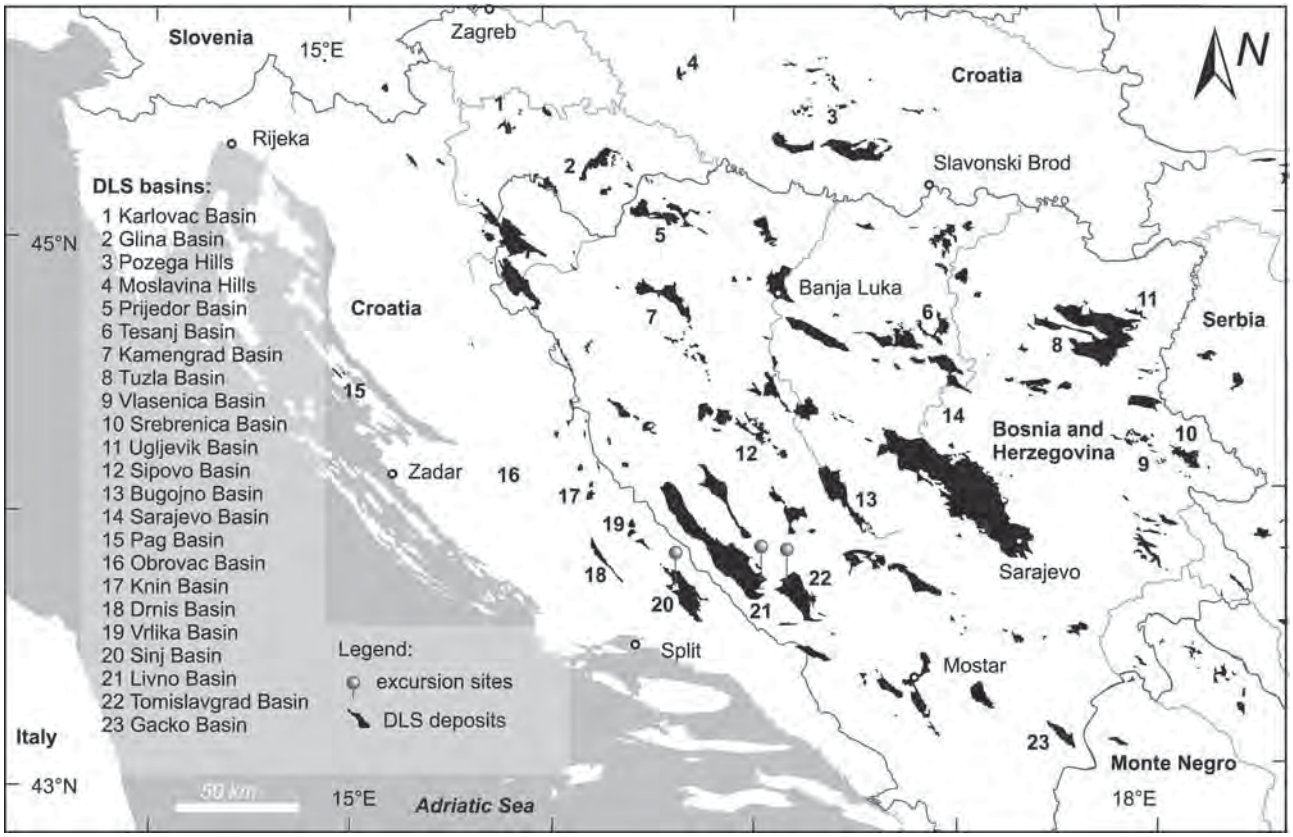

Fig. 67: Distribution of Miocene lacustrine deposits attributed to the Dinaride Lake System (data from basic geological map M 1:100.000 of former Yugoslavia). Positions of excursion sites are indicated.

DLS cover parts of Croatia, Bosnia and Herzegovina, Montenegro, Serbia, Hungary and Slovenia (Fig. 67). During its maximum extent, the lake system covered an area of ca. 75.000 km^2.

The long-living lakes left up to 2000-m-thick sedimentary successions distributed across the Dinaric Alps (Figs. 66 and 67). The current investigations provided a deep-time window to DLS in constructing the integrative Ar/Ar geochronologic and palaeomagnetic age model for its key basins (De Leeuw et al. 2012). Those results supported the establishment of a powerful bio-magnetostratigraphic tool allowing the stratigraphic correlations and a precise insight into the complex environmental history of that previously less-known region. In particular it could be demonstrated

Fig. 68: Palaeogeographic setting of the Dinaride-Anatolian Island during the early Middle Miocene (modified after Rögl 1999).

Fig. 69: Positions of excursion sites in the Dinaride intra-montane basins filled by Miocene lacustrine deposits of the Dinaride Lake System (data from basic geological map M 1:100.000 of former Yugoslavia).

that the lakes recorded a suite of climatic parameters (Jiménez-Moreno et al. 2008, 2009; Mandic et al. 2009, 2011, Harzhauser et al. 2012). Moreover the lake level changes in Pag (Jiménez-Moreno et al., 2009) and Gacko (Mandic et al. 2011) basins were proven as cyclic and presumably driven by astronomical forces. The captured fluctuations therein provide actually a high-resolution archive that considering its length allows not only establishing relations between the global warming and its regional effects but also the weighting of the potential effect of MMCT (Holbourn et al. 2005, Lewis et al. 2008) and regional geodynamics to its disintegration.

In particular the early and the middle DLS stages (Fig. 66) coinciding with the MCO comprise partly vast coal deposits. Its late DLS stage is characterised in contrast by depositional hiatus or introduction of coarse clastic sedimentation. Yet, whereas in the northern DLS, thick successions of fluvial conglomerates are known from the Sarajevo Basin (Hrvatovic 2006), such conglomerates are missing in the southern DLS including the Tomislavgrad-Livno and Sinj basins (Fig. 68). There local debris flow deposits (sandstones and breccias) are recorded between ~15.2 and ~15.0 Ma in the Sinj Basin (Mandic et al. 2009, De Leeuw et al. 2010) and between 14.8 and ~13.0 Ma in the Tomislavgrad-Livno Basin (De Leeuw et al. 2011). In all three basins the coarse clastic deposition coincide with the terminal phase of the main DLS depositional sequence indicating synsedimentary tectonics and relief building as cause for basinal inversion terminating the lacustrine deposition in the late Middle Miocene. The three southern intra-montane basins of the Outer Dinarides will be visited to show the late syn- to post-orogenic sedimentation within the orogenic belt.

The Sinj Basin (Fig. 70), with a surface area of ~140 km^2, is located in the hinterland of Split in SE Croatia. Its sigmoidal plan-view shape suggests an origin as a strike-slip basin, although the shape can as well be an artefact of post-depositional wrench-fault tectonics related to the formation of the South Adriatic strike-slip basin. The basin formed in a karst environment. Whereas the pre-Neogene basement is dominated by Mesozoic platform carbonates along the basin margins, extensive Permian evaporite deposits with a direct sedimentary contact with the basal lake sediments occur beneath the basin. Doming of those evaporites decreased subsidence rates within the basin. The presence of steep hinterland topography is pinpointed by massive breccia intercalations into marginal lake deposits. The basin-fill succession consists of fresh-water lacustrine limestones and marls, more than 500 m thick, with the lignite intercalations and large mammal remains in the uppermost part marking the ultimate shallowing of the basin. The late depositional phase is characterized by a cyclic architecture attributed to orbitally-forced regional climatic fluctuations. Based on the main range of δO^{18} values between -2 and -6 typical for freshwater settings, Harzhauser et al. (2012) interpret Lake Sinj as a pure freshwater system. The lake existence duration is estimated at about 3 Ma, between ~18 and ~15 Ma BP, correlating largely with the Miocene Climatic Optimum (De Leeuw et al. 2010). This ancient lacustrine basin is well known since the Darwin time for its strictly endemic mollusc fauna, serving as a textbook example of adaptive fauna radiation (Neubauer et al. 2011).

The Livno and Tomislavgrad (=Duvno) basins (Fig. 71) are located in the SW Bosnia and Herzegovina. They represent two different, tectonically-disconnected karst poljes developed at about 1000 m a.s.l. During the DLS deposition, they formed a single basin with an area of about 590 km^2, the second largest intra-montane basin in the Dinarides after the Sarajevo Basin. The basin-fill succession is more than 2000 m thick, comprising two depositional sequences bounded by an angular unconformity. The lower sequence is ~1700 m thick, composed of Early to Middle Miocene fresh-water deposits that commence with ~10 m thick coal bed bearing elephant remains and pass upwards into a monotonous, limestone-dominated lacustrine succession. At a stratigraphic height of ~850 m the first intercalation of margin-derived debris-flow deposits occurs. The successive coarse-clastic intercalations are thickening and coarsening upwards, including up to 10 m thick volcaniclastic beds. The succession culminates in megabreccia bed, ~26 m thick, near the top, which suggests strongly that active tectonics was the main cause for the cessation of deposition in the large original basin. The basin subsequently became split into two parts and the second cycle of sedimentation followed above an angular unconformity overlain by lacustrine claystones passing upwards into lignite-dominated deposits. The Holocene witnessed an expansion peat deposition. The Livno Basin, with an area of 410 km^2, is the largest karst peatland basin of the Dinarides.

4.2. Sinj Basin

Stop 3/3: Lucane section

Lucane section (Fig. 72) is exposed along the Sutina Creek W of Sinj (top at N 43°43'11'' E 16°35'25''). Located at the western margin of the Sinj basin it allows the study of the complete infill succession (Fig. 70). Already described by Kerner (1905) it was currently a subject of multiproxy investigation campaign providing new data on stratigraphy, depositional history, palaeobiology, and palaeoclimatology (Jiménez-Moreno et al. 2008, Mandic et al. 2009, De Leeuw et al. 2010, Neubauer et al. 2011). It comprises two partially overlapping sections, representing together a continuous, around 500-m-thick record of lacustrine deposits. Magnetostratigraphic pattern together with facies correspondence prove their precise correlation. The uppermost beds include coal seam intercalations, whereas the basal and the middle part of the infill show exclusively carbonate rocks. The whole succession is intercalated occasionally by volcanic ash layers. Magnetostratigraphic study together with Ar/Ar dating of ash layer provided precise age model for the section proving its continuous sedimentation within a 3 my period from the latest Early to the earliest Middle Miocene (Burdigalian to Langhian) (De Leeuw et al. 2010).

Sedimentological analysis and petrography made it possible to distinguish eight main facies types in the Ostrozac succession (Vranjkovic 2011). Seven facies are carbonate

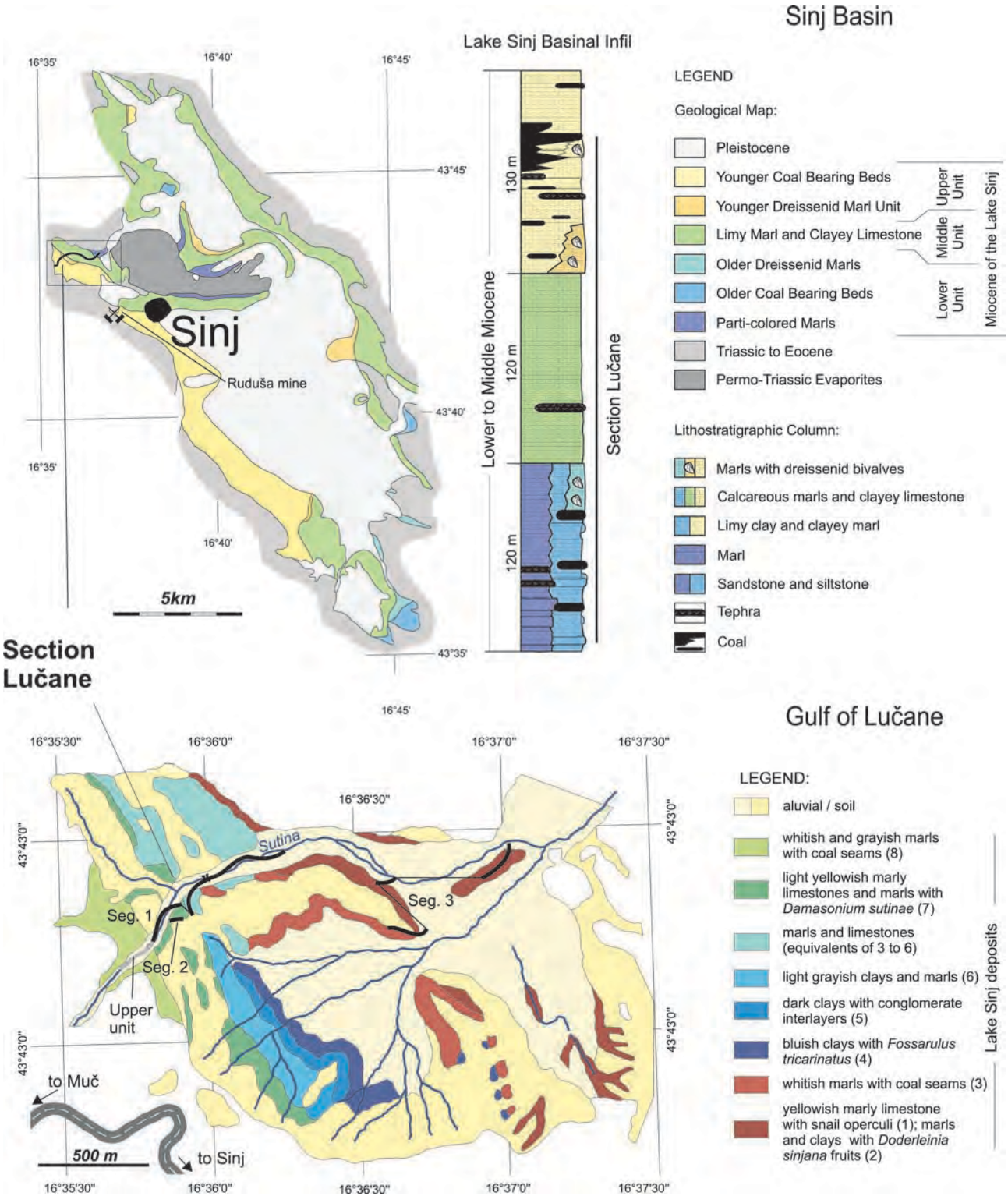

Fig. 70: Geological map of the Sinj basin with schematic lithological section through its infill (above) accompanied by detail geological map of the Lucane embayment (below) (modified after DE LEEUW et al. 2010).

in origin in addition to the coal and tephra facies:

(1) Micrite (Fig. 73a) - consists of very fine-grained lime mudstones. The deposition of the fine-grained components of lacustrine carbonates is dominantly induced by the photosynthetic activity of macrophytes and microphytes. It belongs to deeper and protected lake parts.

(2) Biomicrite (Fig. 73b) - mudstones and wackestones containing degraded, and/or carbonized plant remains, plant encrustations, most commonly related to the stems of the submerged Charophytes and fruits and stems of *Damasonium* plant. Rooted submerged

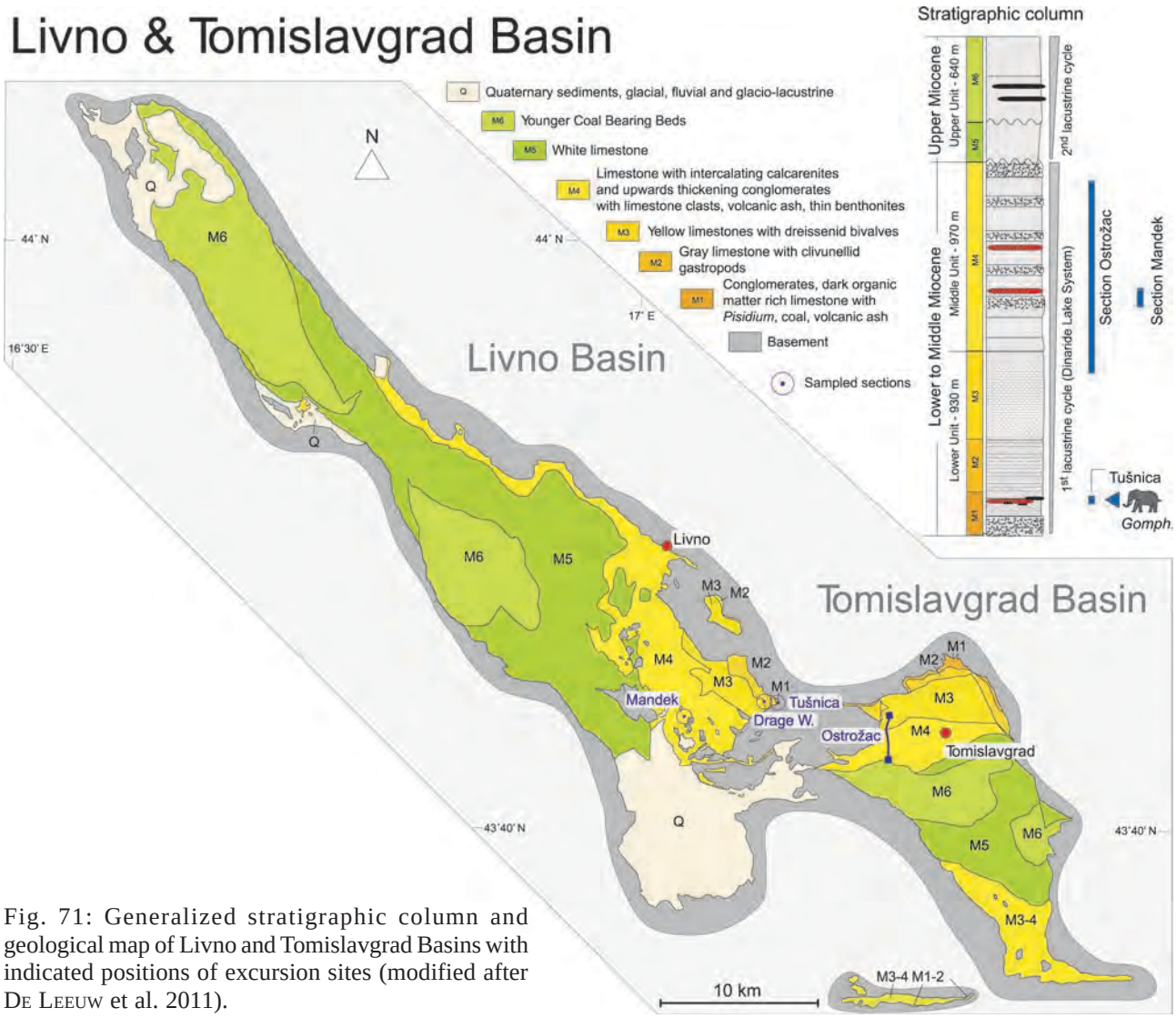

Fig. 71: Generalized stratigraphic column and geological map of Livno and Tomislavgrad Basins with indicated positions of excursion sites (modified after De Leeuw et al. 2011).

macrophytes indicate a vegetated littoral environment of the carbonate lake.

(3) Calcisiltite (Fig. 73c) - accumulation out of sediment-laden density currents (hyperpycnal flow; underflow) following expanded floods.

(4) Laminated micrite (Fig. 73d) - alternation of thin micritic laminae, and micrite to microsparite laminae containing Charophytes plant encrustations.

(5) Coquina - the association of gastropods, bivalves, ostracods, plant encrustations and predominantly oxidized macrophyte remains suggests a calm, very shallow fresh-water environment of a carbonate lake interrupted by higher energy events probably related to storms and earthquakes.

(6) Tephra/clays (Fig. 73e) - pyroclastic fall of volcanic ash derived from distant eruptions.

(7) Breccia - olistoliths and debris flow deposits transported basinward by gravity processes at the margin of the lake.

(8) Coal (lignite) - deposition of allochthonous phytoclasts took place in small delta topset at the mouth of a creek draining a vegetated marsh while 4 meters thick coal seam was accumulated in a swamp-marsh complex.

The ordinance of those facies types in the section proves a continuous record of a shallowing upward sequence for the Sinj basin infill. The sequence starts with basinal micrites and ends with a 4-m-thick peaty coal. Hence the dominant limestone deposition marks the lower and the middle part of the succession. Those limestones are usually light, thin to medium bedded, and commonly soft and porous. The $CaCO_3$ content varies between 82% and 99%, and it primarily refers to the calcite. Depositional environment changes in the uppermost part of the succession due to gradual shallowing of the lake and generally more humid climate (Jiménez-Moreno et al. 2008). The changing conditions resulted into cyclic appearance of coal seams alternating with limestone. That alternation was triggered by a short-term, orbitally forced cyclic fluctuation of humid and dry periods. That phase, characterized by stable hard-water lake conditions, witnessed a strong diversification of the ecosystem followed by a significant morphospace increase in melanopsid and hydrobiid snails (Neubauer et al. 2011).

The palaeoenvironmental analysis combining sedimentology, microfacies analysis, coal petrology and palaeoecology of molluscs and plant remains by Mandic

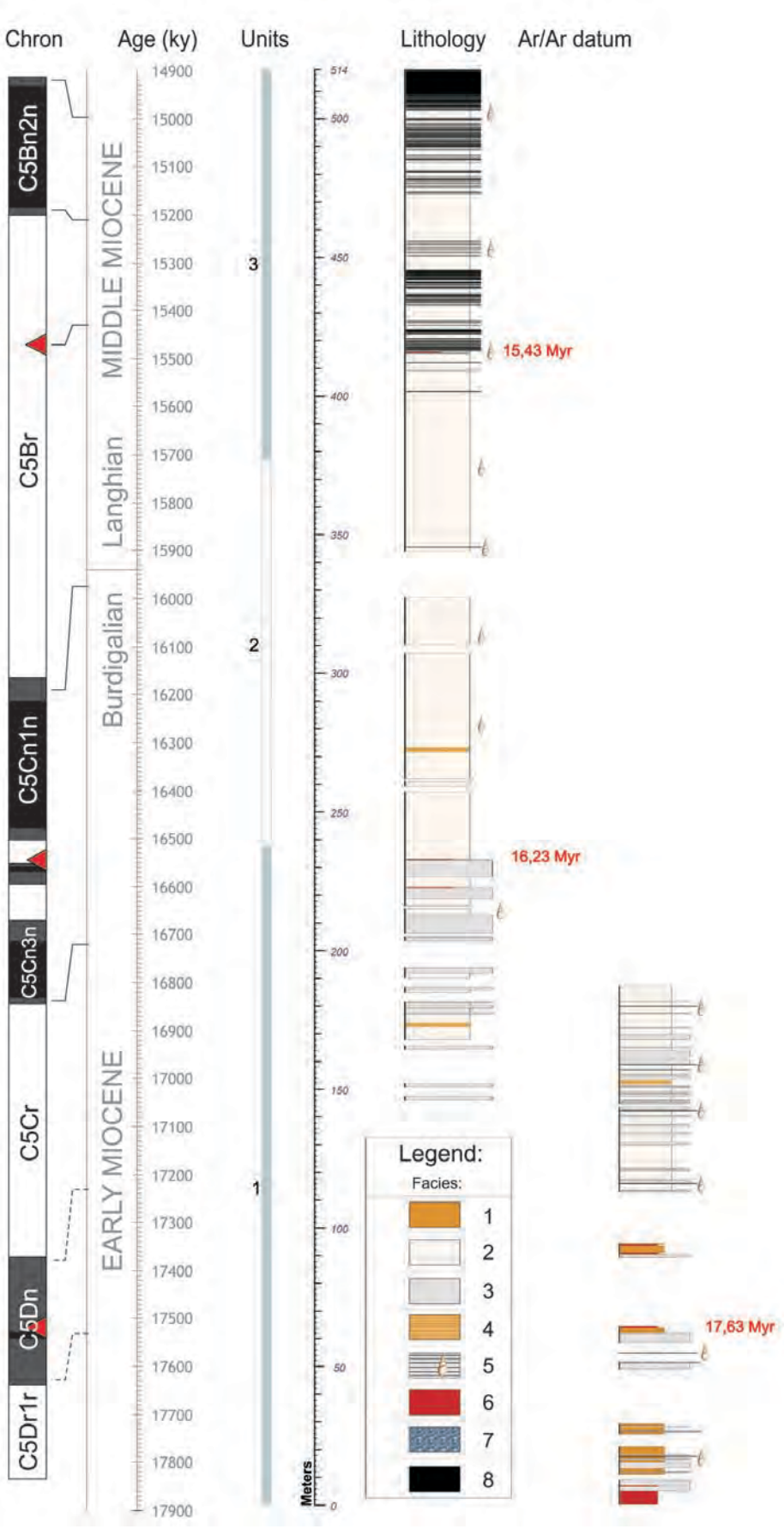

Fig. 72: Age model based on Ar/Ar geochronology and magnetostratigraphic results by DE LEEUW et al. (2010) and facies distribution in the Lucane section by VRANJKOVIC (2011).

et al. (2009), inferred a variety of environments for that part of the section including (1) littoral below the fair weather wave base, (2) littoral above the fair weather wave base, (3) infralittoral with vegetated areas dominated by aquatic, perennial plants, (4) low supralittoral to upper infralittoral with starfruit meadows, (5) areas covered by cyanobacterial mats, (6) carbonate marshes, (7) peripheral swamps, (8) stream catchments areas and vegetated marches, which were (9) more or (10) less frequently flooded. The latter environment was inhabited by large land mammals related to elephants and rhinoceroses.

4.3. Livno and Tomislavgrad Basins

4.3.1. Stop 4/1: Ostrozac Creek section

The 1700-m-thick Ostrozac section (Fig. 74) is situated near the NW margin of the Tomislavgrad basin. It follows the Ostrozac brook, running down the eastern slope of the Tusnica Mountain, for about 2 km. The brook strikes N-S, subnormal to the bedding that is ~150°/30° in the stratigraphically lower part of the section and ~170°/55° in the upper part of the section. The base (N43°43'40.5''

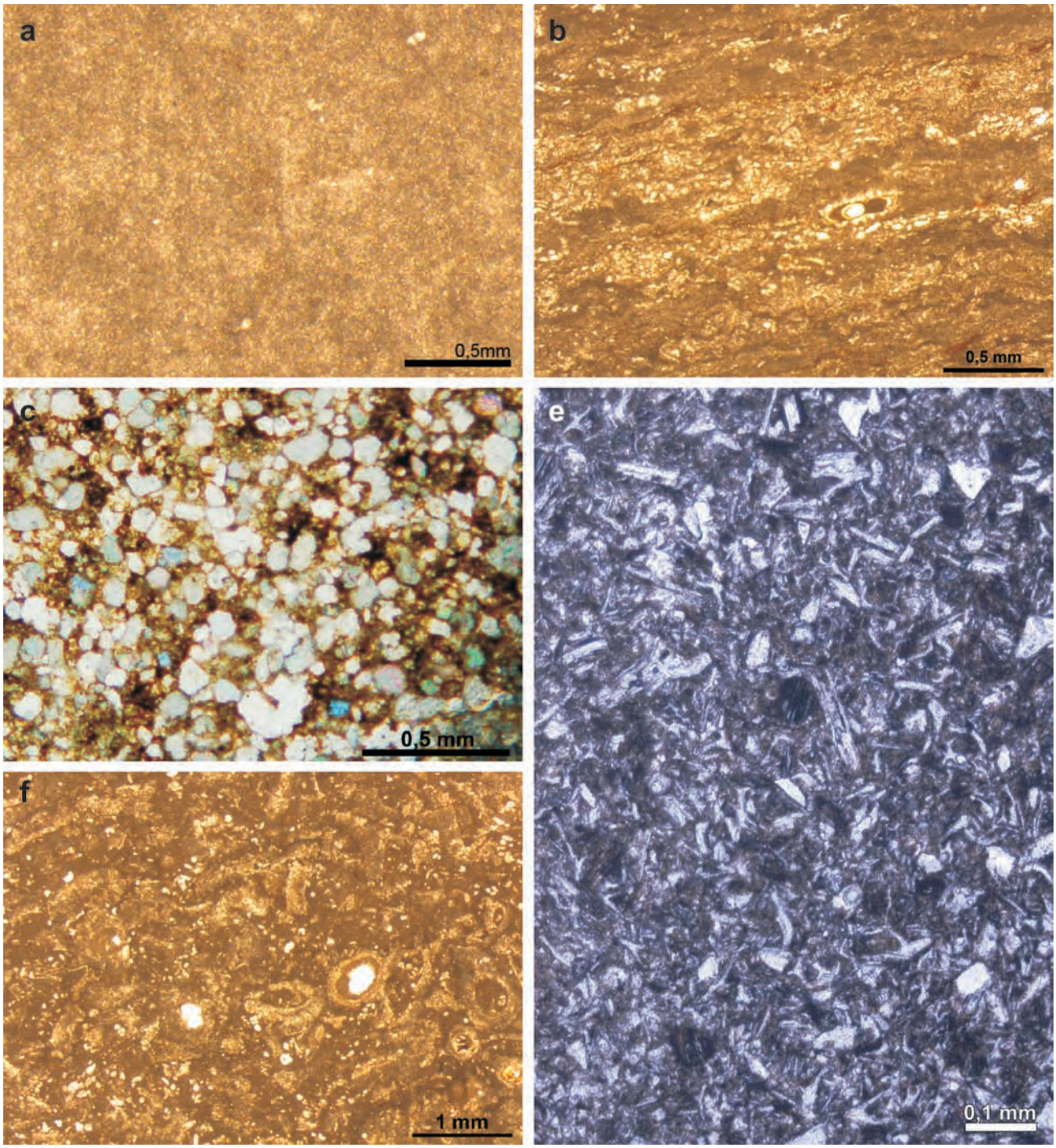

Fig. 73: Microfacies types recognised at Ostrozac section: a. Micrite, b. Biomicrite with characean remains, c. Calcisiltite made of idiomorphic, rhomboedral calcite crystals, d. Laminated micrite with completely preserved, compacted characean remains, e. Diagenetically alternated vitroclastic tuff.

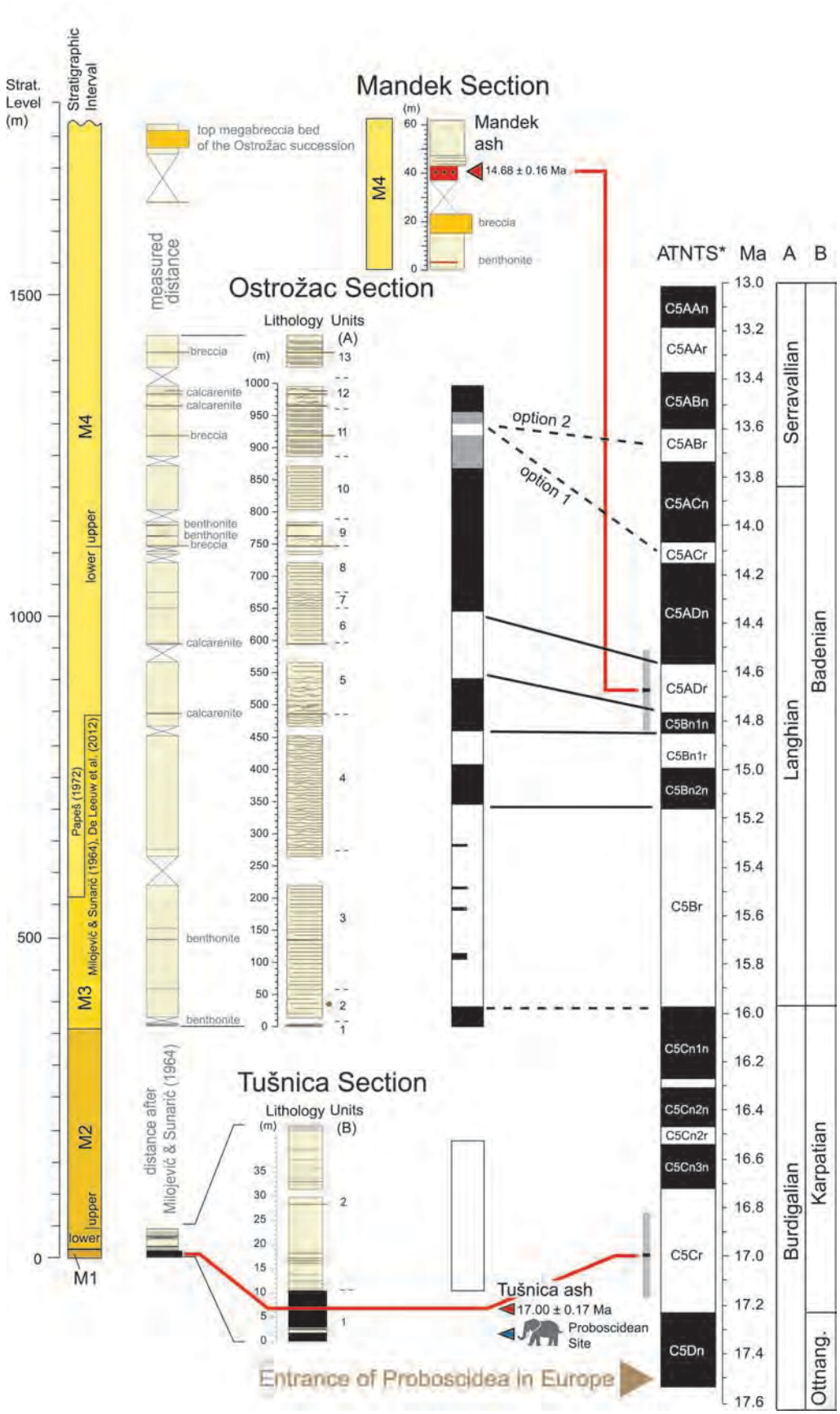

Fig. 74: Lithostratigraphy and lithology (see text for explanation) of three sections representing the main (DLS related) cycle of the basinal infill in Livno and Tomislavgrad Basins accompanied by magnetostratigraphic and geochronologic results by DE LEEUW et al. (2011). ATNTS. Astronomically Tuned Neogene Time Scale by LOURENS et al. (2004). A. Mediterranean (standard geological) stages. B. Central Paratethys stages (modified after DE LEEUW et al. 2011).

E17°10'59.6'') is located about 150 m N of the place where the path to Eminovo Selo meets the road to the abandoned Vucipolje coal mine. The top (N43°43'40.5'' E17°10'59.6'') reaches the town of Josanica where a large megabreccia crops out just north of a large curve in the main road to Tomislavgrad. The section comprises 13 lithostratigraphic units ordered below from the base to the top.

Unit 1 (8.2 m) is made by light coloured lacustrine limestones intercalated by clay layers and volcanic ash beds. These already pertain to stratigraphic interval M3. The well bedded limestone, light beige, gray, yellowish or brownish in colour, is dominantly fine-grained, although some coarser-grained intervals are present as well. The beds are around 10 cm thick. The intercalations are at maximum 20 cm thick and are predominantly found in the lower part of the unit.

Unit 2 (49.6 m) is an interval of brownish limestone with roots of water plants (Fig. 75a) follows. The limestone is somewhat softer than before.

Unit 3 (215.9 m) comprise thick interval of planar bedded limestones (Fig. 75b) with a bed thickness of 5-20 cm. In this interval, plant remains disappear completely. A single bentonite layer appears in its middle part.

Unit 4 (211.2 m) shows ripple bedded limestones (Fig. 75c, d) with only few plain bedded intervals. The ripples are commonly about 1 cm thick and there's about 10 cm of distance between consecutive crests. Some intercalations of plant remains occur in association with horizons of coarser grained limestone.

Unit 5 (111.2 m) starts with an about 5 cm thick calcarenite layer situated within laminated limestones with plant-stems preserved on its bedding plains. Ripple and trough cross beds characterize this unit. Slump and channel structures occur in combination with more calcarenite intercalations. These are red or brownish in colour and consist of badly sorted, angular lithoclasts.

Unit 6 (54.0 m) is dominated by bedded limestone (Fig. 75e), Unit 7 (24.4 m) by ripple bedded limestone, whereas Unit 8 (72.2 m) represents a thinning upward succession of bedded limestone.

Unit 9 (42.0 m) dominantly composed of alternating cross-bedded and massive limestones starts with the initial breccia layer of the Ostrozac succession. The breccia is about 2 m thick and consists of angular, badly sorted carbonate lithoclasts from basement rocks. Two, up to 0.5 thick, volcanic ash layers occur in this unit as well. Both the tephra and breccia beds are laterally continuous and can be traced for at least several 100 m. The breccia thickens in westward direction.

Unit 10 (97.2 m) of thick bedded limestones is followed by Unit 11 comprising the thin bedded limestone with intercalated calcarenite layers (Fig. 75f) and inversely graded breccias (Fig. 75g). Unit 12 (48.3 m) displays a unique carbonate facies with frequent micro-breccia intercalations and ooid intervals.

Unit 13 (394.9 m) the topmost interval is badly exposed due to valley infill through artificial lake. It consists of marly limestones with recurrent breccia intercalations. The topmost breccia (Fig. 75h) is a 26.3 m thick megabed with limestone blocks of up to 2 m in diameter. More marly limestones follow up to the discordant contact (Milojevic & Sunaric 1964, Papes 1975) with the deposits of the younger lacustrine cycle. The measured thicknesses and the succession of lithologic units correspond very well with data presented by Milojevic & Sunaric (1964).

The strata exposed in the lower part of the Ostrozac section are indicative of predominantly shallow water conditions. The rippled structure of these limestone beds points out that they accumulated in the shallow littoral zone. The calcarenites and breccias that characterize interval M4 are badly sorted, which implies short transport. We interpret them as debris-flows indicative of local seismic activity in conjunction with uplift of the basin margins from which the material originates. The coarsening upwards sequence, which these calcarenites and breccias built, preludes the end of the first lacustrine phase.

The angular discordance between the first and second lacustrine cycle provides additional evidence for tectonic activity at the end of the first lacustrine phase. This interpretation is in line with that of Milojevic & Sunaric (1964) and Papes (1975), who suggested that uplift of the Tusnica Mountain began during deposition of Unit M4. They postulate that this divided the Livno-Tomislavgrad basin in two. During the second lacustrine phase, two independent lakes developed.

4.3.2. Stop 4/2: Tusnica Coalpit section

The 45 m thick Tusnica section (Fig. 74) is located in the Drage opencast coalmine situated at the foot of the Tusnica Mountain near the eastern boundary of the Livno Basin (Fig. 71). It was logged along the SSE-NNW striking wall of the quarry. The base of the section is situated at N43°44'17.3'' E17°05'35.0'' (WGS84) and the top at N43°44'19.2'' E17°05'32.9''.

The lower 10.5 m of the section are dominated by coal subdivided in three seams. The lower two seams are separated by a ~1 m thick organic material rich sandy limestone interval with lymneid snails and plant remains. A volcanic ash bed separates the middle and the upper coal seam (Fig. 76a). The ash layer is ~20 cm thick, laterally continuous, grayish-whitish in colour, and consists of sandy and silty clay with dark mica flakes. The transition from coal to ash and vice versa is very sharp. A transitional zone with clayey and coaly inter-layers starts above the upper coal seam. It is followed by dominantly dark brown and grayish well bedded limestones (Fig. 76b) rich in organic matter that dominate the remaining 30 m of the section. These beds belong to interval M2 (Milojevic & Sunaric 1964) and contain scattered fish and plant remains. In the main coal seam, remains of *Gomphoterium angustidens* were found and Malez & Sliskovic (1976) therefore considered it to be of Middle Miocene age. The same level was, in contrast, thought to pertain to the upper part of the Early Miocene based on its pollen content (Pantic 1961). $^{40}Ar/^{39}Ar$ measurements reveal that the Tusnica volcanic ash, found in between the coal seams at the base of the basin infill, is 17.0 ±0.17 Ma old (De Leeuw et al. 2011). Milojevic & Sunaric (1964) described coal seams and organic matter rich limestone beds of Tusnica

Fig. 75: Ostrozac section: a. Subaquatic plant root remains. b. Well bedded limestone. c. Ripple bedded limestone. d. Trough cross-bedded limestone. e. Bedded limestone of the unit 10. f. Calcarenite intercalation. g. Breccia of the unit 11. h. Top megabreccia.

Fig. 76: Tusnica Coalpit: a. Three coal seams delineated by carbonate (below) and ash layer (above). b. Organic rich, well bedded limestone.

type from the abandoned Vucipolje coal mine at 1 km lateral distance from the base of the Ostrozac section. They apparently belong to the same coal bed disturbed tectonically due to rise of the Tusnica mountain block.
The coals exposed in the Tusnica and Vucipolje testify of swamp conditions during the initial phase of basin formation. Coal formation is terminated when the basin floods and a long-lived lake establishes itself. As the lake deepened suboxic bottom conditions developed, as indicated by the organic matter rich limestones of the Tusnica mine and overlying clivunellid limestones (Unit M2). Although the clivunellid bearing interval M2 is in general badly exposed in the Livno as well as the Tomislavgrad basin, fragments crop out at Drage West site located about 300 m W of the main entrance to the Tusnica coalmine (N43°44'29.0'' E17°04'55.6'').
The little quarry displays there light and dark brownish bedded limestones with endemic deep water gastropod *Clivunella katzeri*, small dreissenid bivalves and plant remains such as *Taxodium*-related *Glyptostrobus europaeus* and pertains to the upper part of interval M2. The clivunellid limestone interval is about 300 m thick (Milojevic & Sunaric 1964) and reaches up to the base of the Ostrozac section (De Leeuw et al. 2011).

4.3.3. Stop 4/3: Lake Mandek section

The Mandek section (Fig. 74) is located 10 km south of Livno, just E of the Mandek village, on the shore of artificial lake Mandek (Fig. 71) and belongs to stratigraphic unit M4. The section was logged from North to South along the gulley of the Vojvodinac brook (Fig. 77a) which runs normal to the bedding. The outcrop was already mentioned by Luburic (1963).
The section starts with about 15 m of lacustrine limestone starting by 30 cm thick bentonitic tephra layer. A prominent 8-m-thick breccia horizon follows, topped by about 14 m interval of presumable lacustrine limestone completely covered by vegetation. About 6 m thick coarse grained volcanic ash, weakly lithified and whitish in colour follows on top. Finally upsection the ash grades into lacustrine carbonates, dominated by fine-bedded limestone. Ash horizons of the Lake Mandek section are both indicated on the geological map by Papes (1972). A sample of the 6 m thick main ash layer was collected in a small pit (Fig. 77b) about 100 m E of the gulley at N43°43'49.9'', E017°01'21.6''. The lowermost tephra analyzed by Luburic (1963) represent vitroclastic volcanic ash composed mostly by volcanic glass (~80%) calcite (~18.5%) quartz (~1%) and biotiote (~0.5%). The glass particles are elongated, angulated and filled by gas inclusions. It is well sorted fine sand to silt. Absence of larger grains, together with angular grain shape point to their transport from larger distance. That coincides with the fact that no Miocene volcanic rocks have been detected in radius of at least 100 km. The extreme depth of the main ash horizon however provides mystery about the transportation of such sediment quantity from the long distance.
$^{40}Ar/^{36}Ar$ dating on feldspar crystals found in the main

Fig. 77: Mandek section: a. Overview of the section - white dot (right up) is the main ash site. b. Main volcanic ash layer topped by lacustrine limestone. Positions in sections are indicated in previous figure.

tephra bed of Mandek provides an age of 14.68 ±0.16 Ma providing its correlation with the middle Langhian of the standard geological scale and lower Badenian of the Central Paratethys scale (Middle Miocene). Considering its association with the mega-breccia beds this datum allows the dating of important tectonic event for the Dinarides. This event marks the start of the disintegration of the Dinaride Lake System due to extensive relief building and was recorded throughout the Dinarides such as Zenica-Sarajevo basin where massive fluvial conglomerates marks the corresponding event (HRVATOVIC 2006). Event coincides with the initial marine flooding of the southern Pannonian Basin (CORIC et al. 2009, MANDIC et al. 2011) and could reflect the compensation of the extensional tectonics therein (DE LEEUW et al. 2012). Indeed the new magneto-stratigraphic and geochronologic data could prove the complete cessation of lacustrine sedimentation synchronous with these movements for the smaller Dinaride basins such are Gacko (MANDIC et al. 2011) or Sinj Basin (DE LEEUW et al. 2010).

References

ALLEN, J.R.L. (1982): Sedimentary Structures: Their Character and Physical Basis. - Developments in Sedimentology, **30**: 1255 p., Elsevier, Amsterdam.

BABIC, Lj. & ZUPANIC, J. (1983): Paleogene clastic formations in northern Dalmatia. - In: BABIC, Lj. & JELASKA, V. (eds.): Contributions to Sedimentology of some Carbonate and Clastic Units of the Coastal Dinarides. Excursion Guidebook. 37-61, International Association of Sedimentologists 4th Regional Meeting, Split.

BABIC, Lj. & ZUPANIC, J. (1988): Coarse-grained alluvium in the Paleogene of northern Dalmatia (Croatia, Yugoslavia). - Rad JAZU, **441**(23): 139-164.

BABIC, Lj. & ZUPANIC, J. (1990): Progradacijski sljedovi u paleogenskom klasticnom bazenu Vanjskih Dinarida, od sjeverne Dalmacije do zapadne Hercegovine. - Rad JAZU, 449(24): 319-343.

BABIC, Lj. & ZUPANIC, J. (2008): Evolution of a river-fed foreland basin fill: the North Dalmatian Flysch revisited (Eocene, Outer Dinarides). - Natura Croatica, **17**: 357-374.

BAHUN, S. (1963): Geoloski odnosi okolice Donjeg Pazarista u Lici (trijas i tecijarne Jelar-naslage. - Geol. vjesnik, **16**: 161-170.

BAHUN, S. (1974): Tektogeneza Velebita i postanak Jelar naslaga. - Geol. vjesnik, **27**: 35-51.

COLLINSON, J.D. & THOMPSON, D.B. (1982): Sedimentary Structures. - 207 p., Allen and Unwin, London.

CORIC, S., PAVELIC, D., RÖGL, F., MANDIC, O., VRABAC, S., AVANIC, R., JERKOVIC, L. & VRANJKOVIC, A. (2009): Revised Middle Miocene datum for initial marine flooding of North Croatian Basins (Pannonian Basin System, Central Paratethys). - Geologia Croatica, **62**: 31-43.

DECELLES, G. P. & GILEST, A.K. (1996): Foreland basin systems. - Basin Research, **8**: 105-123.

DE LEEUW, A., MANDIC, O., KRIJGSMAN, W., KUIPER, K. & HRVATOVIC, H. (2012): Paleomagnetic and geochronologic constraints on the geodynamic evolution of the Central Dinarides. - Tectonophysics, **530-531**: 286-298.

DE LEEUW, A., MANDIC, O., KRIJGSMAN, W., KUIPER, K., HRVATOVIC, H. (2011): A chronostratigraphy for the Dinaride Lake System deposits of the Livno-Tomislavgrad Basin: the rise and fall of a long-lived lacustrine environment in an intra-montane setting. - Stratigraphy, **8**/1: 29-43.

DE LEEUW, A., MANDIC, O., VRANJKOVIC, A., PAVELIC, D., HARZHAUSER, M., KRIJGSMAN, W. & KUIPER, K.F. (2010): Chronology and integrated stratigraphy of the Miocene Sinj Basin (Dinaride Lake System, Croatia). - Palaeogeogr., Palaeoclim., Palaeoecol., **292**: 155-167.

DE RAAF, J. F. M., BOERSMA, J. R. & VAN GELDER, A. (1977): Wave-generated structures and sequences from a shallow marine succession: Lower Carboniferous, County Cork, Ireland. - Sedimentology, **24**: 451-483.

DOTT, R.H. JR. & BOURGEOIS, J. (1982): Hummocky stratification: significance of its variable bedding sequences. - Bull. Geol. Soc. Am., **93**: 663-680.

EINSELE, G. & SEILACHER, A. (eds.) (1982): Cyclic and Event Stratification. - 536 p., Springer-Verlag, Berlin.

GUSIC, I. & JELASKA, V. (1990): Stratigrafija gornjokrednih nasalga Braca u okviru geodinamske evolucije Jadranske karbonatne platforme. - Djela Jugoslavenske akademije znanosti i umjetnosti, **69**: 160 p., JAZU, Zagreb.

HAMBLIN, A.P. & WALKER, R.G. (1979): Storm-dominated shallow marine deposits: the Fernie-Kootonay (Jurassic) transition, southern Rocky Mountains. - Can. Jour. Earth Sci., **5**: 1673-1690.

Harms, J.C., Southard, J.B., Spearing, D.R., Walker, R.G. (1975): Depositional environments as interpreted from primary sedimentary structures and stratification sequences. - SEPM Short Course, 2, 161 p., Lecture Notes. Society of Economic Paleontologists and Mineralogists, Dallas.

HARMS, J.C., SOUTHARD, J.B. & WALKER, R.G. (1982): Structures and sequences in clastic rocks. - SEPM Short Course, 9, 249 p., Lecture Notes. Society of Economic Paleontologists and Mineralogists, Calgary.

HARZHAUSER, M. & MANDIC, O. (2008): Neogene lake systems of Central and South-Eastern Europe: Faunal diversity, gradients and interrelations. - Palaeogeogr., Palaeoclim., Palaeoecol., **260**/3-4: 417-434.

HARZHAUSER, M. & MANDIC, O. (2010): Neogene dreissenids in Central Europe: evolutionary shifts and diversity changes. - In: VAN DER VELDE, G., RAJAGOPAL, S., BIJ DE VAATE, A. (Eds.): The Zebra Mussel in Europe, 11-28, 426-478, Backhuys Publishers, Leiden.

HARZHAUSER, M., MANDIC, O., LATAL, C. & KERN, A. (2011): Stable isotope composition of the Miocene Dinaride Lake System deduced from its endemic mollusc fauna. - Hydrobiologia, **682**/1: 27-46.

HARZHAUSER, M. & PILLER, W.E. (2007): Benchmark data of a changing sea - Palaeogeography, Palaeobiogeography and Events in the Central Paratethys during the Miocene. - Palaeogeogr., Palaeoclim., Palaeoecol., **253**: 8-31.

HERAK, M. & BAHUN, S. (1980): The role of calcareous breccias (Jelar Formation) in the tectonic interpretation of the High Karst Zone of the Dinarides. - Geol. vjesnik, **31**: 49-59.

HOLBOURN, A., KUHNT, W., SCHULZ, M. & ERLENKEUSER, H. (2005): Impacts of orbital forcing and atmospheric carbon dioxide on Miocene ice-sheet expansion. - Nature, **438**: 483-487.

HRVATOVIC, H. (2006): Geological Guidebook through Bosnia and Herzegovina. - 172 p., Geological Survey of Federation BiH, Sarajevo.

ILIC, A. & NEUBAUER, F. (2005): Tertiary to recent oblique convergence and wrenching of the Central Dinarides: Constraints from a palaeostress study. - Tectonophysics, **410**: 465-484.

IVANOVIC, A., SAKAC, K., MARKOVIC, S., SOKAC, B., SUSNJAR, M., NIKLER, L. & SUSNJARA, A. (1973): Osnovna geoloska karta SFRJ 1:100.000. List Obrovac. (Basic Geological Map of SFRY, Obrovac Sheet). - Inst. geol. istraz. Zagreb (1962-1967), Savezni geol. zavod, Beograd.

JIMENEZ-MORENO, G., DE LEEUW, A., MANDIC, O., HARZHAUSER, M., PAVELIC, D., KRIJGSMAN, W. & VRANJKOVIC, A. (2009): Integrated stratigraphy of the early Miocene lacustrine deposits of Pag

Island (SW Croatia): palaeovegetation and environmental changes in the Dinaride Lake System. - Palaeogeogr., Palaeoclim., Palaeoecol., **280**/1-2: 193-206.

Jiménez-Moreno, G., Mandic, O., Harzhauser, M., Pavelic, D. & Vranjkovic, A. (2008): Vegetation and climate dynamics during the early Middle Miocene from Lake Sinj (Dinaride Lake System, SE Croatia). - Review of Palaeobotany and Palynology, **152**: 270-278.

Kerner, F.v. (1905): Gliederung der Sinjaner Neogen-formation. - Verhandlungen der Geologischen Reichanstalt in Wien, **1905**/6: 127-165.

Kerner, v. M.F. (1920a): Erläuterungen zum Nachtrag zur Geologischen Karte der im Reichsrate vertretenen Königsreiche und Länder der Österr.-Ungar. Monarchie. SW Gruppe Nr. 119, Knin und Ervenik (Zone 29, Col. XIV der Spezialkarte der vormaligen Österr.-Ungar. Monarchie im Maßstabe 1:75.000). - Verlag Geol. Reichsanst., 1-32, Wien.

Kerner, v. M.F. (1920b): Erläuterungen zum Nachtrag zur Geologischen Karte der im Reichsrate vertretenen Königsreiche und Länder der Österr.-Ungar. Monarchie. SW Gruppe Nr. 117, Zara (Zone 29, Col. XII der Spezialkarte der vormaligen Österr.-Ungar. Monarchie im Maßstabe 1:75.000). - Verlag Geol. Reichsanst., 1-16, Wien.

Korbar, T. (2009): Orogenic evolution of the External Dinarides in the NE Adriatic region: a model constrained by tectonostratigraphy of Upper Cretaceous to Paleogene carbonates. - Earth-Science Reviews, **96**: 296-312.

Kreisa, R.D. (1981): Storm-generated sedimentary struc-tures in subtidal marine facies with examples from the Middle to Upper Ordovician of southwestern Virginia. - J. Sedim. Petrol., **51**: 823-848.

Leckie, D.A. & Walker, R.G. (1982): Storm- and tide-dominated shorelines in Cretaceous Moosebar-Lower Gates interval: outcrop equivalents of Deep Basin gas trap, western Canada. - Am. Assoc. Petrol. Geol. Bulletin, **66**: 138-157.

Lewis, A.R., Marchant, D.R., Ashworth, A. C., Hedenäs, L., Hemming, S R., Johnson, J.V., Leng, M. J., Machlus, M.L., Newton, A.E., Raine, J.I., Willenbring, J. K., Williams, M. & Wolfe, A.P. (2008): Mid-Miocene cooling and the extinction of tundra in continental Antarctica. - Proc. Natl. Acad. Sci. USA, **105**(31):10676-10680.

Lowe, D.R. (1982): Sediment gravity flows II. Depositional models with special reference to the deposits of high-density turbidity currents. - J. Sedim. Petrol., **52**: 279-297.

Lowe, D.R. (1988): Suspended-load fallout rate as an independent variable in the analysis of current structures. - Sedimentology, **53**: 765-776.

Luburic, P. (1963): Pojave tufova i bentonita u naslagama slatkovodnog neogena u Livanjsko-Duvanjskom ugljonosnom nasenu u jugozapadnoj Bosni. - Geoloski glasnik Sarajevo, **8**: 203-211.

Malez, M. & Sliskovic, T. (1976): Starost nekih naslaga ugljena u tercijaru Bosne i Hercegovine na osnovi nalaza vertebrata. - Geoloski glasnik Sarajevo, 21: 39-56.

Mandic, O. Pavelic, D., Harzhauser, M., Zupanic, J., Reischenbacher, D., Sachsenhofer, R.F., Tadej, N. & Vranjkovic, A. (2009): Depositional history of the Miocene Lake Sinj (Dinaride Lake System, Croatia): a long-lived hard-water lake in a pull-apart tectonic setting. - Journal of Paleolimnology, **41**: 431-452.

Mandic, O., de Leeuw, A., Vukovic, B., Krijgsman, W., Harzhauser, M. & Kuiper, K.F. (2011): Palaeoenvironmental evolution of Lake Gacko (NE Bosnia and Herzegovina): impact of the Middlle Miocene Climatic Optimum on the Dinaride Lake System. - Palaeogeogr., Palaeoclim., Palaeoecol., **299**/3-4: 475-492.

Mandic, O., De Leeuw, A., Bulic, J., Kuiper, K., Krijgsman, W. & Jurisic-Polsak, Z. (2012): Paleogeographic evolution of the Southern Pannonian Basin: $^{40}Ar/^{39}Ar$ age constraints on the Miocene continental series of northern Croatia. - International Journal of Earth Sciences, **101**/4: 1033--1046.

Middleton, G.V. & Hampton, M.A. (1973): Turbidites and deep water sedimentation. sediment gravity flows: mechanics of flow and deposition. - Short Course Lecture Notes, 38 p., Soc. Econ. Paleont. and Mineralog., Pacific Section.

Milojevic, R. & Sunaric, O. (1964): Pokusaj stratigrafskog rasclanjavanja slatkovodnih sedimenata Duvanjskog basena i neki ekonomsko geoloski momenti u razvoju ugljenih facija. - Geoloski glasnik Sarajevo, **9**: 59-75.

Mrinjek, E. (1993a): Conglomerate fabric and paleocurrent measurment in the braided fluvial system of the Promina Beds in northern Dalmatia (Croatia). - Geol. Croat., **46**/1: 125-136.

Mrinjek, E. (1993b): Sedimentology and depositional setting of alluvial Promina Beds in northern Dalmatia, Croatia. - Geol. Croat., **46**/2: 243-261.

Mrinjek, E. (1994): Internal architecture of alluvial Promina Beds in northern Dalmatia, Croatia. - Acta geol., **24**/1-2: 1-36.

Mrinjek, E. (2008): The Promina Beds in canyon of Krka River and Bribirske Mostine. - In: Marjanac, T. (ed.): Guidebook, 5th ProGEO International Symposium, Rab Island, Croatia, Progeo - Croatia, Zagreb.

Mrinjek, E., Pencinger, V., Sremac, J. & Luksic, B. (2005): The Benkovac Stone member of the Promina formation: a Late Eocene succession of storm-dominated shelf deposits. - Geologia Croatica, **58**/2: 163-184.

Mrinjek, E., Pencinger, V. & Sremac, J. (2007): The stacked shallow coarse-grained mouth-bar type deltas in Promina formation: a Late Eocene prograding succession in Bribir area, Northern Dalmatia, Croatia. - 25th IAS meeting, Abstracts, Patras, Greece.

Mrinjek, E. & Pencinger, V. (2008): The Benkovac Stone - a building stone from the Promina Beds: a Late Eocene heterolithic succession of storm-dominated shelf deposits with highly diverse trace fossils. Guidebook, 5th ProGEO International Symposium, Rab Island, Croatia, 105-125, Progeo - Croatia, Zagreb.

Mrinjek, E., Pencinger, V., Maticec, D., Miksa, G., Bergant, S., Velic, I., Velic, J., Prtoljan, B. & Vlahovic, I. (2010a): Sedimentology, origin and depositional setting of sandstone beds within the oldest Promina deposits (Middle to Upper Eocene) of Northern Dalmatia, Croatia. - In: Horvat, M. (ed.): Abstracts Book, 4th Croatian Geological Congress, Sibenik, October 14-15, 2010, 24-25, Zagreb.

Mrinjek, E., Pencinger, V., Maticec, D., Miksa, G., Bergant, S., Velic, I., Velic, J., Prtoljan, B. & Vlahovic, I. (2010b): Carbonate olistoliths and megabeds within Middle to Upper Eocene Promina deposits: a sedimentary response to thrusting and fold growth an the Dinaric foreland basin. - In: Horvat, M (ed.): Abstracts Book, 4th Croatian Geological Congress, Sibenik, October 14-15, 2010, 26-27, Zagreb

Mrinjek, E., Pencinger, V., Nemec, W., Vlahovic, I. & Maticec, D. (2011): The effects of blind-thrust folding on foreland sedimentation: examples from the Eocene-Oligocene Dinaric foreland basin of Croatia. - Abstracts, 28th IAS Meeting, Zaragoza, Spain, 443.

Myrow, P.M. & Southard, J.B. (1996): Tempestite deposition. - Jour. Sed. Res., **66**: 875-887.

Mutti, E., Bernoulli, D., Lucchi, F. R. & Tinterri, R. (2009): Turbidites and turbidity currents from Alpine „flysch" to the exploration of continental margins. - Sedimentology, **56**, 267-318.

Neubauer, T.A., Mandic, O. & Harzhauser, M. (2011): Middle Miocene Freshwater Mollusks from Lake Sinj (Dinaride Lake System, SE Croatia; Langhian). - Archiv für Molluskenkunde, **140**/2: 201-237.

Nikler, L. (1982): Znacaj i karakteristike smeđih ugljena Dalmacije. - Geol. vjesnik, **35**: 181-194.

Ogorelec, B., Dolenec, T. & Drobne, K. (2007): Cretaceous-Tertiary boundary problem on shallow carbonate platform: carbon and oxygen excursions, biota and microfacies at the K/

T boundary sections Dolenja Vas and Sopada in SW Slovenia, Adria CP. - Palaeogeog., Palaeoclim., Palaeoecol., **255**: 64-76.

ORI, G.G. & FRIEND, P.G. (1984): Sedimentary basins, formed and carried piggyback on active thrust sheets. - Geology, **12**: 475-478.

PANTIC, N. (1961): O starosti slatkovodnog tercijara sa ugljem u Bosni na osnovu paleofloristickih istrazivanja. - Geoloski anali Balkanskog poluostrva, **28**: 1-22.

PENCINGER, V. (2012): Sedimentological and stratigraphical characteristics of the Promina beds in the northwestern Dalmatia. - Unpubl. PhD Thesis, University of Zagreb.

PAPES, J. (1972): Osnovna geoloska karta SFRJ 1:100.000. List Livno (Basic Geological Map of the SFRY. Livno Sheet). - Savezni geoloski zavod, Beograd.

PEMBERTON, S.G., MACEACHERN, J.A. & FREY, R.W. (1992): Trace fossil facies models: environmental and allostratigraphic significance. - In: WALKER, R.G. & JAMES, N.P. (eds.): Facies Models: Response to Sea Level Change. Geol. Assoc. of Canada, St. John's, 47-72.

PERVESLER, P. & UCHMAN, A. (2004): Ichnofossils from the type area of the Ground Formation (Miocene, Lower Badenian) in northern Lower Austria (Molasse Basin). - Geol. Carpath., **55**: 103-110.

PRTOLJAN, B., BERGANT, S., KRSTULOVIC, M., HAJEK-TADESSE, V., MRINJEK, E. & VLAHOVIC, I. (2009): Eocene flysch of the Konavle area (SE Croatia) - is it really Eocene and is it really flysch? - Abstracts, 27th IAS Meeting, Alghero, Italy.

Reading, H.G. & Collinson, J.D. (1996): Clastic coasts. - In: READING, H.G. (ed.): Sedimentary Environ-ments: Processes, Facies and Stratigraphy. 3rd ed., Blackwell Science, Oxford, 154-231.

REINECK, H.-E. & SINGH, I.B. (1975): Depositional Sedimentary Environments. - 439 p., Springer-Verlag, Berlin.

RÖGL, F. (1999): Mediterranean and Paratethys. Facts and Hypotheses of an Oligocene to Miocene Paleogeography (Short overview). - Geologica Carpathica, **50**/4: 339-349.

SAKAC, K. (1960): Geoloska grada i boksitne pojave podrucja Novigrad-Obrovac u sjeverozapadnoj Dalmaciji. - Geol. vjesnik, **14**: 323-342.

SAKAC, K. (1969): Analiza eocenskog paleoreljefa i tektonskih zbivanja u podrucju Drnisa u Dalmaciji s obzirom na postanak lezista boksita. - Geol. vjesnik, **23**: 163-179.

SANDERS, J.E. (1965): Primary sedimentary structures formed by turbidity currents and related resedimentation mechanisms. - In: MIDDLETON, G.V. (ed.): Primary Sedimentary Structures and Their Hydrodynamic Interpretation. Soc. Econ. Paleontol. Mineral. Spec. Publ., **12**: 192-219.

SCHMID, S.M., BERNOULLI, D., FÜGENSCHUH, B., MATENCO, L., SCHEFER, S., SCHUSTER, R., TISCHLER, M. & USTASZEWSKI, K. (2008): The Alpine-Carpathian-Dinaridic orogenic system: correlation and evolution of tectonic units. - Swiss Journal of Geosciences, **101**/1: 139-183.

SCHUBERT, R. (1909): Geologische Spezialkarte der im Reichsrate vertretenen Königsreiche und Länder der Österr.-Ungar. Monarchie neu aufgenommen und herausgegeben durch die k.k. Geologische Reichsanstalt. Medak und Sv. Rok 1:75.000 (Zone 28, Col. XIII). - Geol. Reichsanst., Wien.

SCHUBERT, R. (1910): Erläuterungen zum Nachtrag zur Geologischen Karte der im Reichsrate vertretenen Königsreiche und Länder der Österr.-Ungar. Monarchie. SW Gruppe Nr. 116, Medak und Sv. Rok (Zone 28, Col. XIII der Spezialkarte der vormaligen Österr.-Ungar. Monarchie im Maßstabe 1:75.000). - Verlag Geol. Reichsanst., 1-32, Wien.

SCHUBERT, R. (1920a): Geologische Spezialkarte der im Reichsrate vertretenen Königsreiche und Länder der Österr.-Ungar. Monarchie. Knin und Ervenik 1:75.000 (Zone 29, Col. XIV). - Geol. Reichsanst., Wien.

SCHUBERT, R. (1920b): Geologische Spezialkarte der im Reichsrate vertretenen Königsreiche und Länder der Österr.-Ungar. Monarchie. Zara 1:75.000 (Zone 29, Col. XII). - Geol. Reichsanst., Wien.

SEPKOSKI, J.J. Jr. (1982): Plat-pebble conglomerates, storm deposits, and the Cambrian bottom fauna. - In: EINSELE, G. & SEILACHER, A. (eds.): Cyclic and Event Stratification. Springer-Verlag, Berlin, 372-385.

STEUBER, T., KORBAR, T., JELASKA, V. & GUSIC, I. (2005): Strontium-isotope stratigraphy of Upper Cretaceous platform carbonates of the island of Brac (Adriatic Sea, Croatia): implications for global correlation of platform evolution and biostratigraphy. - Cret. Res., **26**/5: 741-756.

TARI KOVACIC, V. & MRINJEK, E. (1994): The role of Palaeogene clastics in the tectonic interpretation of Northern Dalmatia (Southern Croatia). - Geol. Croatica, **47**/1: 127-138.

UCHMAN, A. (1995): Taxonomy and paleooecology of flysch race fossils: The Marnoso-arenacea Formation and associated facies (Miocene, Nothern Apennines, Italy). - Beringeria, **15**: 3-115.

UCHMAN, A. (1999): Ichnology of the Rhenodanubian Flysch (Lower Cretaceous-Eocene) in Austria and Germany. - Beringeria, **25**: 67-173.

UCHMAN, A. (2001): Eocene flysch trace fossils from the Hecho Group of the Pyrenees, northern Spain. - Beringeria, **28**: 3-41.

UCHMAN, A., JANBU, N.E. & NEMEC, W. (2004): Trace fossils in the Cretaceous-Eocene flysch of the Sinop-Boyabat Basin, Central Pontides, Turkey. - Ann. Soc. Geol. Polon., **74**: 197-235.

VLAHOVIC, I., TISLJAR, J., VELIC, I. & MATICEC, D. (2005): Evolution of the Adriatic Carbonate Platform: paleogeography, main events and depositional dynamics. - Palaeogeog., Palaeoclim., Palaeoecol., **220**: 333-360.

VLAHOVIC, I., TISLJAR, J., VELIC, I. & MATICEC, D. (2007): Immense Tertiary carbonate Jelar breccia, Dinarides, Croatia: a new view. - In: BUSH, D. (ed.): 2007 GSA Annual Meeting and Exhibition: Abstracts with Programs. 146, Denver, Geological Society of America.

VLAHOVIC, I., TISLJAR, J., VELIC, I., ENOS, P., MATICEC, D., PLETIKOSIC, N., PERKOVIC, D., PRTOLJAN, B., VELIC, J., MRINJEK, E. & MIKSA, G. (2011): Tertiary carbonate breccia conundrum in the Karst Dinarides of Croatia: very massive and very neglected. - In: BÁDENAS, B., AURELL, M. & ALONSO-ZARZA, A.M. (ed.): Abstracts, 28th IAS Meeting of Sedimentology 2011. 460, Zaragoza, IAS.

VRANJKOVIC, A. (2011): Klimatski zapisi u miocenskim slatkovodnim naslagama Sinjskog bazena. - Unpubl. PhD Thesis, University of Zagreb.

WALKER, R.G, DUKE, W.L. & LECKIE, D.A. (1983): Hummocky stratification: significance of its variable bedding sequences: Discussion. - Geol. Soc. Am. Bull., **94**: 1245-1251.

WALKER, R.G. & PLINT, A.G. (1992): Wave- and storm- dominated shallow marine systems. - In: WALKER, R.G. & JAMES, N.P. (eds.): Facies Models: Response to Sea Level Change. - Geol. Assoc. of Canada, St. John's, 219-238.